DAJA45-92-M-0334 . . R&D 6971-EE-02

Abstracts Booklet

International Conference

on

Narrow Gap Semiconductors

NGS

19 - 23 July 1992

University of Southampton

UK

Organised in conjunction with

BRITISH ASSOCIATION FOR CRYSTAL GROWTH

Booklet funded by GEC Sensors

Post-deadline Abstracts

International Conference

on

Narrow Gap Semiconductors

NGS

19 - 23 July 1992

University of Southampton

UK

Organised in conjunction with

BRITISH ASSOCIATION FOR CRYSTAL GROWTH

Measurement of the Two-Photon absorption coefficient of InSb using a Free-Electron Laser

B.N.Murdin, C.Merveille, A.K.Kar and C.R.Pidgeon

Department of Physics, Heriot-Watt University, Edinburgh EH14 4AS, Scotland.

D.A.Jaroszynski, J-M.Ortega, R.Prazeres and F.Glotin

Laboratoire pour l'Utilisation du Rayonnement Électromagnétique, Bâtiment 209D, Université de Paris-Sud, 91405 Orsay Cedex, Paris, France.

Abstract

We have performed the first experiment on the Free-Electron Laser (CLIO) at the Laboratoire pour l'Utilisation du Rayonnement Électromagnétique (LURE).

Strong power limiting has been observed in a transmission experiment on InSb at wavelengths longer than the absorption edge. This is associated with induced free-carrier absorption produced by direct interband two-photon transitions.

We have estimated the Two-Photon Absorption (TPA) coefficient (β) of InSb to be 2cm/MW at 8.9μm (utilising the tuneablity of the FEL for wavelengths other than hitherto available with CO_2 lasers), by fitting the power-limiting effect to a simple theory. The result distinguishes between different theoretical models for the process.

FELIX, A FREE-ELECTRON LASER FACILITY OPERATING IN THE MID AND FAR INFRARED

D. Oepts, R.J. Bakker, D.A. Jaroszynski, A.F.G. van der Meer, C.A.J. van der Geer, and P.W. van Amersfoort
FOM-Instituut voor Plasmafysica 'Rijnhuizen', Associatie Euratom-FOM,
P.O.Box 1207, 3430 BE Nieuwegein, Nederland

The Free Electron Laser for Infrared eXperiments, FELIX, is designed to provide a source of powerful, tunable, short-pulse radiation in the wavelength range 8 - 80 µm (1250 - 125 cm^{-1}). Two stages of electron acceleration and two undulators are used to cover this range in two sections of 8-30 µm and 20-80 µm, respectively. The longer wavelength part has become operational last year, and saturated output has been obtained from 16 to 110 µm. The shorter wavelength part is expected to start operation this summer. User experiments can be accomodated on a provisional basis until the user facility becomes fully operational in 1993.

The radio-frequency linear accelerators of FELIX provide an electron beam consisting of micropulses of a few picoseconds length, repeated at 1 GHz during macropulses of up to 20 µs. These macropulses are again repeated at a few Hertz. The optical output of the laser has a similar time structure. However, the length of the optical micropulses is not determined only by the length of the electron pulses, and can be varied between about 1 and 20 ps by adjustment of the resonator length.

Over the present range of operation, we have measured output energies from 1 to 10 µJ per micropulse. This amounts to an average power of 1 - 10 kW in the macropulse, and peak micropulse powers in the MW range. A peak power density of the order of 1 GW/cm^2 can be obtained in a focussed beam.

Tuning of the output frequency over one octave can be performed in a matter of minutes by changing the undulator strength. Setting of a different scanning range may take some 15 minutes.

Preliminary user experiments have been performed in the fields of two photon absorption, photon drag effect, and absorption in low-T_c superconductors.

Shubnikov-de Haas effect for highly Si-doped InAs0.2Sb0.8/InSb strained layer superlattices (SLSs)

Tan Le[1,2], J J Harris[1], W T Yuen[2], R A Stradling[1,2], C C Phillips[2], A G Norman[1] and I T Ferguson[1].

1. Interdisciplinary Research Centre for Semiconductor Materials, Blackett Laboratory, Imperial College, London SW7 2BZ, UK.
2. Physics Department, Blackett Laboratory, Imperial College, London SW7 2BZ, UK.

The Shubnikov-de Haas (SdH) effect has been observed with highly silicon doped $InAs_{0.2}Sb_{0.8}$/InSb SLSs of period 200A, consisting of 100A $InAs_{0.2}Sb_{0.8}$ and 100A InSb. The samples were grown at T_G=440°C on semi-insulating GaAs substrates by molecular beam epitaxy (MBE) with a nominal silicon sheet density of $1\times10^{12}cm^{-2}$, and with the following profiles: a) in the wells, b) in the barriers, or c) uniform doping.

The silicon incorporation as a donor is known to be strongly dependent on growth temperature (T_G). A sample grown at T_G=330°C showed virtually 100% activation of silicon as a donor whereas samples grown at T_G=440°C had about a factor of two lower concentration.

The SdH oscillations show a strong 1/cosθ dependence where θ is the angle of the magnetic field to the growth direction, characteristic of a two dimensional electron gas (2DEG). With the samples having profiles (b) and (c), broad features are observed which are possibly related to magnetic breakdown when the magnetic field is applied parallel to the interfaces. Numerical calculations have shown the Fermi energies above the bottom of the wells to be 109meV (for the sample doped in wells and grown at T_G=440°C), 111meV (sample doped in the barriers), and 164meV (sample with uniform doping).

ABSTRACTS BOOKLET

Sponsors

The conference has been financially underwritten by the British Association for Crystal Growth.

We gratefully acknowledge financial support from the following:

Defence Research Agency
GEC-Marconi Materials Technology
GEC Sensors
Leica (Cambridge)]
MCP Wafer Technology
Philips Infrared
Rockwell International Science Center
S.A.T.

We would also like to thank the Royal Society for assistance to overseas participants.

Exhibition

The following organisations will be exhibiting at the conference:

CTI-Cryogenics
Epichem
Hiden Analytical
Hydrogen Engineering Applications
IOP Publishing
LOT-Oriel
MCP wafer Technology
Nippon Mining (UK)
Oxford Applied Research

PROGRAMME OUTLINE - by first authors

Time	Monday	Tuesday	Wednesday	Thursday
	Introduction	5. Magnetism/ Magnetooptics	8. CMT (structure)	11. III-V (devices)
8.45	Welcome	Dietl-inv	Arias-inv	Lakrimi-inv
9.00	McGill Opening			
9.15		Geist	Monterrat	Phillips
9.30	1. Novel Growth Abstreiter-inv	Story Eggenkamp	Dutton Bubalac	Bougnant Ashley
10.00	Norman-inv	Manasses-inv	Tardot-inv	Malutenko-inv
10.30	Coffee			
	2. DMS (mainly Fe)	6. II-VI growth	9. Linear and NL optics	12. Special Symposium Chair:D G Seiler
11.00	v.Ortenberg-inv	Maxey-inv	Vodopyanov-inv	Levine-inv
11.30	Skierbizewski	Lusson	Klann	Sheng Li
11.45	Wilamowski	Funaki	Hofmann	Sizman
12.00	Szuszkiewicz	Mitra	Kremser	Fraenkel
12.15	Dobrowolski	Astles	Littler	Morimoto
12.30	Lahderanta	He	Kushev	Mironov
12.45	Lunch	Lunch	Lunch	Lunch
	3. II-VI (elect/opt.)	POSTERS	10.Material (mainly IV-VI)	12. contd.
13.45	Meyer-inv	P1.1 to P12.2	Tacke-inv	Heremans-inv
14.15	Cheong		Lambrecht	Gornik-inv
14.30	Kraus		Zogg	
14.45	Takita		Herrmann	Takyanagi-inv
15.00	Esquivias		Schweitzer	
15.15	Andrukhiv			Dawson-inv
15.30	TEA	TEA	Conference Excursion	------------ 15.45- TEA
	4. III-V (InAs/GaAs)	7. Dots/Novel Confinement		
16.00	Mendes-inv	Ploog-inv		------------ 16.15 Oswald-inv
16.30	Miles	Tournie		
16.45	Waterman	Zawadzki		16.45 Shen-inv
17.00	Golding	Freytag		
17.15	Omaggio	Kubisa-inv		Close
17.30	Golding			
17.45	Inoui			Landwehr

NGS Conference Programme, 20-23 July, 1992

Monday, July 20

8.45 R A Stradling, Imperial College
Introduction

9.00 T C McGill, California Institute of Technology
Opening address

1. Novel Growth

9.30 G. Abstreiter (invited), J Olajos, R Schorer, P Vogel and W Wegscheider
1.1 Properties of Sn-Ge superlattices

10.00 A G Norman (invited), T-Y Seong, I T Ferguson, G R Booker, B A Joyce and R A
1.2 Stradling
Structural properties of natural superlattices

10.30 **Coffee**

2. Dilute Magnetic Semiconductors (mainly Fe)

11.00 M von Ortenberg (invited),
2.1 High magnetic field studies of HgFeSe

11.30 C Skierbiszewski, Z Wilamowski and J Kossut
2.2 The band structure of mixed crystal $Hg_{1-x}Fe_xSe$

11.45 Z Wilamowski, W Jantsch and G Hendorfer,
2.3 Spin relaxation in semimetallic HgSe:Fe

12.00 W Szuszkiewicz, C Julien, M Balkanski and B Witkowska
2.4 Hybridisation-mediated spin dependent p-d interaction in semimagnetic semiconductors:experimental proof

12.15 W Dobrowolski, E Grodzicka, J Kossut and B Witkowska
2.5 Iron doping: a tool to improve electrical properties of $Hg_{1-x}Zn_xSe$

12.30 E Lahderanta, R Laiho, A V Lashkul, A Makinen and V S Zakhvalinski
2.6 High temperature magnetic freezing in $(Cd_{1-x}Mn_x)_3As_2$

12.45 **Lunch**

3. II-VI (Electronics and Optics)

13.45 C A Hoffman, J R Meyer (invited) and F J Bartoli
3.1 Semimetallic HgTe-HgCdTe superlattices

14.15 H M Cheong, J H Burnett, W Paul, P M Young and J F Schetzina
3.2 Pressure dependence of IR photoluminescence spectra from HgTe/HgCdTe superlattices

14.30 M M Kraus, Y S Wu, C R Becker and G Landwehr
3.3 IR photoluminescence on MBE grown $Hg_{1-x}Cd_xTe$ layers

14.45 K Takita, S Kuroda and H J Kwon
3.4 Observation of magnetophonon resonance oscillations in open gap $Hg_{1-x-y}Cd_xMn_yTe$ grown by LPE

15.00 I Esquivias, J Baars and D Brink
3.5 Electrical properties of the anodic oxide-HgZnTe interface

15.15 A M Andrukhiv, V I Ivanov-Omskii, A M Litvak, K E Mironov and V V Ratnikov
3.6 Growth and properties of $Zn_xCd_yHg_{1-x-y}Te$ LPE layers

15.30 **Coffee**

4. III-V (InAs/GaSb)

16.00 E E Mendes (invited)
4.1 Tunneling in crossed-gap systems

16.30 R H Miles, D H Chow, A T Hunter, J N Schulman and T C McGill
4.2 Far Infrared $Ga_{1-x}In_xSb/InAs$ superlattices

16.45 J R Waterman, B V Shanabrook, R J Wagner, M J Yang, J L Davis and J P
4.3 Omaggio
The effect of interface bond type on the structural and optical properties of MBE grown GaSb/InAs superlattices

17.00 T D Golding, J T Zborowski, J A Dura, A Viliante, D W Donnelly, B C Covington
4.4 and E MacDonald
Investigation of InAs/(In,Ga)Sb superlattices grown by molecular beam epitaxy on the [100] and [111] orientations

17.15 J P Omaggio, R J Wagner, J R Meyer, C A Hoffman, M J Yang, D H Chow and R
4.5 H Miles
Magnetooptic and magneto-transport study of $InAs/Ga_{1-x}In_xSb$ superlattices

17.30 T D Golding, J A Dura, H Wang, J T Zborowski, A Viliante and J H Miller Jr.
4.6 Investigation of Sb/GaSb multilayer structures for potential application as a narrow bandgap system

17.45 M Inoue, H Furuse, N Nasu, M Yano and Y Iwai
4.7 Optical analysis of InAs heterostructures grown by migration enhanced epitaxy

Tuesday, July 21.

5. Magnetism and Magnetooptics

8.45 T Dietl (invited)
5.1 Mesoscopic phenomena in dilute magnetic semiconductors

9.15 F Geist, H Pascher, N Frank, G Bauer and M Kriechbaum
5.2 Exchange interaction in semimagnetic IV-VI multi-quantum well structures

9.30 T Story, P J T Eggenkamp, C H W Swuste, H J M Swagten and W J M de Jonge
5.3 Electron spin resonance study of the narrow gap semiconductor PbSnMnTe

9.45 P J T Eggenkamp, T Story, H J M Swagten, C W H M Vennix, M M H Willekens
5.4 and W J M de Jonge
Carrier-induced magnetic properties in small gap semiconductors

10.00 J Manasses (invited), Y Guldner, J P Vieren and J P Faurie
5.5 Properties of HgZnTe-CdTe and HgTe-CdTe superlattices

10.30 **Coffee**

6. II-VI Growth

11.00 C Maxey (invited), I Gale, J B Clegg and P A C Whiffin
6.1 Doping studies in MOVPE of $Cd_xHg_{1-x}Te$

11.30 A Lusson, R Druilhe, Y Marfaing and E Rzepka
6.2 CdTe/CdHgTe interdiffused quantum wells

11.45 M Funaki, J E Lewis, T D Hallam, Li Chaorong, S K Halder, K Durose, A W
6.3 Brinkman and B K Tanner
The MOVPE growth and characterisation of $Hg_{1-x}Mn_xTe$

12.00 P Mitra, T R Schimert, F C Case, L T Claiborne and H L Wilson
6.4 Properties of HgCdTe layers grown by isothermal vapour phase epitaxy at high pressures

12.15 M G Astles, N Shaw and G Blackmore
6.5 Techniques for improving the properties of liquid phase epitaxial CdHgTe for IR photodiodes

12.30 L He, C R Becker, R N Bicknell-Tassius, S Scholl and G Landwehr
6.6 Optimized MBE growth of (100) HgCdTe on CdZnTe

12.45 Lunch

Posters

1.45 P1.1 to P12.2

7. Dots and Novel Confinement

16.00 K H Ploog (invited) and O Brandt
7.1 InAs monolayers and quantum dots in a crystalline GaAs matrix

16.30 E Tournie, O Brandt and K H Ploog
7.2 Optical properties of InAs quantum wells emitting between 0.9 and 2.5 microns

16.45 W Zawadzki and M Kubisa
7.3 Magnetooptical properties of quantum dots in InSb

17.00 B Freytag, U Rossler and O Pankratov
7.4 Subbands in inversion layers on NGS for E_{gap} tends to zero

17.15 M Kubisa (invited)
7.5 Kinetic confinement of electrons in semiconductor heterostructures

Wednesday, July 22

8. CMT (Structure)

8.45 J.Arias (invited), M Zandian and R Zucca
8.1 HgCdTe infrared laser diodes grown by MBE

9.15 E Monterrat, L Ulmer, N Magnea, H Mariette, J L Pautrat, K Kheng and F
8.2 Fuchs
Optical spectroscopy of CdTe/CdHgTe quantum wells and superlattices

9.30 D T Dutton, E O'Keefe, P Capper, C L Jones, S Mugford and C Ard
8.3 Type conversion of $Cd_xHg_{1-x}Te$ grown by liquid phase epitaxy

9.45 L O Bubalac, S J C Irvine, E R Gartner, W P Lin and J Bajaj
8.4 As and Sb diffusion in MCT for junction formation

10.00 A Tardot (invited), A Hamoudi, P Gentile, N Magnea and J L Pautrat
8.5 Interdiffusion study in CdTe/HgTe superlattices

10.30 Coffee

9. Linear and Nonlinear Optics

11.00 K L Vodopyanov (invited), H Graener, C C Phillips and I Ferguson
9.1 Middle infrared picosecond spectroscopy of MBE InAs epilayers at 300K

11.30 R Klann, T Hofer, R Buhleier, T Elsaesser and A Lambrecht
9.2 Ultrafast recombination processes in lead chalcogenide semiconductors via picosecond optical nonlinearities

11.45 W Hofmann, H Pascher and G Denninger
9.3 Nuclear spin polarization in InSb detected by spin flip Raman gain spectroscopy

12.00 C Kremser, K Unterrainer, Gornik, P Pfeffer, W Zawadzki, B Murdin and C R
9.4 Pidgeon
Crossed field hot hole cyclotron resonance: non-parabolic and quantum effects

12.15 C L Littler, X N Song, Z Yu, J L Elkind, D G Seiler and J R Lowney
9.5 Investigation of trap levels in bulk and LPE $Hg_{1-x}Cd_xTe$ using resonant impact ionization spectroscopy

12.30 D B Kushev and N N Zheleva
9.6 Characterization of free carriers in IV-VI laser materials from IR reflectivity

12.45 Lunch

10. Material Properties (mainly IV-VI)

13.45 M Tacke (invited)
10.1 IV-VI material properties relevant to laser diodes

14.15 A Lambrecht, H Bottner, M Agne, R Kurbel, A Fach, B Halford, U Schiessl and M
10.2 Tacke
MBE of laterally structured lead chalcogenides for the fabrication of buried heterostructure lasers

14.30 H Zogg, C Maissen, S Blunier, S Teodoropol, R M Overney, T Richmond and J E
10.3 Tomm
Thermal mismatch strain relaxation mechanisms in heteroepitaxial lead chalcogenide layers on Si-substrates

14.45 K H Herrmann, K P Mollmann, P Schafer, J W Tomm, H Bottner, M A Fach, M
10.4 Griesinger and J Sebastian
Properties of narrow gap PbSe quantum wires

15.00 M O Schweitzer, F M Leibsle, T s Jones, C F McConville and N V Richardson
10.5 An STM study of InSb(100)-c(8x2)

15.30 Conference Excursion

Thursday, July 23

11. III-V Devices

8.45 M Lakrimi (invited), R W Martin, C Lopez, D M Symons, E T R Chidley, R J
11.1 Nicholas, N J Mason and P J Walker
Piezoelectric effects in superlattices

9.15 C C Phillips, R H Thomas, H L Vaghjiani, I T Ferguson and A Norman
11.2 Interband and intersubband transitions in InAs doping superlattices studied by absorption and photoconductivity spectroscopies

9.30 G Bougnot, J P R David, A Giani, S K Haywood, G Hill, A Krier, F Mansoor, N J
11.3 Mason, R J Nicholas, F Pascal-Delannoy, M Pate, L Ponnampalam and P J Walker
The growth and fabrication of new antimony containing III-V heterostructures for devices in the 2-4 micron region

9.45 T Ashley, A B Dean, C T Elliott, A D Johnson, G J Pryce, A M White and C R
11.4 Whitehouse
A heterojunction minority carrier barrier for InSb devices

10.00 V K Malutenko (invited)
11.5 Exclusion effects in semiconductors revisited : narrow gap semiconductors, non-traditional use

10.30 Coffee

12. Special Symposium on Novel Structures and Applications

11.00 B F Levine (invited)
12.1 Quantum well infrared photodetectors

11.30 Sheng S Li, M Y Chuang and S S Yu
12.2 Current conduction in bound-to-miniband transition III-V multiquantum well IR detectors

11.45 R Sizman, P Helgesen, S Lovold and A Paulsen
12.3 The absorption linewidth of bound to extended state transitions in GaAs/AlGaAs quantum wells-dependence on excited level position

12.00 A Fraenkel, E Finkman, G Bahir, A Brandel, G Livescu and M T Asom
12.4 *Increased responsivity and detectivity in asymmetric quantum well infrared detectors*

12.15 T Morimoto, M Chiba, G Kido and A Tanaka
12.5 Stimulated emission due to magnetoelectric photo-effect in NGS at the quantum limit

12.30 O A Mironov, V T Igumenov and V M Konstantinov
12.6 Galvanomagnetic properties of InSb/(100)GaAs heterostructures for microminiature Hall transducers

12.45 Lunch

12. Special Symposium (continued)

13.45 J Heremans (invited)
12.7 III-V magnetic sensors

14.15 E Gornik (invited)
12.8 Hot electron and subband far infrared detectors

14.45 H Takayanagi (invited), T Akazaki and J Nitta
12.9 Superconducting structures on narrow gap semiconductors

15.15 L R Dawson (invited)
12.10 Applications of narrow gap strained layer superlattices

15.45 Coffee

16.15 J Oswald (invited)
12.11 Review of nipi structures for IR detectors

16.45 S C Shen
12.12 CMT versus quantum well structures for IR detectors

Conclusion

17.15 G Landwehr, University of Wurzburg, Germany
Closing Address

Posters

P1.1 L V Kradinova, A M Polubotko, V V Popov, V D Prochukhan, Yu V Rud and V E Skoriukin
Novel ...less compounds, magnetics: $CuFeS_2$ and $CuFeTe_2$

P2.1 C Skierbiszewski, Z Wilamowski, T Suski and J Kossut
Why different types of donors can either enhance or reduce electron mobility in NGS

P2.2 I I Lyapilin, I G Kuleev and V V Karyagin
Transport phenomena in a quantum well containing mixed valence impurities

P2.3 I M Tsidilkovski, I I Kuleev and I I Lyapilin
The "anomaly" of electron scattering by a correlated system of charged donors

P2.4 Z Wilamowski, H Przybylinska, W Joss and M Guillot
Anisotropy of the magnetic interactions in HgFeSe

P3.1 F Fuchs, K Kheng, K Schwarz and P Koidl
Fourier transform photoluminescence excitation spectroscopy on medium band gap HgCdTe

P3.2 V A Pogrebnyak, D D Khalameida and V M Yakovenko
Block boundaries conductivity and size effect in mosaic (HgCd)Te crystals

P3.3 M I Vasilevskiy, S N Ershov and V V Nikonorov
A possibility of observation of the correlated disorder effects in A_2B_6 semiconductor through the exciton spectroscopy

P3.4 S Barton, P Capper, A McAllister, C L Jones and N Metcalfe
Transient and steady state lifetime measurements on epitaxially grown $Cd_xHg_{1-x}Te$

P3.5 Yu I Mazur, V P Denisov, S I Kriven, V V Strelchuk and G G Tarasov
Raman investigation of NG solid solutions of HgCdMnTe

P3.6 Y I Mazur, S I Kriven, G G Tarasov and N V Shevchenko
Vibrational modes activated by structural disordering in FIR transmission of HgCdMnTe

P3.7 S G Gasan-zade, G A Shepelsky, M V Strikha and F T Vas'ko
Dominant recombination mechanism change in uniaxially pressed $Hg_{1-x}Cd_xTe$

P3.8 J H Chu, R Sizmann, K Liu, Z Y Mi, S C Shen and F Koch
Electron subband structure in inversion layer of p-type $Hg_{0.79}Cd_{0.21}Te$

P3.9 J H Chu and S C Shen
The study of far infrared phonon spectra in $Hg_{1-x}Cd_xTe$

P3.10 Susan J Zachman, Eliezer Finkman and Gad Bahir
Bias effects on the electrical characterization of deep levels in HgCdTe

P3.11 G Grabecki, A Wittlin, T Dietl, P A A Teunissen, S A J Wiegers and J A J Perenboom
Precision of the Hall quantization in naturally occurring 2-D system HgCdMnTe bicrystals

P3.12 E Bangert, P Boege, V Latussek and G Landwehr
The optical absorption coefficient of HgTe-CdTe superlattices-theory and experiment

P4.1 B Foste, U Kunze, G Zwinge and A Schlachetzki
Field-effect controlled resonant interband tunneling in electron surface layers on InAs and $In_{.53}Ga_{.47}As$

P4.2 M J Yang, P J Lin-Chung, R J Wagner, J R Waterman, W J Moore, B V Shanabrook and M Fatemi
FIR spectroscopy of strained AlSb/InAs/AlSb quantum wells

P4.3 J Scriba, A Wixforth, J P Kotthaus, C Bolognesi, C Nguyen, G Tuttle, J H English and H Kroemer
The effect of Landau quantization on cyclotron resonance in a non-parabolic quantum well

P4.4 C Gauer, J Scriba, A Wixforth, J P Kotthaus, Ch Nguyen, G Tuttle, J H English and H Kroemer
Photoconductivity in AlSb/InAs quantum wells

P5.1 P Pfeffer and W Zawadzki
Insulator-metal transition in HgTe in crossed magnetic and electric fields

P5.2 G Zheng, J Shen, S Guo and D Tang
Influence of heavy hole scattering on the magnetotransport behaviour of p-type zero-gap $Hg_{1-x}Mn_xTe$

P5.3 G Nachtwei, N J Bassom, W Kraak, R J Nicholas and M Watts
Magnetotransport investigations at InSb and $Hg_{1-x}Cd_xTe$ bicrystals in tilted magnetic fields

P5.4 W Zawadzki, E Dudziak, L Z Jedral, E Placzek-Popko and J Bozym
Phonon assisted interband magnetooptical transitions in HgCdMnTe

P5.5 K H Hermann, K P Mollmann, J W Tomm, H Bottner, A Lambrecht, M Tacke, I V Kolesnikov, A E Yunovich, A I Fedorenko, O A Mironov and A Y Sipatov
Band offsets in Eu-containing lead chalcogenides and lead chalcogenide superlattices from spectroscopical data

P5.6 A Nateprov, I Laue, M von Ortenberg and E Arushanov
Shubnikov de Haas oscillations in $Cd_3(As_xP_{1-x})_2$

P6.1 N L Bazhenov, S I Gasanov and V I Ivanov-Omskii
Excess currents in narrow gap $Cd_xHg_{1-x}Te$ p-n junctions

P6.2 N T Gordon, S Barton, P Capper, C L Jones and N Metcalfe
Electron mobility in p-type epitaxially grown $Cd_xHg_{1-x}Te$

P6.3 N Hoffmann, K Jacobs, L Parthier, T Teubner, K H Herrmann, W Hoerstel, K P Mollmann and J W Tomm
HgCdTe layers grown by MBE on GaAs using different buffer layers

P6.4 N N Berchenko, J S Budzhak, K R Kurbanov and G Sasvari
Identification of extended defects in n-$Hg_{1-x}Cd_xTe$ by galvanomagnetic measurements

P6.5 J C Tedenac, M C Record, R M Ayral-Marin, L Konczewicz, J Jun and J L Robert
Crystallization of HgSe bulk crystals under high gas pressure and their electrical characterisation

P7.1 V K Dugaev, V I Litvinov, O A Mironov, P P Petrov and M Oszwaldowski
Energy spectrum in quantum dots of IV-VI NGS

P8.1 V I Ivanov-Omskii, K E Mironov and K D Mynbaev
$Cd_xHg_{1-x}Te$ doping by ion beam treatment

P8.2 I G Gale, C D Maxey, J B Clegg, S Mugford, S Barton, P Capper and C L Jones
Assessment of doped $Cd_xHg_{1-x}Te$ structures using bevelled sections

P8.3 O A Soltanovich, E B Yakimov and N A Yarykin
Effect of trap athermal recharge on DLTS measurements in NGS

P8.4 J Bonnet-Gamard, J Bleuse, H Mariette, L Ulmer, N Magnea and J L Pautrat
Cavity structure effects on $Cd_xHg_{1-x}Te$ photopumped heterostructure lasers

P8.5 A Rogalski, A Jozwikowska, K Jozwikowski and J Rutkowski
The performance of p^+-n $Hg_{1-x}Cd_xTe$ photodiodes

P8.6 Y S Wu, C R Becker, A Waag, R N Bicknell-Tassius and G Landwehr
Removal of Oxygen and Carbon contamination from (100) CdZnTe substrates

P8.7 Richard Sizman, Torbjorn Skauli, Thierry Colin, Kjersti Gjonnes and Stian Love
IR absorption and structural properties of HgCdTe quantum wells

P8.8 V V Zav'ialov and V F Radantsev
Magnetotunneling in Pb-p-HgCdTe Shottky barriers

P8.9 T I Deryabina and V F Radantsev
Stationary character of 2D states in inversion and accumulation layers on zero gap HgCdTe

P9.1 A V Germanenko, V V Kruzhaev, G M Minkov, E L Rumyantsev and O E Rut
Spin-polarized tunneling current in metal insulator gapless semiconductor structures in a magnetic field

P9.2 A B Fedortsov, Y V Churkin, A S Ivanov, K F Komarovskikh, D G Letenko and L E Vorobjev
Contactless local determination of the recombination parameters of NGS using laser interferometry

P9.3 J I L Hughes and H A MacKenzie
A new technique for the interpretation of photo-Hall measurements in NGS

P9.4 K H Herrmann and U Muller
Interband and intraband contributions to refractive index in NGS

P10.1 I I Zazavitsky, B N Matsonashvili and B T Trofimov
Photoconductivity spectrum and kinetics of $Pb_{1-x}Sn_xTe$/PbTe/BaF2 multiquantum well structures

P10.2 I A Chernick and S N Lykov
The resonant defect superconductivity in narrow gap A_4B_6 semiconductors

P10.3 E V Bogdanov
Sasaki effect in the narrow gap semiconductor $Bi_{1-x}Sb_x$ alloys

P10.4 A I Lebedev and I A Sluchinskaya
Ferroelectric phase transitions in quaternary lead tin chalcogenides

P10.5 B A Akimov and D R Khokhlov
Lead telluride-based photodetectors: a new approach

P10.6 D R Khokhlov, I I Ivanchik, A de Visser and A V Nikorich
Magnetic field-induced localization in $Pb_{1-x}S_xnTe(In)$

P10.7 C L Mitsas, E K Polychroniadis and D I Slapkas
Structural dependence of the optical absorption in $TiBiSe_2$ thin films near the fundamental absorption edge

P10.8 Jianren Xu, Bernard Halford and Maurus Tacke
The electrical characteristics of $Pb_{1-x}Eu_xSe$ homojunctions

P10.9 V G Kantser and N M Malkova
Two-dimensional electronic states on the interface of stressed piezoelectric semiconductors

P10.10 M Griesinger, H Bottner, S Kuhn, A Seifert and M Tacke
MBE of lead chalcogenides at increased residual gas pressures

P10.11 O A Mironov, A I Fedorenko, V V Zorchenko, A Yu Sipatov, O N Nashchekina, A A Konchits and I M Zaritskii
Dislocation superlattices based on lead and tin chalcogenides as models for high T_c superconductors

P10.12 V I Litvinov and M Oszwaldowski
Interface energy spectrum of real PbTe/SnPbTe heterojunction

P10.13 H A Kenawy, H A Zayed, A M Abo-Elsoud and A M Ibrahim
Effect of annealing on the electrical and structural properties of $Sb_{1-x}Se_x$ thin films

P11.1 Qian Dingrong
Element of a new infrared device - optical transistor

P11.2 M O Schweitzer, W T Yuen, T S Jones, C R McConville, N V Richardson and R A Stradling
Damage induced changes in the electronic properties of InSb(100): implications for surface preparation

P11.3 O M Bulashenko, A G Kollyukh, V K Malyutenko and B A Morozhenko
Anisotropy and polarization of hot electron intraband luminescence

P12.1 B A Akimov, A V Albul and E V Bogdanov
Low temperature switching in PbTe(Ga) at high electric fields

P12.2 V A Gorbyiev, I D Zalevski, V B Kulikov, A I Petrov, M V Chukichev and A E Yunovich
IR photoconductivity and luminescence of multiple quantum wells $GaAs/Ga_{1-x}Al_xAs$

1.1
Properties of Sn/Ge Superlattices

G. Abstreiter, J. Olajos, R. Schorer, P. Vogl and W. Wegscheider
Walter Schottky Institut, Technical University Munich
D-8046 Garching, Germany

Short-period strained-layer α-Sn/Ge superlattices can be synthesized by a low temperature molecular beam epitaxy technique which allows a large variation of substrate temperature. Thin, tetragonally distorted α-Sn layers are stabilized on Ge substrates by growth conditions far away from equilibrium. In the present contribution we discuss the following aspects:

- theory of bandstructure of short period Sn/Ge superlattices
- possibilities for the achievement of an intrinsically direct band gap with the Sn/Ge system
- optimization of growth conditions
- experimental characterization of Sn_1Ge_m and Sn_2Ge_m superlattices with transmission electron microscopy, x-ray diffraction and Raman spectroscopy
- determination of the fundamental band-gap of Sn_1Ge_m superlattices by photocurrent and absorption measurements

1.2

Structural Properties of Natural Superlattices

A. G. Norman[1], T-Y. Seong[2], I. T. Ferguson[1], G. R. Booker[2] and B. A. Joyce[1]

[1]IRC for Semiconductor Materials, Blackett Laboratory, Imperial College of Science, Technology and Medicine, Prince Consort Road, London SW7 2BZ, UK
[2]Department of Materials, University of Oxford, Parks Road, Oxford OX1 3PH, UK

ABSTRACT

The occurrence of phase separation in ternary and quaternary Group III-V semiconductor alloy epitaxial layers can lead to the formation of compositionally modulated microstructures, termed "natural superlattices"[1-3], whose physical properties resemble those of artificially grown superlattices. Monolayer natural superlattices may also be generated during epitaxial growth of these materials by a process of surface atomic ordering. Such natural superlattice structures are increasingly being found to occur in a wide range of ternary and quaternary Group III-V alloy semiconductor epitaxial layers grown by a variety of techniques such as molecular beam epitaxy (MBE) and metalorganic chemical vapour deposition (MOCVD). The occurrence of these natural superlattices can have a pronounced effect on the electrical and optical properties of the layers. In this paper we will present the results of recent structural studies of natural superlattice structures in epitaxial layers performed using transmission electron microscopy and diffraction. Particular attention will be given to the natural strained layer superlattice structures recently discovered in MBE $InAs_{1-x}Sb_x$ and $GaAs_{1-x}Sb_x$ layers grown at low temperatures[1-3] which arise from a process of surface phase separation, and the surface induced CuPt-type atomic ordering on {111} planes which is observed in (001) orientation epitaxial layers of many III-V alloys including both $InAs_{1-x}Sb_x$ and $GaAs_{1-x}Sb_x$. The current understanding of the formation mechanisms for these natural superlattices and the effects of their presence on the physical properties of the layers will also be discussed.

References

1. Seong T-Y., Norman A. G., Hutchison J. L., Ferguson I. T., Booker G. R., Stradling R. A. and Joyce B. A., Inst. Phys. Conf. Ser. No. 117 (1991) 485
2. Ferguson I. T., Norman A. G., Joyce B. A., Seong T-Y., Booker G. R., Thomas R. H., Phillips C. C. and Stradling R. A., Appl. Phys. Lett. 59 (1991) 3324
3. Ferguson I. T., Norman A. G., Seong T-Y., Thomas R. H., Phillips C. C., Zhang X. M., Stradling R. A., Joyce B. A. and Booker G. R., Inst. Phys. Conf. Ser. No. 120 (1992) 395

2.1

HIGH MAGNETIC FIELD STUDIES OF HgSe(Fe)

Michael von Ortenberg

Institut für Halbleiterphysik und Optik, Hochmagnetfeldanlage,
Technische Universität Braunschweig, D-3300 Braunschweig, F.R. Germany

In the ternary *semimagnetic* compound $Hg_{1-x}Fe_xSe$ some of the Hg-ions are statistically substituted by Fe-ions. The most interesting features of this material are related to the donor properties of the Fe-ion, whose energy level lies about 210 meV above the band edge degenerate with the quasi-free conduction-band states. For sufficiently large $x \geq 0.0003$ the Fermi energy gets pinned to the donor level. In this *mixed-valence regime* a multitude of interesting phenomena is observed: pronounced reduction of the microscopic scattering as effective in the mobility and Dingle temperature, fluctuations between delocalized and localized states giving rise to a *3-dimensional analogue of the Quantum-Hall Effect,* and spin-fluctuations. These effects are demonstrated in data of numerous experiments of magnetospectroscopy (transport, magnetization, IR- , and FIR-spectroscopy) in DC-magnetic fields up to 18 T and pulsed fields up to 100 T. The optical spectra are dominated by *a non-local* interaction between electromagnetic radiation and charge carriers. Different theoretical approaches ranging from an effective Wigner condensation over short-range correlation are discussed in relation to the experimental data. Due to the pronounced reduction of scattering HgSe(Fe) proves to be an ideal matrix to study the *semimagnetic* behaviour of different paramagnetic substitutes as in the quaternary compound $Hg_{1-x-y}Fe_xMn_ySe$. Special interest is dedicated to possible *Q2D* modifications of the compounds in hetero structures and super lattices.

2.2

THE BAND STRUCTURE OF MIXED CRYSTAL $Hg_{1-x}Fe_xSe$.

C. Skierbiszewski[1], Z. Wilamowski[2] and J. Kossut[2]

[1] High Pressure Research Center, Polish Academy of Sciences, Sokolowska 29/37, 01-142 Warsaw, Poland

[2] Institute of Physics, Polish Academy of Sciences, Al. Lotnikow 32/46, 02-668 Warsaw, Poland

In ternary semiconducting compounds $A_{1-x}B_xC$ positions of the conduction and valence band edges are normally functions of the mole fraction x. In particular, in zero-gap HgSe the energy gap (E_g) opens when a fraction of Hg atoms are substituted by, e.g., Cd or Mn.

Because mixed crystals $Hg_{1-x}Fe_xSe$ were obtained in a limited range of x ($x < 0.2$) it is difficult to study $E_g(x)$ relationship by traditional methods, e.g., by interband absorption. Furthermore high concentration of free carriers in these materials make optical measurements very difficult to interpret. For this reasons information concerning $E_g(x)$ in $Hg_{1-x}Fe_xSe$ is not completely clear. In this work we analyzed:

a) the dependence of electron concentration vs. x

b) the mobility, taking the spatial correlations of impurity charges and the chemical disorder scattering into account

c) the dependencies of these two quantities on hydrostatic pressure.

From this indirect analysis we conclude that :

a) the crossover from the zero-gap band to the open band-gap configuration takes place at $x = 0.08$

b) the extrapolated energy gap to hypothetical FeSe ($x = 1$) is 3.5 eV

c) the drop of the mobility as a function of x observed at low temperatures for $x > 0.002$ is due to chemical disorder (alloy scattering)

d) it is necessary to assume that the Fe - related impurity level broadens considerably as x is increased (d - band formation).

e) an additional broadening of the impurity level, if it exceeds the value of the Coulomb gap, necessarily leads to destruction of the spatial correlation in the system of ionized impurities.

2.3

SPIN RELAXATION IN SEMIMETALIC HgSe:Fe

Z. Wilamowski[1], W. Jantsch[2] and G. Hendorfer[2],

[1]*Institut of Physics PAS, Warsaw;* [2] *J. Kepler University, Linz.*

Narrow gap semiconductors offer the possibility to investigate in detail the role of conduction electrons in spin relaxation processes. In wide gap semiconductors the coupling of local magnetic moments to conduction electrons is usually too weak to govern the relaxation of the local magnetic moment. On the other hand, in the case of classical metals the influence of conduction electrons is too strong. As a consequence the EPR line in metals is very broad and cannot be investigated thoroughly. The most interesting concentration range of conduction electrons is achieved in narrow- and zero gap semiconductors. In those cases the sp-d coupling is strong enough to create the dominant mechanisms of spin relaxation and it is weak enough to allow investigation of the EPR line width. Moreover, in narrow gap semiconductors it is possible to change the electron concentration, which makes the investigations much more valuable.

HgSe:Fe is a peculiar case. In this material two different charge states of substitutional iron can coexist. Fe^{3+} ions are characterised by a very weak spin-lattice coupling and a long spin lattice relaxation time. In contrast, the spins of Fe^{2+} ions are strongly coupled to the lattice but because of the ground singlet state of the Fe^{2+} ion this coupling is effectively cut off at low temperatures. We deal thus with a set of three spin - subsystems (Fe^{3+}, Fe^{2+} and conduction electrons) where the couplings can be controled by changing the temperature and iron doping. A different doping level results in the concentration changes of each type of spins.

The analysis of the EPR line width of Fe^{3+} in HgSe reveals new spin relaxation mechanisms. Apart from the Korringa-like mechanism and dipole-dipole broadening the following mechanisms were observed:

1. Pseudo dipolar Fe^{3+}-Fe^{3+} coupling due to an anisotropic RKKY exchange. It leads to a very specific angular dependence of the line width at low temperatures.
2. The shortening of the spin relaxation time due to the capture and emission of an electron by the iron impurity. This process is activated by an energy originating from Coulomb potential fluctuations. The effect is observed as a decrease of the EPR line amplitude with increasing temperature.
3. Indirect, energetic relaxation of the Fe^{3+} spins. At sufficiently high Fe^{2+} concentrations, because of the RKKY coupling between Fe^{3+} and Fe^{2+} ions, the relaxation path: Fe^{3+} --> conducting electrons --> Fe^{2+} --> lattice becomes the most effective one.

One can conclude that EPR allows to investigate different types of coupling and the basic dynamic properties of a magnetic system in narrow gap semiconductors.

2.4

HYBRIDISATION-MEDIATED SPIN DEPENDENT p-d INTERACTION IN SEMIMAGNETIC SEMICONDUCTORS: EXPERIMENTAL PROOF

W.Szuszkiewicz[a)], C.Julien[b)], M.Balkanski[b)], B.Witkowska[c)]

a) Institute of Experimental Physics, Warsaw University
b) Laboratoire de Physique des Solides, Université Paris VI
c) Institute of Physics, Polish Academy of Sciences

For a zero-gap semiconductor the dominant part of the spin dependent exchange interaction between Γ_8 band electrons and paramagnetic ions comes from a strong p-d hybridisation. Recently it was demonstrated that the Heisenberg Hamiltonian is a good approximation of the p-d interaction for the Fe^{2+} ground state (^5E) resulting from the crystal field splitting. On the contrary, for the Fe^{2+} excited state ($^5T_2$) the non-Heisenberg terms have to be taken into account to describe this interaction [1], some energy broadening of this level can therefore be expected.

In order to verify this suggestion we analysed the Fe^{2+} crystal field optical transitions for HgSe doped with iron. Usually it is impossible to observe these transitions for such a system because they correspond to the spectral region of a high interband absorption coefficient. However, for highly doped n-type samples in the infrared a "transmission window" is always created. The low energy edge of this "window" is determined by the plasma edge, while the $\Gamma_8{}^v \rightarrow \Gamma_8{}^c$ transitions give the high energy "cut-off". It is posible to shift the "transmission window" into the spectral region of the expected Fe^{2+} crystal field transitions by simultaneously doping HgSe with Fe and Ga.

Transmission spectra have been measured for different HgSe samples containing 1×10^{19} cm^{-3} or 3×10^{19} cm^{-3} of gallium and from 3×10^{19} cm^{-3} up to 1.4×10^{20} cm^{-3} of iron. The obtained absorption spectra at helium temperature consist of two parts: a strong peak lying at (2423 ± 3) cm^{-1} (corresponding to the not splitted zero-phonon transitions) and a broad bump lying in the range 2540-2650 cm^{-1} (caused by the optical phonon-assisted transitions). The transmission spectra taken for CdTe:Fe samples with the same iron impurity concentrations (for which the broadening of the excited state $^5T_2$ could not be expected) demonstrated well separated zero-phonon transitions. From the comparison of the results the broadening of the $^5T_2$ excited Fe^{2+} state in HgSe:Fe resulting from the p-d hybridisation was estimated to be not higher than about 20-30 cm^{-1}.

[1] J.Blinowski, P.Kacman and H.Przybylińska, Solid State Commun. 79, 1021 (1991)

2.5

Iron doping: a tool to improve electrical properties of $Hg_{1-x}Zn_xSe$

W. Dobrowolski, E. Grodzicka, J. Kossut and B. Witkowska

Institute of Physics, Polish Academy of Sciences,
Al. Lotników 32/46, 02-668 Warszawa

It has been predicted theoretically [1] and later experimentally proved [2] that $Hg_{1-x}Zn_xSe$ alloy possesses potential advantages - compared to $Hg_{1-x}Cd_xTe$ or $Hg_{1-x}Cd_xSe$ - as a stable material for application in detection of electromagnetic radiation.

In the present paper we show that the electrical properties of $Hg_{1-x}Zn_xSe$ alloy can be greatly improved by means of doping with iron. In our study we investigated $Hg_{1-x}Zn_xSe$: Fe crystals grown by the Bridgman method in a composition range $0 \leq x \leq 0.14$, with iron doping up to $5 \cdot 10^{19}$ cm^{-3}. Transport properties (Hall effect and conductivity) were studied in a broad temperature range 3.5 K - 300 K. We show that, similarly to the case of HgSe:Fe [3], the iron in $Hg_{1-x}Zn_xSe$ acts as a *donor resonant* with the conduction band continuum. This property of Fe donors stabilizes the free electron concentration n (no passive annealing) and leads to sizable enhancement of the free electron mobility at temperatures at which the charged center scattering is a mobility limiting mechanism.

The energy of the resonant Fe level is determined from n vs. x dependence. Furthermore, this quantity together with previously determined energy gap vs. x relationship [4] provided an estimate of the conduction band offset in $Hg_{1-x}Zn_xSe$.

[1] A. Sher, A.-B. Chen, E.E. Spicer and C.K. Shih, *J. Vacuum Sci. Technol.* **A3**, 105 (1985)

[2] S.D. Cobb, R.N. Andrews, F.R. Szofran and S.L. Lehoczky, *J. Crystal Growth* **110**, 415 (1991)

[3] recent review : J. Kossut, W. Dobrowolski, Z. Wilamowski, T. Dietl and K. Świątek, *Semicond. Sci. Technol.* **5**, S141 (1990)

[4] N.P. Gavaleshko, W. Dobrowolski, M. Baj, L. Dmowski and T. Dietl, in *Proc. 3rd Int. Conf. Physics. of Narrow-Gap Semicond. Warszawa 1977* (Edited by J. Rauluszkiewicz, M. Górska and E. Kaczmarek), PWN - Polish Scientific Publishers, Warsaw and North Holland, Amsterdam, 1988 p. 331

2.6

HIGH-TEMPERATURE MAGNETIC FREEZING IN $(Cd_{1-x}Mn_x)_3As_2$

E. Lähderanta, R. Laiho, A.V. Lashkul, A. Mäkinen and V.S. Zakhvalinski[a]

Wihuri Physical Laboratory, University of Turku, 20500 Turku, Finland
[a]Institute of Applied Physics, Academy of Sciences of Moldova, 277028 Kishinev, Moldova

$(Cd_{1-x}Mn_x)_3As_2$, shortly CMA, is a semimagnetic n - type semiconductor with $E_g \sim -0.095$ eV (1). Single crystals of CMA with x = 0.04 and 0.10 were prepared by moving slowly a temperature gradient along an ampule containing the melted stoichiometric mixture of pure Cd_3As_2 and Mn_3As_2 (modified Bridgman method). The magnetic susceptibility of the grown crystals were investigated in a wide range of temperatures and magnetic fields by using a SQUID magnetometer.

Below a certain temperature T_f (~ 200 K for x = 0.10) results show a difference between values of $\chi_{dc}(T)$ measured for samples cooled in zero magnetic field (ZFC) and in a field (FC), respectively (see the figure). This difference grows with increasing Mn concentration. It can be seen only in relatively weak applied fields (H ≤ 300 Oe for x = 0.10). This is obviously the reason why the freezing of moments around 200 K was not observed in investigations (2,3) made in a field of several kilogauss. Our observations indicate that at T_f freezing of magnetic moments takes place in CMA with x ≥ 0.04. When the field is increased the difference of $\chi_{dc}(FC) - \chi_{dc}(ZFC)$ diminishes and the temperature dependence of χ_{dc} approaches the Curie-Weiss law with a large negative value of the Curie temperature.

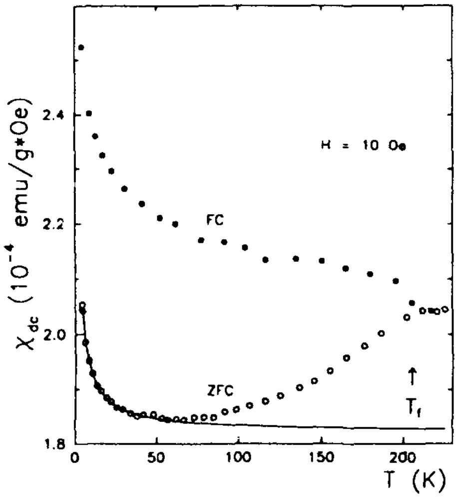

Temperature dependence of $\chi_{dc}(ZFC)$ and $\chi_{dc}(FC)$ for CMA with x = 0.10. The solid line is a fit of the Curie-Weiss law to the ZFC curve.

An interesting feature is that in addition to the freezing of magnetic moments at high temperatures, as discussed above, there is a low temperature spin glass transition in CMA at $T_{sg} \leq 5$ K (2,3). Before this work two consecutive spin glass like freezing phenomena were known to exist only in $(Zn_{1-x}Mn_x)_3As_2$ (4). We attribute these effects to formation of a complex system of magnetic clusters.

1. J.J. Neve et. al., J. Phys. C: Solid State Phys. **15**, 4795 (1982).
2. C.J.M. Denissen et. al., Phys. Rev. **B33**, 7637 (1986).
3. Z. Celinski and W. Zdanowicz, Acta Phys. Pol. **A69**, 1067 (1987).
4. E. Lähderanta et. al., Proc. Int. Conf. Magn., ICM-91, Edinburgh, Sept. 1991, J. Magn. Magn. Mater. (to be published).

3.1

Novel Magneto-Transport and Magneto-Optical Processes in Semimetallic HgTe-CdTe Superlattices

C. A. Hoffman, J. R. Meyer, and F. J. Bartoli
Code 6551, Naval Research Laboratory, Washington, DC 20375

Recent observations of novel electronic processes in semimetallic HgTe-CdTe superlattices will be reviewed, in the context of distinctive features in the superlattice band structures. It will be demonstrated that most of the observed phenomena are either directly or indirectly related to an anti-crossing of the HH1 band, which is nearly dispersionless in the growth direction k_z, and the E1 band, which has strong dispersion in k_z. For example, it has recently been demonstrated that there is a critical magnetic field B_{crit} above which one can magnetically activate a bipolar plasma whose density increases linearly with $B - B_{crit}$. Dramatic experimental confirmation of the effect is provided by low-temperature magneto-optical data showing the emergence of minority holes in an n-type superlattice whenever $B > B_{crit}$. Similarly, a rapid variation of the momentum relaxation time with energy gap, and hence k_z, leads to the observation of broad quantum Hall plateaus in superlattices with strong 3D dispersion. This contradicts the previous theoretical understanding of how dimensionality influences the quantum Hall effect, since it occurs even in structures for which the miniband width is comparable to or larger than the Landau level spacing. Other topics to be discussed include recent technological advances toward more sophisticated stuctures (e.g., controlled modulation doping, setback doping, and superlattice IR detector arrays), comprehensive new theoretical descriptions of magneto-transport and magneto-absorption in HgTe-CdTe superlattices, and novel processes predicted to occur in HgTe-CdTe quantum wires (giant subband splittings, quantized ballistic conductance per well in *fractional* units of e^2/h, magnetic closure of the energy gap, etc.)

3.2

Pressure Dependence of Infrared Photoluminescence Spectra from HgTe/HgCdTe Superlattices

H. M. Cheong, J. H. Burnett, W. Paul, and P. M. Young
Department of Physics and Division of Applied Sciences, Harvard University, Cambridge, Massachusetts 02138, USA
J. F. Schetzina
Department of Physics, North Carolina State University, Raleigh, North Carolina 27695, USA

We have investigated the pressure dependence of the band gap of HgTe/HgCdTe superlattices (SL's) using infrared photoluminescence (PL) spectroscopy at liquid nitrogen temperature up to 30 kbar. We observed several PL peaks with energies ranging from ~130 meV to ~700 meV. The most prominent peak at ~130 meV, which has been attributed to the recombination across the SL band gap, moves higher in energy with a pressure coefficient of ≤1 meV/kbar. Other peaks at higher energies, whose origins are not clear, have similar pressure coefficients of 0-2 meV/kbar. A calculation based on the envelope function approximation, assuming that the valence band-offset value is 350 meV and pressure independent, indicates that the SL band gap increases with pressure at a rate of ~6.5 meV/kbar near zero pressure, and this rate increases to ~8 meV/kbar at ~20kbar. Neither a small valence band offset value (~40 meV) nor varying input parameters changes this rate by more than 10%. The calculated pressure dependence of the SL band gap of≥6 meV is far outside the error bars of the measured pressure dependence of the main peak, ≤1 meV/kbar. Possible explanations, including a modification of the current model of HgTe/HgCdTe SL bands and reinterpretation of the PL peaks, will be examined.

3.3

Infrared Photoluminescence on molecular beam epitaxially grown $Hg_{1-x}Cd_xTe$-layers

M.M. Kraus, Y.S. Wu, C.R. Becker, G. Landwehr
Physikalisches Institut d. Universität Würzburg, D-8700 Würzburg

March 13, 1992

Abstract

$Hg_{1-x}Cd_xTe$ is an important material for infrared device technology. Despite a variety of investigations on molecular beam epitaxially (MBE) grown Hg-based superlattices and modulation doped structures, little attention has been paid to the study of the photoluminescence properties of the constituent materials.

We report here on the first systematic study of infrared photoluminescence on $Hg_{1-x}Cd_xTe$-layers grown by MBE. The Fourier transform photoluminescence of $Hg_{1-x}Cd_xTe$ layers with $0.25 < x < 0.80$ grown on (110) and (211) GaAs was investigated in the spectral range from 150 meV to 800 meV. Emission lines were observed with a full with at half maximum down to 16 meV.

Photoluminescence and transmission properties are compared over the temperature range from 4.2 K to 300 K. The possible influence of Burstein-Moss shift, impurity bands, and band tailing are discussed.

Photoluminescence at high temperatures originates from band to band transitions. However, low temperatures photoluminecence can be attributed both to impurity bands or additional states due to band tailing.

3.4

Observation of Magnetophonon Resonance Oscillations in Open-Gap $Hg_{1-x-y}Cd_xMn_yTe$ Grown by LPE

Kôki TAKITA, Shinji KURODA and Hyuk-Jin KWON

Institute of Materials Science, University of Tsukuba, Tsukuba, Ibaraki 305, JAPAN

$Hg_{1-x-y}Cd_xMn_yTe$ (HCMT) is a new quatenary Hg-based alloy, which has the characteristics both as a narrow-gap and a semimagnetic semiconductors. In this study HCMT crystals of positive energy gap ($E_g > 0$) have been successfully grown on CdTe substrates by the LPE method from Hg solution. The result of Hall measurements showed that the obtained crystals are n-type with carrier concentration $n = 10^{15} \sim 10^{17}\,\mathrm{cm^{-3}}$ and mobility $\mu_H = 10^4 \sim 10^5\,\mathrm{cm^2/V \cdot s}$.

Figure 1 illustrates a typical example of the transverse magnetoresistance ρ at various temperatures. In this figure, the second derivatives $-\partial^2\rho/\partial H^2$ are shown to enlarge minute changes in ρ. One can clearly discern oscillatory structures in this temperature range. These structures are interpreted as due to the magnetophonon resonance (MPR); the transition of electrons between conduction Landau levels with the emission of one LO-phonon. The resonance peak positions (indicated by arrows in the figure) shift towards the higher field with the increase of temperature T. The T-dependence of the observed peak positions is found to be much stronger than those predicted theoretically on the basis of the band calculation. The origin of this anomalous T-dependence will be discussed.

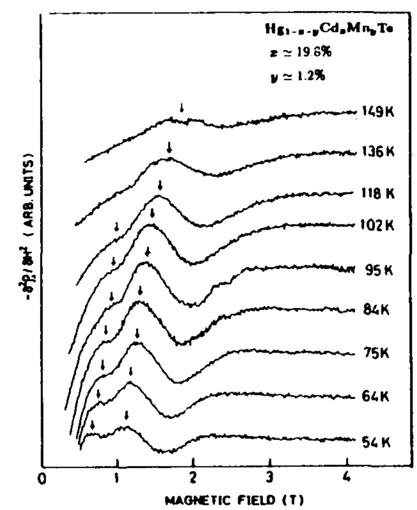

Figure 1 : A typical example of second derivatives of transverse magnetoresistance in $Hg_{1-x-y}Cd_xMn_yTe$ ($x \simeq 19.8\%$, $y \simeq 1.2\%$)

3.5

ELECTRICAL PROPERTIES OF THE ANODIC OXIDE-HgZnTe INTERFACE

I. Esquivias, J. Baars, and D. Brink
Fraunhofer-Institut für Angewandte Festkörperphysik,
Tullastr. 72, D-7800 Freiburg, Germany

D. Eger
Soreq Nuclear Research Center, Yavne 70600, Israel

The electrical properties of the passivating layer-semiconductor interface play a crucial role on device performance. $Hg_{1-x}Zn_xTe$ (MZT) is considered an alternative material to $Hg_{1-x}Cd_xTe$ (MCT) for infrared detectors. To the best of our knowledge, only Eger and Zigelman[1] have studied some properties of insulator layers on MZT. They reported, on the basis of Hall effect measurements, a lower tendency to form inversion layers in p-type MZT passivated with anodic oxide than in MCT. We present here results concerning the electrical properties of the anodic oxide-MZT interface, performed by Capacitance-Voltage (C-V) measurements of Metal-Insulator-Semiconductor (MIS) capacitors.

The MZT samples ($x = 0.167$, $E_g = 114$ meV at 77 K) were grown by LPE[2] and annealed in a Hg atmosphere. Hall effect measurements at variable temperature were performed, and a good fitting between theoretical and experimental curves was achieved by using empirical relations for the dependence of the energy gap and intrinsic carrier concentration with the temperature. An acceptor concentration of 1.6×10^{16} cm^{-3}, with an ionization energy of 8 meV, was determined.

The insulator of the MIS structures consited of 50 nm of conventional anodic oxide and 300 nm of ZnS. MCT samples, with similar energy gap and doping level at 77 K as those of MZT, were simultaneously processed for comparison. The experimental C-V curves were compared with theoretical curves, which were calculated taking into account the conduction band non-parabolicity and Fermi-Dirac statistics, and using the band structure parameters (hole effective mass and Kane matrix element, P_k) of MCT with similar gap. While a good theoretical-experimental fitting was achieved in the MCT samples, significant differences were found in the inversion region of the MZT devices. This was attributed to a different value of P_k in MZT than in MCT. The fixed insulator charge density, Q_{ss}, was lower in MZT than in MCT, but the semiconductor surface was still inverted at 0 V of gate bias.

The Q_{ss} of the MZT devices was found to increase after 10 hours of annealing at 100 °C, while a similar increase was found after only 1 hour in the MCT samples. This confirms the expected better stability of the MZT interfaces with respect to MCT interfaces.

References

1. D. Eger and A. Zigelman, Proc. SPIE, vol. **1484**, p. 48, 1991.
2. A. Sher, D. Eger, A. Zemel, H. Feldstein, and A. Raizman, J. Vac. Sci. Technol. **A4**, 2024, 1986.

3.6

[illegible] $Zn_xCd_yHg_{1-x-y}Te$ [illegible]

A.M.Andrukhiv, V.I.Ivanov-Omskii, A.M.Litvak,

K.E.Mironov, V.V.Ratnikov

A.F.Ioffe Physico-Technical Institute, St.Petersburg, 194021, Russia

A new modification of the LPE method is applied to growth of epitaxial $Zn_xCd_yHg_{1-x-y}Te$ layers with the energy gap 100-400 meV and their unique properties are demonstrated.

The temperature conditions of the process were established by the detailed experimental investigation of the Te rich compositions of the phase diagram by the method of direct visual observation . The model of completely associated solutions applied to this system gave an excellent coincidence of the theoretical and experimental results.

Layers grown on CdZnTe substrates have thickness 10-30 µm, smooth surface with the small steps not exceeding 0.1µm. Structural characteristics of the substrates and the layers were investigated by means of the x-ray topography, two- and three-crystal diffractometry and the positive effect of the isoperiodic substrates was demonstrated.

To obtain the low concentration of the carriers ($n,p=10^{14}-10^{16}cm^{-3}$) the annealing procedures have been developed. The lifetime of nonequilibrium charge carriers defined by the photoconductivity relaxation reaches 40 µs at 77K that proves the low concentration of the recombination centres as well as high structural perfection. Photoluminescence studies near helium temperatures demonstrated one impurity line in n-type material and three ones in p-type. The analysis shows that in the last case two lines are caused by mercury vacancies (singly and doubly ionised) while the third one has the same nature as in n-type material and is caused by the acceptor impurities. It was shown, that the temperature behavior of the band-to-band line could be explained by the contribution of excitons at temperatures low than 60K. Cyclotron resonance in n-type material was observed and effective masses of electrons were evaluated.

The observed effects confirm the high quality of epilayers from the point of view of purity, structure and homogenity.

4.1

Tunneling in Cross-Gap Systems

E. E. Mendez
IBM Research Division, T. J. Watson Research Center
Yorktown Heights, NY 10598, USA

The InAs-GaSb heterostructure constitutes the prototype of cross-gap systems, in which the bottom of the conduction band of the former is lower in energy than the top of the bottom band of the latter. Such an unusual band alignment provides novel properties to structures formed with those two semiconductors, as illustrated in the tunnelling current characteristics of an InAs quantum well cladded by GaSb electrodes, which involves the resonant transport of holes between the electrodes via electron states in the well.

This talk will review interband resonant tunneling in selected heterostructures based on InAs-GaSb (e.g., GaSb-AlSb-InAs-AlSb-GaSb), focusing on the effects of a magnetic field parallel to the tunneling current, that is, perpendicular to the materials interfaces. The unique combination of a large Landau-level separation in InAs (even for very moderate fields) and of a quasi-monoenergetic distribution of holes in the GaSb electrodes has made it possible to do magnetic-level spectroscopy from the current-voltage characteristics and to resolve spin-split states at high fields, from which magnetic-field-induced charge transfer between InAs and GaSb and oscillations of the Landé factor, g, as a function of magnetic field has been demonstrated.

4.2

Far Infrared $Ga_{1-x}In_xSb/InAs$ Superlattices

R.H. Miles, D.H. Chow, A.T. Hunter and J.N. Schulman

Hughes Research Laboratories, Malibu, California 90265

T.C. McGill

California Institute of Technology, Pasadena, California 91125

The type-II, broken gap band alignment between $Ga_{1-x}In_xSb$ and InAs results in long-wavelength infrared energy band gaps for superlattices composed of these materials. The calculated electronic band structure of $Ga_{1-x}In_xSb/InAs$ superlattices is qualitatively distinct from that of conventional LWIR materials such as $Hg_{1-x}Cd_xTe$, which is expected to result in superlattice IR detectors superior in operating temperature and/or detectivity to those based on Hg1-xCd_xTe alloys. Specifically, detectors based on $Ga_{1-x}In_xSb/InAs$ superlattices are ultimately expected to benefit from reduced noise, owing to a substantial reduction in tunnelling leakage currents and the suppression or elimination of intrinsic impact ionization processes.

We will present recent optical data which support these predictions and which illustrate the utility of these superlattices at wavelengths beyond those currently accessible to $Hg_{1-x}Cd_xTe$. In addition, we have extended tight binding calculations of the electronic band structure of these superlattices to describe the InSb- or GaInAs-like nature of the interfaces. We have previously demonstrated the capability to change the nature of our interface through the use of appropriate shutter sequencing and interrupts during MBE growth, and have observed dependencies of the energy gap on interfacial chemistry. Our calculations yield energy gaps and effective masses which are in good agreement with experiment, and suggest dependencies of absorption coefficients and transport processes on the nature of the interfaces. Recent results in the development of $Ga_{1-x}In_xSb/InAs$ superlattice detectors will also be presented.

4.3

The Effect of Interface Bond Type on the Structural and Optical Properties of MBE Grown GaSb/InAs Superlattices

J.R. Waterman, B.V. Shanabrook, R.J. Wagner,
M.J. Yang, J.L. Davis, and J.P. Omaggio
Naval Research Laboratory, Washington, DC 20375

The effect of interface bond configuration on the structural and optical properties of short period (50 Å) GaSb/InAs superlattices has been examined. Since early work in this material system, MBE growth techniques have advanced to allow control of the microscopic nature of the interface between the two constituents. In particular it has been recognized that in an AB/CD superlattice, it is possible to have interface bonds that are either "AD-like" or "CB-like". Structures consisting of 8 monolayers of GaSb and 7 monolayers of InAs with either "GaAs-like" or "InSb-like" interface bonds were grown by MBE on (100) GaAs with a 1 micron GaSb buffer layer. Interface bond type was established by precise control of the shutter opening and closing sequences at the interface. Growths were performed at 390 C to minimize interdiffusion. The number of monolayers of each constituent was determined in-situ using RHEED oscillations, and confirmed with ex-situ x-ray measurements.

X-ray diffraction measurements exhibiting up to 7 satellite lines revealed a marked difference in the average superlattice lattice constant for the two different interface bond type materials, with the "InSb-like" and the "GaAs-like" bonded samples having lattice constants of 6.103 and 5.993 Å respectively. This difference is in good agreement with that expected based on the difference between the bulk Ga-As and In-Sb bond lengths and elastic coefficients, assuming coherent strain. Good agreement between experimental diffraction peak positions and intensities and calculations using a kinematical x-ray scattering model taking into account the interface bonding differences has been achieved.

The high quality of the material is demonstrated by Raman scattering measurements which have revealed, for the first time in this material system, the presence of folded acoustic phonons as well as the previously observed modes characteristic of both "GaAs-like" and "InSb-like" interface bonds. The period determined from the position of the first folded phonon doublet is in excellent agreement with that determined from x-ray diffraction. The "InSb-like" mode is observed in both types of samples, while the "GaAs-like" mode was observed only in the "GaAs-like" interface sample. This is in contrast to previous results on MOCVD grown material where the "GaAs-like" mode dominated the spectra for both types of samples. The "InSb-like" mode was stronger in the sample intended to have that type of interface. This behavior is indicative of the high degree of structural perfection of these samples. The InAs TO phonon energy as determined from far-infrared transmission measurements was 217.7 cm^{-1}, indicating that the InAs layer is coherently strained.

Bandgaps determined from photoconductivity and interband magnetoabsorption measurements were in good agreement with one another, with the "GaAs-like" and "InSb-like" bonded samples having gaps of 0.288 and 0.250 eV respectively. The difference between the two is attributed to interface bonding effects. This effect will bc discussed in terms of band offsets and effective layer thicknesses.

4.4

Investigation of InAs/(In,Ga)Sb superlattices grown by molecular beam epitaxy on the [100] and [111] orientations

T.D. Golding, J.T. Zborowski, J.A. Dura, and A. Viliante
Department of Physics, University of Houston, Houston, Texas, 77204, USA

D. W. Donnelly and B.C. Covington
Department of Physics, Sam Houston State University, Huntsville, Texas, 77341, USA

E. MacDonald
Department of Physics and Astronomy, University of Cardiff, Cardiff, UK

We will present details of the growth characteristics, chemical, electrical, structural and optical properties of $InAs/In_xGa_{1-x}Sb$ ($0 \leq x \leq 0.4$) strained layer superlattices (SLS) grown by molecular beam epitaxy (MBE).

The $InAs/In_xGa_{1-x}Sb$ superlattice is type II, in which the conduction-band minimum of InAs is lower in energy than the valence band maximum of GaSb, resulting in a superlattice that can have a band gap smaller than that of either constituent material, and for sufficently thick periods the system can be metallic.

Our study has investigated growth of the $InAs/In_xGa_{1-x}Sb$ SLS on both the [100] and [111] growth orientations. Epitaxy has been characterized by *in situ* reflection high energy electron diffraction, interface chemistry and structure by x-ray photoelectron spectroscopy and x-ray reflectivity, and the structural properties of the SLS by x-ray diffraction. SLS with period thicknesses in the range 25Å-200Å have been characterized by temperature dependent Fourier transform infrared spectroscopy.

The talk will present comparative aspects of the growth, interface chemistry, structural properties and optical response of structures deposited on both the [111] and [100] orientations.

4.5

MAGNETO–OPTIC AND MAGNETO–TRANSPORT STUDY OF $InAs/Ga_{1-x}In_xSb$ SUPERLATTICES

J.P. Omaggio, R.J. Wagner, J.R. Meyer, C.A. Hoffman and M.J. Yang
Naval Research Lab, Washington, D.C. 20375

D.H. Chow and R.H. Miles
Hughes Research Laboratories, Malibu, California 90265

The band gap of $InAs/Ga_{1-x}In_xSb$ superlattices have been determined by interband magneto–optics and by magneto–transport measurements as a function of magnetic field and temperature. Superlattices with individual layer thicknesses of 24 to 41 Å and x values from 0.24 to 0.29 were grown on (100) GaAs substrates by molecular beam epitaxy (MBE). Interband magneto–optic measurements were taken using a Fourier transform infrared spectrometer with the sample in the Faraday orientation at 4.2 K with magnetic fields of 0 – 12 T. Optical transitions between the valence and conduction (sub–band), n = 0, 1, 2, and 3 Landau levels were observed. In this study, a Kane model with an applied magnetic field ($k^2 \rightarrow \frac{2eB}{\hbar}(n + \frac{1}{2})$) was used to fit the data and determine the band gap. Van der Pauw magneto–transport measurements were also performed and Hall and conductivity data were obtained for magnetic fields in the 0 – 7 T range for temperatures between 4.2 and 300 K. Electron and hole densities and mobilities were determined by performing a mixed conduction analysis of the field dependent data at each temperature. Band gaps determined by the two methods were in good agreement and ranged from 97 to 152 meV. These measured gaps were found to be in good agreement with gaps calculated using a two band (Bastard[1]) model.

The first measurements of carrier effective masses are also reported in this paper. Both electron and hole masses were measured by cyclotron resonance at 4.2 K. Measurements in both the Faraday and Voigt geometries with both n and p–type samples give the masses in both the planer and superlattice growth direction. Both electron and hole masses were found to be around 0.03 m_0 which is on the same order as predicted by Smith and Mailhiot[2]. Furthermore these masses agree with the reduced effective mass obtained from the interband magneto–optic data. The electron masses are a factor of 4 – 5 than in HgCdTe which is critical for the success of this material system. The larger mass is needed for reduced dark leakage currents (from tunneling) in photodiode IR detectors.

Finally, the electron and hole mobilities were determined from the magneto–transport measurements. At 150 K, electron mobilities from 3900 to 4700 cm^2/V–sec were observed and hole mobilities from 800 to 1800 cm^2/V–sec. The temperature dependence indicates that some mechanism other than phonon scattering is limiting mobility.

[1] G. Bastard, Phys. Rev. B, vol. 25, p. 7584 (1982).

[2] D. L. Smith and C. Mailhiot, J. Appl. Phys. vol. 62, p. 2545 (1987).

4.6

Investigation of Sb/GaSb multilayer structures for potential application as a narrow bandgap system

T.D. Golding, J.A. Dura, H. Wang, J.T. Zborowski, A. Viliante, and J.H. Miller, Jr.
Department of Physics, University of Houston, Houston, Texas, 77204, U.S.A.

We will present results of an investigation into the molecular beam epitaxial growth of Sb/GaSb heterojunctions and multilayer structures. The motivation of this study is to utilize spacial quantization effects in the Sb layers to induce a positive valence-conduction band energy gap in the Sb semimetal layers.

The GaSb/Sb system has a number of advantageous features relevant to synthesis of an epitaxial semimetal/semiconductor system. Sb has an rhombohedral structure and is closely lattice matched to GaSb ($\Delta a/a = 0.012$ at 273K). Because the biatomic planar structure of Sb mimics the (111) plane in the zincblende structure registry between the zincblende and rhombohedral lattice is preserved if epitaxy is performed along the [111] directions.

Our studies have shown that Sb can be grown epitaxially on GaSb(111) oriented epilayers at growth temperatures $T_s < 300°C$. Subsequent nucleation and epitaxy of GaSb on Sb epilayers is performed using migration enhanced epitaxy.

We will present details of the growth of the Sb/GaSb multilayer structures and characterization of the resulting epilayers and multilayers. Epitaxy has been characterized by *in situ* reflection high energy electron diffraction and x-ray photoelectron spectroscopy, and the structural properties of the resultant epilayers and multilayers by x-ray diffraction and Rutherford back scattering. The talk will also present results of the optical and electrical characterization of the multilayered structures, with specific regard to evaluation of quantization effects in the semimetal layers.

4.7

Optical Analysis of InAs Heterostructures Grown by Migration Enhanced Epitaxy

M.Inoue , H.Furuse , N.Nasu , M.Yano and Y.Iwai

New Material Research Center, Osaka Institute of Technology
Asahi-ku Ohmiya , Osaka 535 , Japan
Fax # 81-6-957-2133

InAs heterostructures have offered promising new device applications due both to the high speed electron transport and to the unique band alignment on type II staggard and broken-gap systems.[1,2] The heterostructures, InAs/GaSb or AlSb are also very interesting system from the fundamental point of view, arising from the combination of no common anion and cation. Since the different types of interface bonding are available , fine control of MBE growth of the heterointerface is very important to make well defined quantum well structures.[3]

We report here the optical analysis of InAs/GaSb and InAs/Al(Ga)Sb grown by MBE and migration enhanced epitaxy (MEE) to control the atomic bonding at the interface.The Raman spectra measured on the different types of heterointerface have shown the beautiful set of interface phonons as well as zone-folded LA phonon modes. The characteristic phonon spectra observed from the atomically-controlled structures will be discussed in conjunction with the MEE growth operation.

We also report photoluminescence (PL) spectra from InAs ultrathin quantum well structures to study electronic states and carrier distributions in the type II band allignment. The external applied electric fields have induced interesting Stark shift of PL spectra showing the blue shift which can be interpreted from the modulation of electron and hole distributions in the InAs type II heterostructures.

1) K.Yoh,T.Moriuchi and M.Inoue,IEEE Electron Device Lett. 11 (1990) 526.
2) M.Inoue,R.Sakamoto,K.Yoh,T.Kohno and T.Kamiyosi,Proc. IEEE/Cornell Conf on Advanced Concepts in High Speed Semiconductor Devices and Circuits (1991) 403.
3) Y.Iwai,M.Yano,R.Hagiwara and M.Inoue,Surface Science,in Press.

5.1

MESOSCOPIC PHENOMENA IN DILUTED MAGNETIC SEMICONDUCTORS

Tomasz Dietl

Institute of Physics, Polish Academy of Sciences,
Al. Lotników 32/46, PL-02 668 Warszawa, Poland

Mesoscopic phenomena in microstructures that incorporate narrow-gap diluted magnetic semiconductors exhibit a number of novel aspects which originate from strong spin-orbit couplings and impurity spin interactions.

In the first part of this lecture we shall discuss the influence of the spin couplings upon symmetry of the random-matrix ensembles, and the corresponding influence upon quantum interference effects such as quantum localisation, universal conductance fluctuations, and low-frequency noise.[1,2] Particular attention will be paid to the spin-generated noise in spin-glasses, which may constitute a valuable tool to probe glassy dynamics.[2]

In the second part of the lecture, millikelvin transport measurements carried out for microstructures of HgCdMnTe bicrystals[3,4] and PbMnTe epilayers[4] will be described. In those experiments a temperature dependence of the amplitude of the universal conductance fluctuations and of the mean magneto-conductance provided interesting information on the dominant phase- breaking mechanisms and the relevant spin-orbit couplings.

1. B. L. Altshuler and B. I. Shklovskii, *Zh. Eksp. Teor. Fiz.* **91**, 220 (1986); A. D. Stone, Phys. Rev. B 39, 10736 (1989), and references therein.
2. S. Feng, A. J. Bray, P. A. Lee, and M. A. Moore, *Phys. Rev B* **36**, 5624 (1987); M. Cieplak, B. R. Bułka, and T. Dietl, *Phys. Rev B* **44**, 12337 (1991), and references therein.
3. G. Grabecki, A. Lenard, W. Plesiewicz, J. Jaroszyński, M. Cieplak, T. Skośkiewicz, T. Dietl, E. Kamińska, A. Piotrowska, and B. Bułka, *Acta Phys. Polon.* **80**, 307 (1991).
4. G. Grabecki, J. Jaroszyński, A. Lenard, W. Plesiewicz, T. Skośkiewicz, T. Dietl, E. Kamińska, A. Piotrowska, G. Springholz, and G. Bauer, unpublished.

5.2

EXCHANGE INTERACTION IN SEMIMAGNETIC IV-VI MULTI QUANTUM WELL STRUCTURES

F.Geist[1], H.Pascher[1], N.Frank[2], G.Bauer[2], M.Kriechbaum[3]

[1]Phys. Inst. Universität, D-8580 Bayreuth, Germany
[2]Semicond. Physics Group, Universität, A-4040 Linz. Austria
[3]Inst. f. Theoret. Physik, Universität, A-8010 Graz, Austria

Diluted magnetic IV-VI semiconductors like PbMnTe or PbMnSe exhibit a strong dependence of the effective g-factors of the free carriers on temperature and magnetic field. This modification of the spin splittings with respect to the diamagnetic host materials is caused by an exchange interaction between the free carriers and the magnetic moments of the paramagnetic ions. In quantum wells (QW's) or superlattices (SL's) the strength of the exchange interaction depends on the probability to find the carriers within the diluted magnetic component. Thus an analysis of the observed spin splittings yields information on the types of SL's and on the band offsets.

Detailed informations on the bandstructures of SL's and MQW's of PbSe/PbMnSe, the tellurides and the related Eu- compounds are achieved for different concentrations of the magnetic ions and different widths of the quantum wells by photoluminescence, interbandabsorption and by coherent anti Stokes Raman scattering (CARS) using CO_2 lasers. Particularly CARS yields very precise data on the spin splittings of carriers confined in the quantum wells. In type I' MQW's the interband transitions which are direct in real space yield complementary informations.

Data are analyzed in the framework of an envelope function formalism [1] including the effects of the exchange interaction in a molecular field approximation for applied magnetic fields parallel and perpendicular to the layers, respectively using position dependent material parameters [2]. Mainly the band edge energies are varying and the exchange interaction vanishes in the diamagnetic layers. Published material parameters for both constituents are used [3] and not fitted to the experiments reported here.

The g-factors, especially as a function of temperature, obtained by CARS at high magnetic fields where the magnetic length is small compared to the layer width are decisive for the distinction between type I and I' band alignment. At low fields, where considerable penetration of the wavefunctions into the barriers occurs, a precise determination of the band offsets is possible. The analysis of CARS data from various PbMnSe/PbSe QW structures yields a type I' alignment with electrons confined in the PbMnSe layers and holes in the PbSe layers.

[1] M.Kriechbaum,P.Kocevar,H.Pascher,G.Bauer, IEEE J.Quant.El.24,1727,(1988)
[2] H.Pascher,P.Röthlein,M.Kriechbaum,N.Frank,G.Bauer, Superlattices and Microstructures 8, 69, (1990)
[3] G.Bauer,H.Pascher in Semimagnetic Semiconductors and Diluted Magnetic Semiconductors, p.209, ed. M.Averous, M.Balkanski, Plenum Press (1991)

5.3

Electron spin resonance study of the narrow-gap semiconductor PbSnMnTe.

T. Story*, P.J.T. Eggenkamp, C.H.W. Swüste, H.J.M. Swagten, and W.J.M. de Jonge.
Department of Physics, Eindhoven University of Technology (E.U.T.), P.O. Box 513, NL-5600 MB Eindhoven.

It has been shown that in the narrow-gap semiconductor $Pb_{1-y}Sn_yTe$, in which a small amount of Mn is dissolved, the magnetic properties strongly depend on the concentration of holes [1]. It was found that a critical carrier concentration $p_c = 3 \times 10^{20}\ cm^{-3}$ exists, above which a low temperature ferromagnetic phase was observed. Below this carrier concentration no magnetic ordering was found for temperatures higher than 1K. This phenomenon has been explained in terms of the band structure of the host material, in combination with the RKKY interaction, which is dominant in these compounds [2].
We have studied the same regime of carrier concentrations with electron spin resonance. Our samples had compositions of $0.005 \leq x \leq 0.06$, $0.12 \leq y \leq 0.72$ and carrier concentrations ranging from $p = 1.6 \times 10^{19}$ to 1.4×10^{21} cm^{-3}. Electron spin resonance lines were observed in the temperature range $T = 1.3 - 100$K. It was found that for samples with a carrier concentration higher than p_c the width of the ESR line increases fast with increasing temperature ($T > \Theta$, the Curie-Weiss temperature obtained from susceptibility measurements), while the resonance field does not change within the experimental accuracy. If $p < p_c$ neither the linewidth nor the position of the line changed with temperature at temperatures higher than the Curie-Weiss temperature. At low temperatures, the lines become wider in both cases. However, for $p < p_c$ the resonance field shifts down at low temperatures, while for $p > p_c$ an anisotropic behaviour is found.
We will interpret these results in terms of the model mentioned above in combination with the Korringa relaxation process ($T > \Theta$), and the exchange narrowing process ($T < \Theta$). The results will be compared with other existing data for various Mn and carrier concentrations. The role of the electron bottleneck will be discussed.

* now at Institute of Physics, Polish Academy of Sciences, Al. Lotników 32/46, PL-02-668 Warsaw.

[1] T. Story, R.R. Gałązka, R.B. Frankel, and P.A. Wolff, Phys. Rev. Lett. **56**, 777 (1986).

[2] H.J.M. Swagten, W.J.M. de Jonge, R.R. Gałązka, P. Warmenbol, and J.T. Devreese, Phys. Rev. B **37**, 9907 (1988).

5.4

Carrier-induced magnetic properties in small-gap semiconductors.

P.J.T. Eggenkamp[a], T. Story[b], H.J.M. Swagten[a], C.W.H.M. Vennix[c], M.M.H. Willekens[a], and W.J.M. de Jonge[a].

[a] Department of Physics, Eindhoven University of Technology (E.U.T.), PO. Box 513, NL-5600 MB Eindhoven.

[b] Institute of Physics, Polish Academy of Sciences, Al. Lotników 32/46, PL-02-668 Warsaw.

[c] Netherlands Energy Research Foundation ECN, PO. box 1, NL-1755 ZG Petten.

In IV-VI group narrow-gap semiconductors randomly diluted with Mn, the magnetic properties are closely related to the number of (p-type) carriers. It has been shown [1] that an increase of the carrier concentration beyond 3×10^{20} cm^{-3} transforms (Pb)SnMnTe from a paramagnet to a ferromagnet at helium temperatures, the so-called carrier-induced ferromagnetism. This phenomenon could be explained by an RKKY polarisation of carriers, provided that both L and Σ valence bands are taken into account [2]. Very recently, we have shown [3] that in $Sn_{0.97}Mn_{0.03}Te$ the ferromagnetic state collapses for p rougly larger than 10^{21} cm^{-3}, in favour of a spin glass like state. It was pointed out that the (p dependent) oscillatory nature of the RKKY interaction should be responsible for this.
We will present new experimental facts on the latter phenomenon by means of ac susceptibility, magnetisation and specific heat, for temperatures between 100 mK and 50 K and various magnetic fields. The character of the spin glass like state will be analysed and compared with canonical spin glasses, such as Cu(Mn), with special emphasis on the dynamics of the spin system, which is reflected by the frequency dependence of the ac susceptibility.
Furthermore, we will try to explore the rather complicated x, p, T magnetic phase diagram in some detail. It will be pointed out that some sections of the diagram will yield an additional magnetic phase, which might be associated with a so-called re-entrant spin glass. A calculation will be presented based on the Mean Random Field model, which, in analogy with the model of Sherrington and Kirkpatrick, provides a convenient tool to predict the transition between the ferromagnetic and spin glass state. The agreement between the calculations and the experimental data existing so far is satisfactory. This subscribes that the RKKY mechanism is dominating the carrier-induced transitions in the narrow-gap Sn(Mn)Te.

[1] T. Story, R.R. Gałązka, R.B. Frankel, and P.A. Wolff, Phys. Rev. Lett. **56**, 777 (1986).

[2] H.J.M. Swagten, W.J.M. de Jonge, R.R. Gałązka, P. Warmenbol, and J.T. Devreese, Phys. Rev. B **37**, 9907 (1988).

[3] W.J.M. de Jonge, T. Story, H.J.M. Swagten, and P.J.T. Eggenkamp, Europhys. Lett. **17**, 631 (1992).

5.5

Free carriers magnetoabsorption in HgZnTe-CdTe and HgTe-CdTe superlattices.

J.Manassès, Y.Guldner, J.P.Vieren
Laboratoire de Physique de la Matière Condensée de l'Ecole Normale Supérieure,
24, rue Lhomond, 75231 Paris cedex 05, France.
J.P.Faurie
University of Illinois, Chicago, Illinois 60680, USA.

We report transport and far infrared magnetooptical properties of n-type $Hg_{1-x}Zn_xTe$-CdTe ($x < 0.1$) and HgTe-CdTe superlattices. These heterostructures, grown by molecular beam epitaxy, usually present very high electron mobilities.

Hall and conductivity data obtained over a broad temperature range (1.5 - 300K) show that these superlattices are semimetallic or narrow-band-gap semiconductors at low temperature, while they are degenerate intrinsic semiconductors for T > 100K. This constitutes a new interesting situation in semiconductor-superlattice physics, clearly different from that previously reported in p-type HgTe-CdTe superlattices where the bands were not degenerate in the intrinsic regime. The analysis of the data gives the Fermi energy and the band-gap as a function of temperature, in excellent agreement with the calculated band structure using a multiband envelope function formalism and a valence band offset of 360meV.

Far infrared magnetotransmission experiments are reported in the temperature range 1.5 - 300K with the magnetic field **B** applied both parallel and perpendicular to the superlattice growth axis. We show that the semimetallic nature of the heterostructures is characterized by a strong anisotropy of the cyclotron mass. For **B** parallel to the growth axis, the observed magneto-optical transitions are in very satisfactory agreement with the calculated Landau levels and the Fermi energy in the whole temperature range. For **B** perpendicular to the growth axis, a significant drop is observed for several samples in the curve giving the cyclotron mass as a function of the temperature. This drop is associated with the important variation of the conduction-band anisotropy occuring when a superlattice undergoes a semimetal-semiconductor transition. The variation of the cyclotron mass and the temperature of the semimetal-semiconductor transition are found to be in reasonable agreement with the band structure calculations. Finally, the plasma frequency and the influence of the magnetoplasma effects are discussed.

6.1

DOPING STUDIES IN MOVPE OF $Cd_xHg_{1-x}Te$

C.D.Maxey, I.Gale, J.B.Clegg and P.A.C.Whiffin

Philips Research Laboratories, Redhill, Surrey, U.K.

ABSTRACT

In two recent review papers on MOVPE growth of cadmium mercury telluride (CMT) particular emphasis was made to the crucial importance of doping studies to the realization of future device structures. If the full potential of MOVPE growth of CMT is to be realised then full extrinsic doping of heterostructures is required. If the doping and composition junctions can be grown with the correct degree of grading then this will create the potential for the production of device structures leading to either improved performance and/or increased operating temperatures. This paper will review published doping studies and also present some recent results on both acceptor and donor doping studies carried out at the author's laboratory. In these studies IMP growth of CMT has been performed at $\approx$360°C using di-methyl cadmium (DMC) and di-iso propyl tellurium (DIPT) as the MO-precursors while the Hg overpressure was provided by a heated elemental source. Alternative acceptor doping sources to arsine have been investigated including phosphine, tri-phenyl arsenic and phenyl arsenic of which the latter appears to be most suitable. Iodine has continued to show the donor dopant potential in CMT it exhibited with higher temperature ($\approx$400°C) MOVPE growth using di-ethyl tellurium. Characterization of fully doped structures will be described.

6.2

CdTe/CdHgTe INTERDIFFUSED QUANTUM WELLS

A. LUSSON, R. DRUILHE, Y. MARFAING and E. RZEPKA
Laboratoire de Physique des Solides de Bellevue
CNRS, 1 Place A. Briand F-92195 Meudon Cedex, France

The $Cd_xHg_{1-x}Te$ solid solution is characterized by large interdiffusion coefficients of cadmium and mercury. This property is at the basis of the preparation of homogeneous alloys by interdiffusion of MOCVD-grown CdTe and HgTe elemental layers (IMP process). We have extended this method to the preparation of CdHgTe quantum wells confined between CdTe barriers.

The principle of the technique is to grow a CdTe/HgTe/CdTe structure and to control the interdiffusion process occuring during the growth and post-growth periods in order to get a narrow CdHgTe region at the centre of the structure. The result is a graded potential well. The profile of the well depends on the thickness of the HgTe initial layer and on the thermal cycle. The exact shape of this profile has been modelled for different growth parameters using a numerical simulation of the interdiffusion which takes into account the composition dependence of the interdiffusion coefficient.

CdTe/CdHgTe interdiffused structures were grown by MOCVD at 365°C using diisopropyltellurium, dimethylcadmium and metallic mercury as the material sources. Photoluminescence experiments were used to determine the alloy composition near the bottom of the well, which is compared with the predictions of the theoretical model. The energy gaps of the different wells prepared by interdiffusion are in the range of 1 to 1.6 eV. The confinement energy is weak in those structures grown at 365°C due to composition spreading. A larger confinement energy is expected for structures prepared at lower temperatures.

6.3

THE MOVPE GROWTH AND CHARACTERISATION OF $Hg_{1-x}Mn_xTe$.

M.Funaki, J.E.Lewis*, T.D.Hallam, Li Chaorong, S.K.Halder, K.Durose, A.W.Brinkman, B.K.Tanner.

Dept. of Physics, University of Durham, South Rd., Durham, DH1 3LE, U.K.

The replacement of some fraction of the cations in HgTe by the paramagnetic ion, Mn, results in the dilute magnetic semiconductor, $Hg_{1-x}Mn_xTe$ (MMT). In contrast to its Cd counterpart, a band inversion occurs in MMT at x ~ 0.07 giving this material both semiconducting and semimetallic properties and is therefore a promising material for infrared applications.

Following our earlier demonstration of the direct alloy growth (DAG) of MMT by MOVPE, this paper presents a detailed study of the influence of growth conditions and substrate type on the quality of MMT epilayers. Growth was carried out in the range 350-410°C using the precursors DIPTe, tricarbonyl(methycyclopentadienyl)manganese (TCMn), and elemental Hg, on a range of substrates including GaAs (001), (CdZn)Te (111)B, (211)B and (001), usually on a 1 μm CdTe buffer.

Mn concentration was measured by calibrated EDAX, DCXRD, and the position of the optical reflectance peaks in the visible. It has been possible to follow the evolution of the optical transition $\Lambda_{4,5v}-\Lambda_{6c}$ (the E_1 peak) with increasing Mn concentration ($0<x<0.5$), even though it broadens considerably for the higher concentrations. Mn concentration was found to be strongly affected by the growth temperature via the pyrolysis rate of TCMn and the Hg vapour pressure over the growing layer. Mn concentration increased with susceptor temperature until at 410 °C virtually no Hg was detected.

Crystallinity of the layers was checked by RHEED and DCXRD and growth was epitaxial for T < 380 °C but polycrystalline at the higher temperatures. The morphology and crystallinity of layers grown at 380 °C on different substrates was compared. MMT on GaAs (100) shows a mildly faceted background with large rectangular hillocks superposed. Layers grown on (CdZn)Te (100) were very similar to MCT layers, and those on CZT (211)B showed strong faceting. Those grown on CZT (111)B have completely smooth surfaces.
The results of DCXRD investigations of the structural properties of the layers will be presented, together with optical absorption studies of the layers in the near infrared and measurements (Hall constant and electrical conductivity) made in the temperature range 4 -400 K.

* Permanent address: Dept. Physics, SUNY, Plattsburgh, NY 12901, USA.

6.4

Properties of HgCdTe layers grown by isothermal vapor phase epitaxy at high pressures

P. Mitra, T. R. Schimert, F. C. Case and L. T. Claiborne
LTV Aerospace and Defense Co., Missiles Division, Research Department, P. O. Box 650003, Dallas, TX 75265-0003

H. L. Wilson
CECOM Center for Night Vision & Electro-optics, Fort Belvoir, VA 22060-5677

Isothermal vapor phase epitaxy of $Hg_{1-x}Cd_xTe$ (MCT) has been known for over two decades to yield high quality epitaxial films with extremely smooth surfaces. One disadvantage, however, has been the graded alloy composition of the films which limit their applicability in many IR detector device structures. The graded composition is especially severe when the grown MCT layers are thin i.e. 10 microns or less. In this paper we report a modified approach for the growth and anneal of MCT done under high pressure of hydrogen. This process performed in an internally heated pressure vessel is straightforward to implement, relatively inexpensive and has the potential to be a manufacturable method. Furthermore, by controlling the hydrogen pressure in the 700 - 1200 psi range during an anneal at 350 - 500C the gradient in the MCT alloy composition can be controlled and reduced. Using this approach we have grown MCT layers on (111)B CdTe and CdZnTe for LWIR applications with uniformity in thickness within 1.5% (largest difference from the mean thickness) over 6 cm^2 area. Compositional uniformity measured in terms of cutoff wavelengths by FTIR are within 0.1 micron measured for 7.3 micron cutoff at 300K over the same area. For undoped n-type LWIR layers mobilities in the range of $7\text{-}10 \times 10^4$ cm^2/volt.sec and carrier concentrations of $5\text{-}10 \times 10^{14}$ cm^{-3} at 80K have been obtained. Minority carrier lifetimes on these layers have been found to be as high as 1000 nsec at 80K and 1500 nsec at 150K and exhibit characteristic Shockley-Read recombination behavior for MCT layers with low dislocation densities. Long wavelength photoconductive detectors fabricated on these layers have yielded detectivity value D^* of 1.3×10^{10} $cmHz^{1/2}W^{-1}$ measured at a wavelength of 10 micron at 80K. These properties demonstrate the suitability of the high pressure isothermal vapor phase epitaxy process for the growth of MCT layers for LWIR focal plane arrays.

6.5

Techniques for Improving the Properties of Liquid Phase Epitaxial (CdHg)Te for IR Photodiodes

M G Astles, N Shaw and G Blackmore
DRA Electronics Division, RSRE Malvern, St Andrews Road,
Malvern, Worcs WR14 3PS, UK

Abstract

Liquid-phase epitaxy (LPE) is currently the most widely-used thin-film growth technique for (CdHg)Te for the current generation of IR photodiode arrays. Such devices place high demands on the control of alloy composition and electrical properties of the epitaxial layers. This paper will describe the developments in LPE technology at RSRE which have produced dramatic improvements in key material parameters. The following areas will be highlighted:

(i) reductions in background impurities following a systematic study of the sources of impurities in the LPE layers, leading to improved techniques for solution charge preparation, LPE boat purification and epitaxial layer annealing. Typical n-type background electrical properties after Hg-rich isothermal annealing are $n_{77} = 6 \times 10^{13}$ - $1 \times 10^{14} cm^{-3}$, $\mu_{77} = 2.2\text{-}2.4 \times 10^5 cm^2V^{-1}s^{-1}$.

(ii) The use of donor and acceptor impurity doping to provide n- and p-type carrier concentration control in the range 10^{14} to $10^{18} cm^{-3}$. Particular emphasis will be placed on the problems of obtaining controllable acceptor doping in Te-rich LPE.

(iii) the design of a novel graphite sliding boat system which provides Hg overpressure control using powdered HgTe within the graphite slider and which gives extremely reproducible composition ($\Delta x \pm 0.002$, $\Delta\lambda$ $\pm 0.15\mu m$) and thickness (Δt $\pm 1.5\mu m$ at $t=20\mu m$).

The potential of this technology for the growth of fully doped LPE structures will also be discussed and the various materials assessment techniques used (Hall effect, annealing, SIMS, IR transmission) will be fully described.

6.6

Optimized Molecular Beam Epitaxially Growth of (100) HgCdTe on CdZnTe

L. He,* C.R. Becker, R.N. Bicknell-Tassius, S. Scholl and G. Landwehr
Physikalisches Institut der Universität Würzburg
D-8700 Würzburg, Federal Republic of Germany

Molecular Beam Epitaxially (MBE) growth of both high quality intrinsic and extrinsically doped narrow gap $Hg_{1-x}Cd_xTe$ with an x of 0.20-0.22 are important issues in long wavelength detector engineering. They are closely correlated and are very complicated for narrow gap semiconductors in particular. Extrinsic doping techniques and an understanding of the doping mechanism involved can be established only after the growth parameters for intrinsic material with high structural quality and good electrical properties have been determined. In this paper, we present results of a systematic investigation of MBE growth conditions, e.g. the effects of Hg flux on pyramidal hillock density for the (100) orientation and on electrical properties. With an understanding of the necessary growth conditions for intrinsic material, we have been able to achieve p-type As-doping using an atomic sheet doping technique for the first time.

A series of samples with x values between 0.202 and 0.210 were grown at 180°C with Hg/Te flux ratios from 180 to 550. As doping was achieved by interrupting the HgCdTe growth, establishing a cation stabilized surface condition with a Cd source, depositing a fraction of an As monolayer, and then resuming the HgCdTe growth.

Pyramidal hillocks were generated during the first stage of the epitaxy growth whose density has a minimum at a Hg/Te flux ratio of about 280. All samples are n-type. Electron mobility is very sensitive to the Hg/Te flux ratio, reaching a maximum value at a Hg/Te ratio between 270 and 320. This dependence correlates well with hillock observations. The electron concentrations at both higher and lower Hg/Te flux ratios were very high and the effects of Te antisites and Hg interstitials were clearly observed for these two cases. The best result was obtained with a Hg/Te ratio of 280 where the electron concentration was $3.9 \times 10^{14} cm^{-3}$ and the mobility $2.8 \cdot 10^5 cm^2/Vs$ at 1.6 K for x=0.21. Highly doped p type HgCdTe was obtained using an atomic sheet doping technique. The doping sheet density was $6.7 \times 10^{12} cm^{-2}$, or in other words 3% of the Te sites were occupied by As. This result is very encouraging not only because it further conforms the electrical quality of our nondoped n type materials, but also because it provides a new alternative method to both understand the doping mechanism and achieve p type doped materials.

*Permanent Address: Institute of Technical Physics, Chinese Academy of Sciences, Shanghai, People's Republic of China

7.1

InAs Monolayers and Quantum Dots in a Crystalline GaAs Matrix

Klaus H. Ploog* and Oliver Brandt

Max-Planck-Institut für Festkörperforschung
W-7000 Stuttgart 80, Germany

We have developed a new approach to fabricate coherent InAs insertions in a crystalline GaAs matrix by conventional elemental-source molecular beam epitaxy (MBE). The 7 % lattice mismatch between InAs and GaAs requires specific strategies to individually control the InAs/GaAs and GaAs/InAs interface formation which is governed by a unique balance of surface and interface energy as well as kinetic processes. The key parameters during growth are a sequence of growth interruptions and of modulations of the substrate temperature during interface buildup. In particular the temperature modulation results in a complete flash-off of the In floating layer created by surface segregation of the deposited InAs, prior to GaAs overgrowth. The interfaces of the strained InAs insertions are then in registry with the surrounding GaAs matrix and hence free of defects, as determined by high-resolution x-ray diffraction and transmission electron microscopy.

This high level of growth control allows us to fabricate a novel class of artificial materials by using either exactly (001) oriented substrates or vicinal (001) substrates tilted towards [100]. The controlled incorporation of fractions of InAs monolayers into the GaAs matrix offers the exciting possibility to manipulate the translational motion of excitons in the crystal on an atomic scale. We are thus able to tune the dimensionality of the center-of-mass motion of excitons and hence the optical response. Moreover, we are able to obtain isolated InAs quantum dots in a crystalline GaAs matrix on vicinal (001) GaAs substrates. The quantum dots are in average 25 Å apart, equal to the terrace distance which is determined by the substrate misorientation. The absence of any surface and interface states makes this system promising to study the optical response of ultrasmall zero-dimensional systems.

---

* present address: Department of Materials Science, Technical University, W-6100 Darmstadt, Germany

7.2

Int. Conf. on Narrow Gap Semiconductors, Southampton, 1992

Optical properties of InAs quantum wells emitting between 0.9 μm and 2.5 μm

E. Tournié*,[1] O. Brandt,[2] and K. Ploog[1]

Max-Planck-Institut für Festkörperforschung, D-7000 Stuttgart 80 (F.R.G.)

*Phone: xx49 / (0)711-6860246; Fax: (0)711-6874371

InAs quantum wells (QWs) embedded in an $Al_xGa_{0.48-x}In_{0.52}As$ matrix have a significant potential for optoelectronic devices working in the near- as well as in the mid-IR. However, there is still a lack of information concerning their optical properties. In this work we show that the operating wavelength of such QWs can be tuned over the whole range between 0.9 μm and 2.5 μm by adjusting the thickness of the well and/or the barrier composition.

InAs single- and multiple-QWs confined by an $Al_xGa_{0.48-x}In_{0.52}As$ barrier are grown on InP substrates by solid-source MBE. The growth conditions are adjusted so as to avoid islanding of the highly strained (3.2 %) InAs film for any thickness investigated. As a result we obtain QWs of superior optical quality as demonstrated by photoluminescence (PL) experiments between 6 K and 300 K.

InAs/$Al_{0.48}In_{0.52}As$ SQWs with thickness between 4 and 16 monolayers (ML) yield PL in the 0.9 to 1.8 μm range. The SQWs up to 7 ML thick emit up to room temperature. The high temperature PL efficiency is drastically increased by using multiple QWs. In this case, non-radiative recombination centers are activated at temperatures higher than 90 K, with an activation energy as high as 100 meV. InAs/$Ga_{0.47}In_{0.53}As$ SQWs with thickness between 4 and 25 ML emit between 1.7 and 2.5 μm and give PL up to room temperature for any thickness. For all the samples, the PL linewidths are the best obtained so far for this material system. Moreover, the low-temperature PL line arising from the InAs QW is much more intense than the line due to the barrier, indicating a very efficient carrier-capture by these QWs. Finally, the variation of the integrated PL efficiency with the excitation power reveals that the low-temperature emission is due to excitonic recombinations.

Our results demonstrate the high potential of InAs QWs for application in optoelectronic devices.

[1] Present address: Fachbereich Materialwissenschaft, Technische Hochschule Darmstadt, D-6100 Darmstadt (F.R.G.)

[2] Present address: Mitsubishi Central Research Laboratory, Amagasaki, Hyogo 661, Japan

7.3

Magneto-Optical Properties of Quantum Dots in InSb

M Kubisa and W. Zawadzki
Institute of Physics, Polish Academy of Sciences
Warsaw, Poland 02-668

Magneto-optical properties of quantum dots in semiconductors have been considered theoretically using the model of a spherical infinite well. In contrast to the previous treatment[1], we have taken into account the real band structure of InSb-type materials (narrow energy gap and the spin-orbit interaction)[2]. The theory is formulated in terms of one parameter $\eta = R^2/2L^2$, where $L = (\hbar e/B)^{\frac{1}{2}}$ is the magnetic radius and R is the dot radius. The eigenenergies of the system and the resulting energies of the allowed magneto-optical transitions have been computed. For $\eta < 5$ (moderate magnetic fields) analytical expansions for the energies have been found, using the method of Dean[3].

Employing the established band parameters for InSb and the value of R = 55nm, we have been able to describe very well the experimental magneto-optical transitions (00) → (0$\bar{1}$) and (00) → (01), observed by Sikorski and Merkt[4] in the quantum dots in InSb in the field range $0 < B < 4$T. The only adjustable value of R is fixed by the experimental cyclotron energy at $B \simeq 0.1$ T, so that the correct description of the data as functions of magnetic field testifies to the validity of the theory.

1. F. Geerinkx, F. M. Peeters, and J. T. Devreese, J. Appl. Phys. 68, 3436 (1990).
2. W. Zawadzki, J. Phys. C16, 229 (1983).
3. P. Dean, Proc. Camb. Phil. Soc. 62, 277 (1966).
4. Ch. Sikorski and V. Merkt, Phys. Rev. Lett. 62, 2164 (1989).

7.4

Subbands in Inversion Layers on NGS for $E_{gap} \to 0$

B. Freytag[a], U. Rössler[a], O. Pankratov[b]
a.) Inst. Theoret. Physik, Universität Regensburg, D-8400 Regensburg
b.) Fritz-Haber-Institut, D-1000 Berlin

Subband states in n-inversion layers on narrow-gap semiconductors are known to be resonant states due to the Zener coupling to the continuum of the bulk valence band [1,2]. Because the strenght of this coupling increases with decreasing gap E_{gap} and, as a consequence, also the width of the resonance increases the principal question arises, if subbands do exist in inversion layers on a zero-gap semiconductor. Self-consistent numerical calculations indicate the existence of resonant subband states at small energy gaps but cannot be applied to the zero-gap case[1,2]. Moreover, these calculations are based mainly on approximations, like neglecting the free-electron term in $\mathbf{k} \cdot \mathbf{p}$ models. We have studied the zero-gap case analytically and find a principal answer to the problem: The existence of bound states ist connected *with the free electron term*, because it changes the order of the relevant differential equations. Thus, resonant states exist only if the free electron term is not neglected. We have checked this principal analytical result by solving the subband problem, starting from Kane's two band model with and without free electron term and using an analytical potential for the inversion layer. The exact solution for $E_{gap} = 0$ and the numerical solution for very small E_{gap} (0.1 meV) show similar structure in the density of states, which does not exist if the free electron term is neglected.

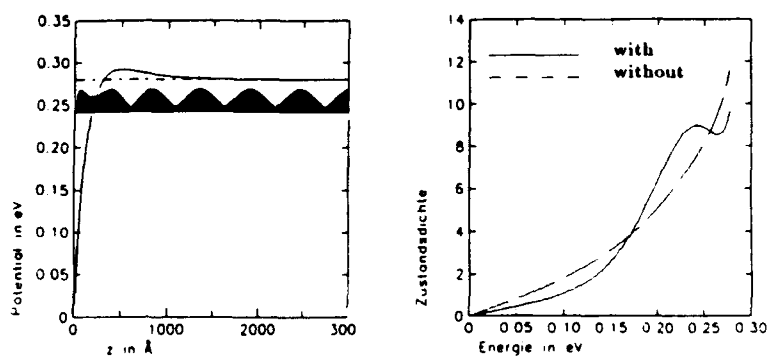

[1] A. Ziegler, U. Rössler, Europhys. Lett. 8 543 (1989)
[2] P. Sobkowicz, Semicond. Sci. Technol. 5 183 (1990)

7.5

Kinetic Confinement of Electrons in Semiconductor Heterostructures

M. Kubisa
Institute of Physics, Polish Academy of Sciences
02-668 Warsaw, Poland

A new type of electron confinement in semiconductor double heterostructures is proposed. The confinement occurs when the effective mass of electrons in the center region is higher than that in the outside regions, and it results from the "kinetic well" produced by the transverse free motion. The system is similar to a moving bicycle: the kinetic forward motion gives it a lateral stability. The resulting energy-wavevector relations for two-dimensional subbands are strongly nonparabolic. The calcualted density of states is similar (but not identical) to that of conventional potentially confined 2D systems. The effect of an external magnetic field on this system is also considered. It is shown that the energies of the kinetically confined states are strongly nonlinear functions of the magnetic field intensity.

8.1
HgCdTe INFRARED LASER DIODES GROWN BY MBE *

J.M. Arias, M. Zandian and R. Zucca

Rockwell International Science Center
Thousand Oaks, California 91360

and

J. Singh

Department of Electrical Engineering and Computer Science
University of Michigan, Ann Arbor, MI 48109

ABSTRACT

Tunable HgCdTe diode lasers could be used as infrared sources for: optical and atmospheric communications, laser radar heterodyne detection, molecular spectroscopy, and atmospheric gas analysis. The small dependence of the lattice constant on the Cd molar fraction, x, of $Hg_{1-x}Cd_xTe$ makes it relatively easy to grow from single epitaxial layers to complex heterostructures across the wide infrared spectral range of 1 to 14 µm without the severe lattice matching constraints usually found with other semiconductor alloys. While HgCdTe has been used extensively to fabricate high performance photodetectors, little has been done to apply its technology to fabricate infrared emitting laser diode devices. The only implementation of a narrow band-gap II-VI compound diode laser was accomplished with HgMnTe.[1]

In this talk we will report the earlier [2] and latest results on the fabrication and successful operation of HgCdTe infrared diode lasers. The stripe-geometry double heterostructure lasers were grown by molecular beam epitaxy (MBE). The active layer thickness ranges between 0.9 and 1.4 µm, and the the p^+ and n^+ confinement layers were in-situ doped up to 10^{18} cm^{-3} with arsenic and indium, respectively. Three double heterostructures were grown, all of which produced working lasers. The devices were operated under pulsed currents at temperatures between 40K and 90K. Emission wavelengths for the three laser structures were 2.9, 3.4, and 3.9 µm. The lowest 77K threshold current density was 521 A/cm^2; which is very close to the prediction of a numerical calculation. Further material growth, device processing and device characterization data (far field patterns, spectral analysis of longitudinal modes, imaging of laser emission, etc.) will be presented. Possibilities for further improvement, as well as technological limitations will be discussed.

1. P. Becla, J. Vac. Sci. Technol., **A6**, 2725 (1988).
2. M. Zandian, J.M. Arias, R. Zucca, R.V. Gil, and S.H. Shin, Appl. Phys. Lett. **59**, 1022 (1991).

---

* Work supported by the Phillips Laboratory under contract No. F29601-90-C-0054

8.2

OPTICAL SPECTROSCOPY OF CdTe/CdHgTe QUANTUM WELLS AND SUPERLATTICES

E. MONTERRAT, L. ULMER, N. MAGNEA, H. MARIETTE[1], J. L. PAUTRAT
Laboratoire de Physique des Semiconducteurs DRFMC / SP2M
Centre d'Etudes Nucléaires de Grenoble, 85X, 38041 Grenoble, France

K. KHENG, F. FUCHS
Fraunhofer Institut für Angewandte Festkörperphysik
72, Tullastrasse, D-7800 Freiburg, Germany

CdTe/$Cd_xHg_{1-x}Te$ (x=0.5) heterostructures emitting in the near IR wavelength range (2-5μm) have been grown by molecular beam epitaxy.

First we will report on the optical properties of $Cd_{0.5}Hg_{0.5}Te$ single quantum wells cladded between CdTe or $Cd_{0.7}Hg_{0.3}Te$ barriers. The well thicknesses vary between 10Å and 300Å. Very efficient transitions characteristic of a type I system are detected on a wide temperature range. Electrons and heavy holes 2D quantization is clearly demonstrated by an important blue shift when the well thickness decreases and, for the narrow well samples, when the potential heights increase.

Second, for superlattice samples, a spectroscopic analysis of luminescence, transmission and photoluminescence excitation (PLE) spectra will be presented.The PLE spectra of CdHgTe heterostructures are obtained for the first time by using Fourier Transform Infrared Spectroscopy. Both the transmission and PLE data reproduce quite well the expected density of states for a two dimensional system with a step-like spectrum corresponding to the various e_ih_i or e_il_i minibands. Up to room temperature the luminescence spectrum exhibits a single line which is very close to the edge of the first absorption step e_ih_i.

All these experimental data are well described by a finite square well model. The quantized energy levels (or minibands) e_ih_i and e_il_i are calculated with a Kronig-Penney model and the associated effective masses are deduced from the Kane approximation. This quantitative study allows to obtain a good fit with the absorption spectra using values for the physical parameters of this system (optical gaps, effective masses, valence band offset, relative contribution heavy / light holes) which will be discussed.

[1]Laboratoire de Spectométrie Physique, Université J. Fourier, Grenoble I

8.3
TYPE CONVERSION OF $Cd_xHg_{(1-x)}Te$ GROWN BY LIQUID PHASE EPITAXY

D.T.Dutton, E.O'Keefe, P.Capper, C.L.Jones, S.Mugford and C.Ard*

Philips Infrared Defence Components, Southampton, Hampshire, U.K.

Abstract

It is important for both photoconductor and photodiode device fabrication to understand the process of p to n conversion in $Cd_xHg_{(1-x)}Te$ (CMT). The purpose of this paper is to report on type conversion of epitaxial CMT as a result of annealing in a mercury overpressure. There are several reasons for studying this conversion mechanism. These include determination of the background donor level, as a measure of material quality, optimisation of anneal times for photoconductors, estimation of junction penetration for photodiodes and removal of mercury vacancies in extrinsically doped material. High quality, long wavelength p-type CMT grown by Liquid Phase Epitaxy (LPE) from a Te-rich melt has been subjected to annealing in an open tube furnace with rapid sample quenching arrangement. Junctions formed by mercury eliminating metal vacancies within the epitaxial layer have been identified by a Hall and strip technique. It has been found that junction penetration depths are dependent upon the square root of anneal time and the junction penetration rate is different from the published results for bulk material [1]. The effect on junction penetration of using layers with different initial acceptor concentrations and background donor levels has been investigated. These findings will be compared with other published data and the mechanism of mercury diffusion will be discussed with regard to initial acceptor and background donor concentrations, as well as Te precipitates and dislocations.

[1] C.L.Jones, M.J.T.Quelch, P.Capper and J.J.Gosney, J.Appl.Phys., 53, (1982) 9080

* Present address - II-VI Inc., Saxonburg, PA, U.S.A.

8.4

As and Sb Diffusion in MCT for Junction Formation

L.O. Bubulac, S.J.C. Irvine, E.R. Gertner, W.P. Lin and J. Bajaj

Rockwell (c.f. Arias)
Rockwell International Science Center, 1049 Camino Dos Rios, Thousand Oaks, Calif. 91360, U.S.A.

HgCdTe is an important narrow band gap semiconductor for infrared detection technology due to wide range of wavelength tunability (0-1.6eV). The p-on-n junction architecture for the photovoltaic devices is increasingly important. Fabrication of p-on-n photodiodes using ion implantation techniques has been developed for this process. In this paper we describe results on the As and Sb diffusion from an ion implanted source and on the quality of the long wavelength p-on-n junctions formed by this process in MOCVD IMP. Diffusion mechanisms of As and Sb have been studied from chemical analysis (secondary ion mass spectrometry-SIMS) and theoretical modelling combined with a technique for measuring the location of the electrical junction (electron beam induced current - EBIC). During the anneal As redistributes from the ion implanted source by a multicomponent mechanism. The electrical junctions are formed by an enhanced diffusion component of As, which, we suggest, is a vacancy mechanism occurring on the cation sublattice of HgCdTe. This mechanism operates when both (a) sources of As on the cation sublattice and (b) cation vacancies, are present in the material. This is the case for the ion implanted regions of MCT. When Sb is diffused from an ion implanted source the junctions seem to form on the gaussian component for which the diffusion coefficient is relatively higher than for As (~4 x 10^{-13}cm^2/s for Sb versus ~2 x 10^{-14}cm^2/s for As at 400°C in Hg atmosphere). In both cases the device quality is good in terms of zero bias resistance area product (RoA) and quantum efficiency. These results can be related to the characteristics of both layer characteristics and junction formation. Examples of photodiodes fabricated by both processes will be given. Thus, an RoA of 73.4Ωcm^2 for a cutoff wavelength of 10.02μm at 77K and a quantum efficiency of ~50% were obtained by As diffusion from an ion implanted sources; and a RoA of 77.7Ωcm^2 for a cutoff wavelength of 9.91μm at 77K and quantum efficiency of ~50% were obtained for Sb. At 77K the transport mechanisms limiting the device performance around zero bias are diffusion limited, indicating good junction properties for these ion implanted devices.

8.5
Interdiffusion study in CdTe/HgTe superlattices

A.Tardot, A.Hamoudi, P.Gentile, N. Magnea, J.L. Pautrat
Laboratoire de Physique des Semiconducteurs
D.R.F.M.C./S.P.2 M.
Centre d'Etudes Nucleaires de Grenoble
BP 85 X
38041 GRENOBLE
FRANCE

The properties of the heterostructures are strongly dependent on the interfacial quality and particularly on its abruptness. Since the interdiffusion coefficients are high in the II-VI semiconductors, this point has to be carefully investigated.

Experiments have been designed to measure the interdiffusion coefficients in CdTe/HgTe (001) superlattices. The interdiffusion coefficients are deduced from double crystal X rays diffraction spectra on post-growth annealed samples. In addition to the central peak (diffraction of the average lattice) the X rays pattern exhibits satellite peaks due to the constructive interference between beams reflected by various periods. The satellites intensity is directly related to the Fourier components of the concentration profile. The interdiffusion process is thus observable on the reduction of the satellites intensities and it enables to measure coefficients ranging from 10^{-16} to 10^{-23} cm^2/s.

The CdTe/HgTe superlattices are coherently grown by Molecular Beam Epitaxy on (001) oriented $Cd_{0.97}Zn_{0.03}Te$ substrates. The annealings are realised in the 200-250°C range for integrated times varying from 1h to 10h. The sample is maintained under a Hg overpressure in order to control the thermodynamic conditions of the thermal treatments. The satellites intensities decrease monotonically with annealing time. We check that the period and the width of the satellites remain constant, indicating a very homogenous interdiffusion. After each annealing, the ratio of the satellites integrated intensities to the central peak is calculated.

A careful analysis of the variation of satellites intensities with time shows that the simple linear model is not applicable. Effects of the strong concentration gradient at the interface and the difference between the intrinsic coefficients of Cd and Hg are taken into account to describe the interdiffusion phenomenon in CdTe/HgTe superlattices. For comparaison we will present results obtained on $CdTe/Cd_{0.93}Zn_{0.07}Te$ superlattices where the linear diffusion model is applicable.

These results will be compared with the available data on the diffusion process in these materials and agree quite well with higher temperature (300-500°C) data.

These experiments show that during the growth process of Hg based heterostructures at 160-180°C, the contribution of interdiffusion to interface sharpness is of the order of one or three monolayers following the concentration gradient. These data agree with the microscopic and spectroscopic investigations.

9.1

Middle Infrared Picosecond Spectroscopy of MBE InAs Epilayers at 300 K

K.L.Vodopyanov *, H.Graener, *EP III Uni.Bayreuth, Postfach 101251, D-8580 Bayreuth,FRG, tel 0921/553179, fax. 0921/552999*
C.C.Phillips, *Physics Dept., Imperial College, London SW7 2AZ, UK, tel. 071/589 5111, fax.071/589 9463*
I.Ferguson, *IRC for Semiconductor Growth,Imperial College, London SW7 2AZ, UK*
*) *Perm. address: General Physics Institute, Vavilov str.38, Moscow 117942*

Pump-probe mid-IR experiments with 10 ps resolution have been performed for the first time on ultrathin (0.09-3.3 μm) undoped MBE InAs epilayers on GaAs substrates at 300 K using a novel pulsed laser system based on Nd:YAG pumped $LiNbO_3$ Parametric Superradiant Generator. This system provided pump and probe pulses independently tunable in the range 2700-3900 cm^{-1} ($h\nu$=0.335-0.485 eV) which is near and above the absorption edge of InAs.

The excess carrier concentrations of 10^{17}-$10^{18}cm^{-3}$ were created at pump intensities of $1\text{-}2\cdot10^{7}$ W/cm^2, leading to the large Burstein-Moss blue shifts, reaching 90 meV , and significant bleaching near the excitation photon frequency with recovery times in the range 3000-35 ps; the latter value being strongly dependent on photon energy, InAs epilayer thickness, high energy proton irradiation dose and other conditions. The Auger coefficient in InAs was measured for the first time to be $1.1\pm0.1\cdot10^{-26}cm^6s^{-1}$. The carrier recombination rate, which was calculated from the bleaching recovery, is governed at the specified carrier densities by : for "thick" (>0.5 μm) samples - Auger effect; for "thin" (<0.5 μm) samples - by the InAs/GaAs interface defect recombination. Shockley-Read recombination played additive role and increased significantly after proton bombardment. A detailed numerical modelling of these effects was made.

Dynamic induced absorption spectra (DIAS) of the samples taken at zero and negative pump-probe delays show a pronounced spectral hole (~100 cm^{-1} wide) burnt into the InAs absorption continuum, centred at the position of the pump frequency, due to generation of nonthermal (hot) carriers. A discussion of this and other sharp features of the DIAS data will be made and preliminary results from $InAs_xSb_{1-x}$ alloys and Strained Layer Superlattices will be presented for the first time.

Using the ultrafast bleaching effect in the InAs MBE layers we have demonstrated passive mode-locking of a 3 μm erbium laser for the first time[1]. Intense (10 MW peak power) picosecond pulses were generated with an extremely simple all solid state cavity design.

1. K.L.Vodopyanov, A.V.Lukashev, C.C.Phillips, I.T.Ferguson Appl. Phys. Lett. 59, 1658 (1991)

9.2

Ultrafast Recombination Processes in Lead Chalcogenide Semiconductors Studied via Picosecond Optical Nonlinearities

R. Klann, T. Höfer, R. Buhleier, and T. Elsaesser
Physik Department E 11, Technische Universität München,
James-Franck-Str., D-8046 Garching, Germany
Phone (089) 3209-2865, FAX (089) 3209-2842
and
A. Lambrecht
Fraunhofer-Institut für Physikalische Messtechnik,
D-7800 Freiburg, Germany

Lead chalcogenides, an important class of narrow-gap semiconductors, have found extensive application for laser diodes emitting in the wavelength range between 3 and 30 μm. Radiationless recombination of electron-hole pairs, e.g. by Auger processes, is expected to influence the performance of laser diodes and to limit the available optical power. A number of theoretical calculations on Auger recombination has been reported, whereas little experimental information is available on fast recombination processes [1]. In this paper, we present the first detailed study of ultrafast recombination in PbSe, by means of temporally and spectrally resolved measurements with picosecond pulses in the mid-infrared.

PbSe crystals grown by molecular beam epitaxy (thickness d=2μm) are studied in the time resolved experiments where an electron-hole plasma is generated by picosecond photoexcitation. The carriers give rise to a bleaching of the inter-band absorption which is monitored by probe pulses of 8 ps duration, tunable in the wavelength range from 4 to 9 μm. For an excitation density of 4×10^{17} cm^{-3}, we observe a transient blue shift of the absorption edge by approximately 12 meV which is due to band-filling by both electrons and holes. The concommittant change of the refractive index by up to $\Delta n=-0.1$ is detected in the wavelength range below the band edge via a shift of the Fabry-Perot resonances of the thin PbSe crystal.

The time dependent change of transmission builds up instantaneously with the pump pulse and shows a relaxation depending on the excitation density N. For N below 5×10^{17} cm^{-3}, the signal decays by carrier recombination on a time scale of several hundreds of nanoseconds. At higher densities of up to 3×10^{18} cm^{-3} , we find an additional fast recombination at early times after excitation. At sample temperatures of 10K and 70 K, the fast recombination leads to a substantial decrease of carrier density within the first 100 ps. A comparative study of the emission spectra occurring after picosecond excitation demonstrates that this effect is due to the onset of stimulated emission, resulting in enhanced recombination rates of electrons and holes. At room temperature, stimulated emission does not occur for densities below 3×10^{18} cm^{-3}. Here, the fast component of recombination is governed by Auger processes, resulting in a decay of carrier density on a time scale of approximately 1 ns. The analysis of the time resolved data gives an Auger coefficient of $1.0\pm0.3\times10^{-28}$ cm^{6}/s. The experimental results will be compared to theoretical calculations of the different fast recombination processes.

[1] R. Klann, R. Buhleier, T. Elsaesser, and A. Lambrecht, Appl. Phys. Lett.59,885(1991)

9.3
NUCLEAR SPIN POLARIZATION IN INSB DETECTED BY SPIN-FLIP RAMAN GAIN SPECTROSCOPY

W. Hofmann, H. Pascher, G. Denninger

(Phys. Inst., Universität, D-8580 Bayreuth, Germany)

The conduction electron spin resonance (CESR) is shifted by the spin polarization of the nuclei via the Fermi contact interaction between the nuclear and electronic spins (Overhausershift). We observe this interaction in n-type InSb by coherent spin-flip Raman scattering using two CO-lasers [1]. In narrow-gap semiconductors with their high effective g-factors this method is very useful to measure the CESR-frequency in a wide range of magnetic fields. The coherent spin-flip Raman scattering of laser radiation with photon energies corresponding to the energy gap is strong enough to produce a considerable amount of saturation of the electronic spin system. Thus due to the large effective g-factor of InSb a high degree of dynamic nuclear polarization (DNP) is achieved by the hyperfine interaction and the Overhausershift is enhanced with respect to thermal equilibrium by a factor of several hundreds.

The Overhausershift is directly proportional to the propability $|\Psi(0)|^2$ to find an electron at the nuclear sites. In thermal equilibrium, when the spin polarization of the nuclei is known, measurements of the Overhausershift directly yield informations on $|\Psi(0)|^2$ of the conduction electrons for ^{115}In and ^{121}Sb, respectively. Investigations of the shift as a function of time either while dynamically polarizing the nuclei or while the nuclei relax from high spin polarization to thermal equilibrium, measure the nuclear spin-lattice relaxation time T_1 of the different isotopes. The observed time constants T_1 are compared with calculations based on a modified Korringa model [2].

Because the Overhausershift directly detects the component of the nuclear polarization parallel to the external magnetic field, experiments where the Overhausershift is observed under pulsed radio frequency irradiation allow a direct observation of Rabi oscillations. From their decay an effective transverse nuclear spin relaxation time T_2^* can be determined. It agrees well with the linewidth of the nuclear magnetic resonance as observed by the Overhausershift technique.

[1] G. Denninger, H. Pascher, Solid State Commun. **78**, 5, 399 (1989).

[2] F. Bridges, W.G. Clark, Phys. Rev. **182**, 2, 463 (1968).

9.4

Cross Field Hot Hole Cyclotron Resonance: Non-Parabolic and Quantum Effects

C. Kremser, K. Unterrainer
Institut für Experimentalphysik, Universität Innsbruck, A-6020 Innsbruck, Austria

E. Gornik
Walter Schottky Institut, TU-München, D-8046 Garching, Germany

P. Pfeffer, W. Zawadzki
Institute of Physics, Polish Academy of Sciences, 02-668 Warsaw, Poland

B. Murdin, C.R. Pidgeon
Department of Physics, Heriot-Watt University, Edinburgh EH14 4AS, U.K.

New results of magneto absorption experiments with p-Ge crystal subjected to high crossed electric and magnetic fields are presented, investigating the coupling between the light and heavy hole bands and non-parabolic effects, which are important for the light hole band at the fields used here. These effects lead to an unequal Landau level spacing which is a key requirement to achieve tunable p-Ge cyclotron resonance lasers [1].

In our experiments we used a sample with a carrier concentration N_A-N_D=6 x $10^{13}cm^{-3}$. One face of the sample was wedged in order to avoid Fabry-Perot interferences. The whole experiment was performed at liquid Helium temperatures. A tunable p-Ge cyclotron resonance laser was used as a novel FIR source giving FIR pulses of 500 ns duration. The laser was placed inside the same cryostat as the investigated sample. Electric field pulses of up to 3.6 kV/cm with a duration of 1 μs were applied to our sample. Magnetic fields of up to 5T were used.

Cyclotron transition energies were recorded for electric fields between 0 and 3.6 kV/cm at laser frequencies between 65 cm^{-1} and 85 cm^{-1}. For a quantitative determination of the light-hole transitions observed in our experiments we have used the Pidgeon and Brown (PB) coupled band model. To obtain a good fit to our data, the influence of the conduction and spin-orbit split off bands is essential. In addition it was found, that for the lowest cyclotron transition warping of the energy surfaces has to be considered. With the PB-model including warping effects good agreement with our data could be obtained both for the electric field and magnetic field dependence of the Landau level transitions. The results are expected to be important for the investigation of stimulated CR-emission in p-InSb and p-Si.

[1] Optical and Quantum Electronics, 1991, 23 (special issue on FIR semiconductor lasers), Mityagin et al., p.287; Gornik et al., p.267; Komiyama et al., p.133; Gavrilenko et al., p.217.

9.5

INVESTIGATION OF TRAP LEVELS IN BULK AND LPE $Hg_{1-x}Cd_xTe$ USING RESONANT IMPACT IONIZATION SPECTROSCOPY

C. L. Littler, X. N. Song, and Z. Yu
Department of Physics, University of North Texas
J. L. Elkind
Central Research Laboratories, Texas Instruments, Inc.
D. G. Seiler and J. R. Lowney
National Institute of Standards and Technology

A new technique for studying low concentrations of trap levels in narrow (x = 0.22 - 0.24) gap $Hg_{1-x}Cd_xTe$, has been used to investigate both bulk and LPE samples of this material. In this technique, known as Resonant Impact Ionization (RII), electrons are photoexcited across the energy gap via the absorption of one photon from a CO_2 laser and then subsequently well into the conduction band by absorption of a second photon. The photoexcited carriers then relax from a higher-lying conduction-band Landau level to a lower one via impact ionization of a valence electron into a trap level. For a resonance to occur the transition energies ΔE_{LL} between conduction-band Landau levels must equal the transition energies ΔE_{II} between the highest valence-band Landau level and an impurity or trap level in the gap. Landau levels that are more than a photon energy above the lowest conduction-band Landau level are not populated and do not contribute. In the case of the bulk samples, mercury (Hg) intersitials were deliberately introduced into a x = 0.22 and a x = 0.24 sample, where each sample was divided into two parts and the second part of each slice was used as a control. The results from the interstitially-doped samples provide direct evidence that the Hg intersitials create trap levels at $\simeq$ 45 and 60 meV above the valence band edge. In addition, enhancement in the two-photon magnetoabsorption (TPMA) strength is observed in samples where the 60 meV level resides approximately at the middle of the energy gap. Work on LPE samples of HgCdTe has recently begun the samples also show RII structure due to deep trap levels.

*This material is based in part upon work supported by the Texas Advanced Technology Program under grant # 003594018 and a grant from Texas Instruments, Inc.

9.6

CHARACTERIZATION OF FREE CARRIERS IN IV-VI LASER MATERIALS FROM INFRARED REFLECTIVITY

D.B.Kushev, N.N.Zheleva

Semiconductor Physics and Technology Institute

University of Sofia, BG 1126 Sofia, Bulgaria

The infrared reflectivity is an useful optical method for determination of free carrier parameters: nondestructive, quick and contactless. An approach for characterization of some narrow gap semiconductors from the minimum of bulk reflectivity spectra in the plasma frequency region is presented. An estimation of the concentrations, effective masses, relaxation time and optical mobility of free carriers in the IV-VI laser materials $Pb_{1-x}Sn_xTe$ $(0<x<0.3)$, $Pb_{1-x}Sn_xSe$ $(0<x<0.33)$ and $PbS_{1-x}Se_x$ $(0<x<1)$ is given. The method is described and illustrated graphically by nomograms for fast estimation of parameters in each band (conduction and the two valence bands). The limitations of the method are discussed. Very often an interference is observed in the epitaxial film reflectivity spectra. An empirical method for estimation of the bulk reflectivity minimal value and its position from the nearest interference reflectivity minimum is proposed. The relations are derived in an optimal way using design of experiments and are valid for wide range of the parameters: plasma and damping frequencies, high frequency dielectric constant and thickness of the layer.

10.1

IV-VI Material Properties Relevant to Laser Diodes

M. Tacke

Fraunhofer-Institut für Physikalische Messtechnik
Heidenhofstrasse 8, W-7800 Freiburg, Germany

Nearly all material parameters of semiconductors are important for designing and understanding diode lasers. Mechanical properties must be considered when mounting the laser chips, chemical properties influence the choice of contacting procedures and materials. Central importance of course comes to those parameters that govern the efficiency of the lasing process.

The laser gain must compensate laser material losses. Hence these losses must be low. In the mid IR, the optical losses are mainly due to free carrier absorption, but probably also to impurity induced attenuation. Good quantitative knowledge on the absorption processes is necessary for the calculation of the threshold gain.

The gain itself depends on the radiative recombination probability and the carrier concentration, the quasi Fermi level position, to be more specific. This is where the band structure enters. The carrier concentration relative to the laser current should be high, hence long minority carrier lifetime due to nonradiative processes is vital.

At present, minority carrier recombination probably is the most important material property, however still not well known. It strongly influences the typical present operation temperature near liquid nitrogen temperatures, which prohibits wide spread use of the lasers.

The main use of the mid IR diode lasers is gas analysis by absorption spectroscopy. In this context laser radiation noise is important. One of the central parameters is the relative change of the gain and the real part of the refractive index upon changes of the carrier concentration.

The talk aims at giving a feeling for the relative importance of such parameters for the IV-VI mid IR lasers.

10.2

Molecular Beam Epitaxy of Laterally Structured Lead Chalcogenides for the Fabrication of Buried Heterostructure Lasers

A. Lambrecht, H. Böttner, M. Agne, R. Kurbel, A. Fach, B. Halford, U.Schießl, and M. Tacke

Fraunhofer Institute for Physical Measurement Techniques (IPM),
Heidenhofstr. 8, D-7800 Freiburg, Germany
Phone: 49-(0)7 61-88 57-0, FAX: 49-(0)7 61-88 57-224

Laser diodes based on IV-VI-compounds are important sources for tunable infrared radiation in the 3 to 20 μm spectral region. Their major application is trace gas analysis of atmospheric pollutants. Most recent developments focus on the fabrication of buried heterostructure (BH-) lasers by molecular beam epitaxy (MBE). MBE-overgrowth of lateral structures in the 2-5 μm range is a prerequisite for the future fabrication of advanced submicron structures as distributed feedback lasers. Here studies on overgrowth of the laterally structured IV-VI- compounds PbSe, PbEuSe, PbSrSe and PbSnSe obtained by different methods are presented for the first time.

Definition of lateral structures can be achieved either by photolithography or by shadow masked growth. Photolithography using a wet chemical etch is hampered by the chemistry of the etchant which results in strongly composition and dimension dependent etch rates, so that our studies show a poor reproducability. Therefore structure definition by ion beam etching (Ar^+) is favourable. It is not material selective and structure shape can be controlled to a certain extent.
For improved MBE-overgrowth some second processes have to be used to ensure a clean, well defined surface and an optimum shape for MBE-overgrowth. Sharp edges result in deep cracks or grooves aside a well grown ridge. We were sucessfully employing a chemomechanical polish similar to substrate preparation to obtain a suitable smooth shape.
By directly growing the active stripe of a BH-laser through a shadow mask much of the problems encountered with photolithography can be avoided. We report on PbSe and PbSnSe - BH-lasers with active widths in the 20 μm range which were obtained by shadow mask growth. The masks were prepared by anisotropic chemical etching of Si(100).
The overgrowth results were investigated employing scanning electron microscopy (SEM). A selective chemical etch was used to reveal layers of different composition. An optimization of this preparation technique gave a sharp analytic tool to investigate overgrowth in detail.

The main effect of lateral structurization is a change of the laser farfield intensity distributions. Double heterostructure lasers usually have multi lobe farfields. BH-lasers frequently show aperture filling single lobe fields. The obtained data are qualitatively explained by a waveguide model.

10.3

Abstract for
International conference on narrow gap semiconductors,
Southampton, 19-23 July 1992

THERMAL MISMATCH STRAIN RELAXATION MECHANISMS IN HETEROEPITAXIAL LEAD-CHALCOGENIDE LAYERS ON Si-SUBSTRATES

H. Zogg, C. Maissen, S. Blunier, S. Teodoropol, R.M. Overney[1], T. Richmond[1], J.W. Tomm[2]

AFIF (Arbeitsgemeinschaft für industrielle Forschung) at Swiss Federal Institute of Technology, ETH Hönggerberg, CH-8093 Zürich, Switzerland

[1]Institute of Physics, University of Basel, CH-4056 Basel, Switzerland
[2]Humbolt University, O-1040 Berlin, Germany

Narrow gap IV-VI lead-chalcogenides are grown by MBE on 3" Si(111)- and Si(100)-substrates. Epitaxy is achieved with the aid of a ≈200 nm thick BaF_2/CaF_2 buffer layer. The layers are applied for the fabrication of photovoltaic IR-sensor arrays both for the 3-5 µm and 8-12 µm range [1].

Due to the thermal mismatch between IV-VIs, fluorides and Si, the layers would crack on cool down from growth temperature if no relaxation of mechanical strain could occur.

For *(111)-oriented* structures, this relaxation is by glide of dislocations on (100) planes (which are inclined with respect to the (111)-surface) both for the fluoride and IV-VI layers. We determined the morphology of slip steps resulting from dislocations which have glided across the layers using a STM (scanning tunnelling microscope) for the IV-VI layers and an AFM (atomic force microscope) for the (insulating) buffer layers. Two types of dislocations are found: A set of glissile dislocations with Burgers vector inclined with respect to the surface is responsible to overcome the thermal mismatch, while most of the large lattice mismatch (up to 19%) is overcome by sessile dislocations with Burgers vector parallel to the interface. The glissile dislocations in the IV-VI layers remain mobile down to cryogenic temperatures even after multiple cool-down cycles; near no strain is observed by x-ray diffraction, Rutherford backscattering channeling, or photoluminescence measurements. The amount of strain relaxation can be tailored by using ternary compounds like $PbSe_{1-x}Te_x$. With suitable compositions x, strain relaxation occurs at elevated temperatures only, while the layers strain elastically on cool down to cryogenic temperatures.

Contrary to (111)-oriented structures, *(100)-oriented* layers are strained and can crack at low temperatures. This is because the resolved shear stress is zero for the primary {100}<110> glide system in (100)-orientation.

[1] H. Zogg, C. Maissen, J. Masek, T. Hoshino, S. Blunier, A.N. Tiwari, Semicond Sci. Technol. 6, 1991, pp. C36-C41.

Please send all correspondence to H. Zogg, AFIF, ETH Hönggerberg, CH-8093 Zürich, FAX ++41 1 371 241, Phone 41 1 377 2209 (or ..2156 or ..2143)

10.4

Properties of Narrow-Gap PbSe Quantum Wires

K. H. Herrmann, K.-P. Möllmann, P. Schäfer, J. W. Tomm[1)]
H. Böttner, M. A. Fach, M. Griesinger[2)]
J. Sebastian[3)]

1) Humboldt-Universität Berlin, Institut für Festkörperphysik, O-1040 Berlin, FRG
2) Fraunhofer-Institut für Physikalische Meßtechnik W-7800, Freiburg, FRG
3) Paul-Drude-Institut für Höchstfrequenztechnik, O-1086 Berlin, FRG

We present the first report on the preparation and investigation of an artificial lead salt based structure containing a one-dimensional electron gas. Starting point for the preparation were thin PbSe layers grown by Molecular Beam Epitaxy. Holographic lithography was used for delineating quantum wires. The result were 2 mm long wires with a cross-section of about 650*650 nm^2 separated by 650 nm wide barriers.

Photoluminescence spectra indicate a giant blue shift of the edge emission by 50 meV (to be compared with $E_g \approx 145$ meV for bulk material). The energy of the main asymmetric luminescence line well agrees with an additional edge in the photocurrent spectra.

The shift observed exceeds the value calculated taking into account the geometrical width (about 0.5 meV) by orders of magnitude.

Possible explanations for this effect will be discussed:

* thermally induced or built-in strain (estimated to give a blue shift of about 5 meV),
* a wire cross section reduced by lateral depletion layers,
* the influence of a resonant level within the conduction band which was found earlier or transitions via states generated by the surface treatment,
* transitions between excited states as a consequence of the heating of the carrier plasma due to reduced electron-phonon interaction.

These hypotheses will be discussed on the basis of several sets of experiments. We think, that there is reason to believe, that the use of quantum size effects in binary lead salts is a real alternative to the application of mixed crystal systems for 'short wavelength' device applications to meet the 2..3 μm region.

10.5
An STM Study of InSb(100)-c(8x2)

M.C. Schweitzer[1], F.M. Leibsle[1], T.S. Jones[2], C.F. McConville[3], N.V. Richardson [1]

[1] IRC in Surface Science, University of Liverpool, Liverpool, L69 3BX, UK
[2] Department of Chemistry & IRC in Semiconductor Materials, Imperial College, London, SW7 2AY, UK.
[3] Department of Physics, University of Warwick, Coventry, CV4 7AL, UK

Abstract

The preparation of chemically clean surfaces of the (100) surface of InSb prior to growth by MBE generally requires *in situ* treatment by cycles of ion bombardment and annealing. Low energy diffraction (LEED) studies after such a treatment, shows a sharp, stable c(8x2) pattern after annealing to 625K. We present the first atomic resolution scanning tunnelling microscopy (STM) images, which demonstrate that after such a cleaning process, automatically flat terraces are obtained over areas in excess of 1000Å. The c(8x2) structure is clearly seen in the STM images consisting of ordered rows of indium dimers. A structural model is presented which is consistent with these observations.

11.1
PIEZOELECTRIC EFFECTS IN SUPERLATTICES

M. Lakrimi, R.W. Martin, C. López, D.M. Symons, E.T.R. Chidley, R.J. Nicholas, N.J. Mason, and P.J. Walker.

Physics Department, Clarendon Laboratory, The University of Oxford, Parks Road, OXFORD OX1 3PU, U.K.

ABSTRACT

The last decade has seen the introduction of new high quality structures based on strained materials. It has also been predicted that the optical and electrical characteristics could be modified through growth along <111> directions compared to the usual <100>. In zincblende and wurtzite structures, the strain is shown to cause large internal piezoelectric fields, of order 1×10^5 V/cm, which modify the structure and alter its performance. The existence of this electric field has already been demonstrated by different groups using various methods. We present results from intrinsic InAs/GaSb and InGaSb/GaSb structures grown by MOVPE. The effects of the piezoelectric field have been assessed by comparative studies of simultaneously grown [100], [111]A, and [111]B structures.

Evidence for the existence of the piezoelctric field was provided by photoluminescence and interband photoconductivity studies on InGaSb/GaSb quantum wells. The measured Stark shifts of the order of 10-100 meV were well correlated by the estimated strain induced piezoelectric field, of about 1×10^5 V/cm. Magnetotransport data on two-dimensional holes confined in these $In_xGa_{1-x}Sb/GaSb$ quantum wells will be discussed with emphasis on the influence of the cap layer thickness, yielding differences between [111]A and [111]B orientations. In [111]A, the depletion field adds to the piezoelectric field, thus producing a sharper triangular well, whilst in [111]B, there is partial cancellation leading to a flatter well. Comparison between simultaneously grown thick cap [100], [111]A, and [111]B samples reveals significant carrier density enhancement for the [111] growth without the need for extrinsic doping; and this is shown to be a consequence of the piezoelectric field. Mobility enhancement was also found. Hole mobilities of up to 33,000 cm^2/Vs, with a Fermi velocity of 2×10^7 cm/s, were achieved in [111]A oriented InGaSb/GaSb superlattices without any external bias.

InAs/GaSb is an unusual type-II system, with the conduction band of InAs lying approximately 150 meV below the valence band of GaSb. For sufficiently thin InAs layers, the system is semiconducting (positive bandgap). For InAs thicknesses in excess of 85 Å, the system is semimetallic (negative bandgap) and contains holes in the GaSb and electrons in the InAs layers. The effects of the piezoelectric field are probed through magnetotransport and infra-red studies in both the semimetallic and the semiconducting regimes, respectively.

The carrier densities are found to be higher in [111] samples over their [100] counterparts. The absorption coefficient, α, of [111] oriented InAs/GaSb superlattices was also found to be significantly enhanced compared to [100] equivalents. The change is attributed to increased overlap between the electrons and holes wavefunctions rather than to a reduced bandgap (the Stark shift is estimated to be of order 10 meV for a 200 Å period). For example, at about 0.3 eV, α is found to increase from 2300 cm^{-1} in [100] to 1400 cm^{-1} in [111]. This considerable enhancement gives potential scope for piezoelectric based structures for the fabrication of long wavelength detectors

11.2

Interband and Intersubband Transitions in InAs Doping Superlattices Studied by Absorption and Photoconductivity Spectroscopies.

C C Phillips, R H Thomas and H L Vaghjiani, Physics Dept., Imperial College, London, SW7 2AZ, UK.
I T Ferguson and A Norman, Interdisciplinary Research Centre for Semiconductor Materials, Imperial College, London, SW7 2AZ.

Doping superlattices ("nipi" structures) in narrow gap binaries are of particular interest because they offer the possibility of reducing the effective bandgap to allow cooled detector operation in the 3-5μm and 10-14μm atmospheric windows [1,2]. Here we report the results of a study of a range of nipi structures grown, for the first time, in InAs. Pronounced bandgap lowering and dramatically increased minority carrier lifetimes are found in MBE epilayers grown on IR transparent GaAs substrates.

Using an overall nipi periodicity of 50nm with n- and p- sheet dopant concentrations of ~ 3 x 10^{12} cm^{-2} produced a fractional change in effective bandgap, $\Delta E_g/E_g$, of 25%. This has resulted in photoconductive detector structures with usable sensitivities out to λ~4.0μm (compared with the λ=2.98μm low temperature cutoff of bulk InAs detectors), and tuneable minority carrier lifetimes of up 400μsec were measured at 15K.

Experimental absorption and photoconductivity spectra were modelled with a detailed bandstructure calculation which allows for the pronounced non-parabolicity effects in these structures and enables effective detector design using optical constant data measured in undoped test layers[3]. The measured nipi absorption spectra are consistent with oscillator strength sum rules governing the modifications to the JDOS spectrum introduced by the perturbing nipi potential on the bandedge states. Etalon effects arising from the dielectric mismatch with the GaAs substrate are used to provide extremely accurate MBE growth rate calibrations.

We have also studied, for the first time in this material, asymmetric nipis (a-nipi's) in which the n-dopant sheet concentration exceeds that in the p-layers, producing occupied i=0 subbands and allowing the i=0→1 intersubband transition energies to be observed in a 15K waveguide subband absorption measurement. Impurity disorder broadening has only a second order effect here, and narrow (≈24meV wide) transitions were seen at energies in good agreement with our depolarisation shifted self-consistent subband energy model.

Intriguingly, evidence for transitions at these intersubband energies is also seen in the normal incidence transmission spectra although this is formally forbidden by the dipole selection rules in this geometry. Possible explanations for this effect and potential device applications will be discussed.

References

1) C C Hodge et al. Semicond. Sci. and Tech. 5, s319-322 (1990)

2) C C Phillips App. Phys. Lett. 56,(2), 151-153 (1990)

3) S N P Smith et al. accepted for Semicond. Sci. and Tech.

G.Bougnot*, J.P.R.David#, A.Giani*, S.K.Haywood+, G.Hill#, A. Krier†, F.Mansoor+, N.J.Mason‡, R.J.Nicholas‡, F.Pascal-Delannoy*, M.Pate#, L.Ponnampalam+, P.J.Walker‡

* University of Montpellier; # University of Sheffield;
+ University College London; † University of Lancaster; ‡ University of Oxford;

The growth and fabrication of new antimony containing III-V heterostructures for devices in the 2 - 4 μm region

The 2 - 4 μm wavelength range is very important from both a military and an environmental perspective. The growth, by MOVPE, of a range of antimonide based materials systems suitable for providing devices responsive to this wavelength range is reported. Photodetectors with external quantum efficiencies of 60% at 2.5 and 2.2 μm have been fabricated from InGaSb containing an n-p junction. The use of various superlattice, ramp and step buffer layers to minimise the effect of the mismatch between the GaSb substrate and the layer will be presented along with I/V and C/V characteristics.

In order to examine the possibility of tuning the wavelength of emission or detection by using strained layer superlattices of InGaSb/GaSb, such superlattices have been grown in the depletion region of a GaSb n-p or p-i-n junction. The effect of the strain within the wells induced by varying the thickness and indium content will be reported.

Novel heterostructures have been grown to produce devices without the need for conventional doping. Using the crossed gap alignment of InAs/GaSb we can use n-InAs to inject holes into n-GaSb to form a diode-like structure. This eliminates the need to produce abrupt doping profiles when fabricating devices. Previous experience with n-type doping of GaSb and InAs suggested that a set-back would be useful, to create a n-i-n structure, and to prevent excessive n-doping of the InAs. The dopant was turned off and a nominally undoped GaSb spacer layer was grown, followed by the nInAs. Various set-backs have been tried and the optimum seems to be 200 Å. The devices have V_{TO} of 0.7V [1mA], typical V_R = -12V [0.1mA] and a best V_R of -12V [10μA] for a 100 μm diameter device with some evidence of avalanche breakdown in the structure.

Abrupt doping junctions may also be avoided by using a Schottky barrier to provide the electric field. However, stringent processing conditions are needed to fabricate Schottkys on n-GaSb and they cannot be made at all on p-GaSb because of the low barrier height [0.2eV]. We have overcome these problems using a thin capping layer of highly dislocated GaAs. Surprisingly this has been successful for both re-growth on older structures and contiguous in-situ growth. Devices are either defined by an aluminium dot on the surface, or by etching a mesa and using Ti/Au contacts. Both methods of growth and of device fabrication have been successful. Reverse bias currents of < 1μA at voltages up to 2V have been obtained from p-GaSb of 10^{16} cm^{-3}. Avalanche breakdown occurs at -4.5V in this material and the barrier height is raised to ~0.7eV due to the large valence band offset. Various cap thicknesses have been investigated and the optimum appears to be 200 Å. $In_{0.3}Ga_{0.7}Sb$ layers have been successfully capped and the photoresponse of these structures is being investigated. This GaAs layer could also be used to passivate a GaSb based device and protect it from deterioration over a period of time. **FAX 0865 272400 Dr N.J.Mason**

11.4
A Heterojunction Minority Carrier Barrier for InSb Devices

T. Ashley, A.B. Dean, C.T. Elliott, A.D. Johnson, G.J. Pryce, A.M. White and C.R. Whitehouse
Defence Research Agency, RSRE
St. Andrews Road, Malvern, Worcestershire, WR14 3PS, UK.

InSb devices are of interest for a range of electronic and optoelectronic components, including ultra-high frequency transistors, lasers and photodetectors, particularly when used in a non-equilibrium mode to attain room temperature operation. In all devices, optimisation of the performance is achieved by careful control of the electron and hole densities in the active region of the structure. In the cases of the transistors and infrared detectors the carrier densities are held below their equilibrium values in order to minimise the leakage current arising from thermal generation, whilst in the injection laser, where electron and hole numbers greatly exceed the equilibrium levels, confinement of the carriers is necessary to obtain a small threshold current. Both situations require that diffusion currents from other regions of the device and from its contacts are minimised.

In $n^+\xi p^+$ InSb diodes (where ξ represents near intrinsic n- or p-type), the majority of the leakage, at or near room temperature, comprises an electron diffusion current. This arises from a thermal Auger generation process in the p^+ region. In devices where the p^+ region is relatively thin ($\leq 1\mu m$) electron injection from the metal contact is also significant. Although both of these contributions could in principle be reduced by degenerate doping of the p^+ region, the necessary acceptor levels are beyond those which can be achieved experimentally. Alternatively, the p^+ region could be replaced by a wider-gap semiconductor, but no suitable lattice matched material exists.

In this paper we describe the use of a thin, strained region of $In_{1-x}Al_xSb$ to form a barrier in the conduction band to electron flow from the p^+ to ξ regions, and so reduce the leakage current. Theoretical and experimental results from diodes, grown by molecular beam epitaxy, are presented which show that the zero-bias resistance increases and the reverse-bias leakage current decreases by up to an order of magnitude as the proportion of Al in the $In_{1-x}Al_xSb$ region is increased from zero to 20%. Strain relaxation, which was observed at a composition of 20% for a barrier 20nm thick, prevents further reduction in the current. The theoretical analysis is based on a numerical model which includes the critical factors of non-parabolicity and degeneracy. This model enables analytic expressions for the effective barrier height, the screening of the valence band offset, and the optimum p^+ doping to be tested.

11.5

Exclusion Effects in Semiconductors revisited

Narrow Gap Semiconductors Nontraditional Use

V.K. Malyutenko

Institute of semiconductors, Ukrainian Academy of Sciences, 252650, Kiev - 28, Ukraine

Although nearly four decades have passed since the effect of the minority-carrier exclusion in semiconductors had been detected, it is only within the last few years that the theoretical analysis, supported by detailed experiments has provided the real understanding of this phenomenon nature and its practical use.

A Drastic decrease (by two-three orders) of the electron-hole concentration accompanied by its nonuniform spatial distribution along or across the crystal results in the sublinear $I \sim V^{1/2}$ or N-type current-voltage characteristics. Negative luminescence arises at the spectral range of fundamental absorption due to band-to-band electron transitions modulation ($\omega \geq Eg/\hbar$, E_g is the energy gap). The thermal emission modulation due to intraband electron transitions ($\omega \leq E_g/\hbar$) can be easily detected as well. Nonlinear recombination suppression influences the effective carrier lifetime and noise processes both in the crystal volume and its surface. Such significant excitation of electron subsystem has given life the new nonorthodox semiconductor devices: light emitting diodes for IR, radiative coolers, IR light modulators, noise generators, uncooled photoresistors with significantly improved performance.

In this review the experimental and theoretical results related with the problem of longitudinal exclusion (l-h contact, bipolar drift towards the current lines) and transversal exclusion (crossed electrical and magnetic fields, bipolar drift across the current lines) are being discussed. The main impact is made on the operation principles of new devices, based on the narrow gap semiconductors. The possible trends of future investigations and applications are also discussed.

12.1

Quantum Well Infrared Photodetectors

B. F. Levine
AT&T Bell Laboratories
Murray Hill, NJ 07974

There has been a lot of interest recently in the detection of long wavelength ($\lambda = 7-19\ \mu m$) as well as midwave (3–5 μm) infrared radiation using multiple quantum wells, due to the fact that these quantum well infrared photodetectors (QWIPs) can be fabricated using the mature III-V materials growth and processing technologies. This superior materials control results in high uniformity and has thus allowed the demonstration of large 128×128 staring arrays with excellent imaging performance.

We will discuss the physics of the intersubband absorption, quantum well escape probability, noise and the hot electron and hole transport and recapture processes in $GaAs/Al_xGa_{1-x}As$ as well as other III-V materials. The high detectivities, D*, and low noise equivalent temperature differences, NEΔT, leading to excellent infrared video imaging will also be discussed.

12.2

International Conference on Narrow Gap Semiconductors
(July 19-23, 1992, University of Southampton, UK)

Current Conduction in Bound-to-Miniband Transition III-V Multiquantum Well Infrared Detectors[1]

Sheng S. Li, M. Y. Chuang, and S. S. Yu
Department of Electrical Engineering
University of Florida
Gainesville, FL 32611
U. S. A.

Abstract

We report a study of the current conduction mechanisms in two new types of III-V multiquantum well (MQW) /superlattice (SL) long wavelength infrared photodetectors (LWIP's) based on the bound-to-miniband (BTM) band and step bound-to-miniband (SBTM) transition and resonant tunneling mechanisms. The BTM LWIP's consists of a 40-period of GaAs quantum wells with a well width of 88 Å and a dopant density of $2.0 \times 10^{18}\ cm^{-3}$. The barrier layer on each side of the quantum well consists of a 5-period of undoped $Al_{0.4}Ga_{0.6}As$ (58 Å) /GaAs (29 Å) superlattice layers which were grown alternatively with the GaAs quantum wells. The SBTM LWIP uses a lightly strained $In_{0.07}Ga_{0.93}As$ (106 Å) quantum well with a 5 period of undoped $GaAs/Al_{0.4}Ga_{0.6}As$ superlattice barrier layer structure. Incorporation of a short period superlattice barrier layer in both the BTM and SBTM LWIP's enhances the potential barrier height in the quantum well which results in a significant reduction of the dark current over the conventional GaAs/AlGaAs MQW LWIP's.

Theoretical calculations of the dark current and the transmission coefficient through the global miniband formed inside the quantum well/superlattice barrier layers have been carried out as a function of temperature and bias voltage for both BTM and SBTM LWIP's. The results reveal that dark current in these LWIP's is dominated by the thermionically assisted tunneling conduction from the heavily populated ground states in the quantum wells via the global miniband inside the quantum wells/superlattice barrier layers for $T \geq 60$ K, whereas resonant tunneling conduction prevails for $T \leq 40$ K. The thermionic emission into the continuum bands is negligible due to the high barrier height created by the superlattice barrier layer for both LWIP's. A comparison of the calculated and measured dark current values for these two LWIP's with that of the conventional GaAs MQW LWIP's was also made in this work.

The measured dark currents, absorbance spectra, and spectral responsivity curves for both LWIP's were found in good agreement with the calculated values. The peak detectivity D^* for the SBTM LWIP's was $2.3 \times 10^{10} cm\sqrt{Hz}/W$ at $\lambda = 10.5\ \mu m$ and $T = 63$ K, and for the BTM LWIP's, D^* was found equal to $1.6 \times 10^{10} cm\sqrt{Hz}/W$ at $\lambda = 8.9\ \mu m$ and $T = 77$ K.

[1] This work was supported by the Defense Advanced Research Project Agency under US Navy grant No. N0014-91-J-1976.

12.3
The absorption linewidth for bound-to-extended state transitions in GaAs/AlGaAs quantum wells in dependence on the excited level position

R.Sizmann, P.Helgesen, S.Løvold

Norwegian Defence Research Estabilshment, Div. for Electronics
P.O.Box 25, N 2007 Kjeller, Norway

A.Paulsen

Norwegian Telecom Research, P.O.Box 83, N 2007 Kjeller, Norway

Electrons, which are bound in the ground state subband of a quantum well, are photoionized by exciting them to extended states above the conduction band edge of the barrier material. Because such bound to extended state excitation processes are promising to use for infrared detection in GaAs/AlGaAs quantum well devices, they are intensively investigated in recent publications[1,2].

Here we study the absorption line width for such kind of transitions theoretically and experimentally in dependence on the energy position of the excited state E_1 above the continuum edge of the well E_C. Due to the interaction of the excited *state with the continuum* states the level is not discrete like in the case of a bound state, but broadened. This intrinsic broadening increases with increasing energy difference $E_1 - E_C$.

We study this effect by performing optical transmission experiments in multi quantum well structures, which are n-type doped in the well. For quantum wells with an excited state slightly above the continuum edge we get a good agreement between the calculated line shape and the absorption data.

In contrast to this we observe for samples with a resonant level $\approx 30meV$ above E_C a line width approximately half as large as the calculated one. We assume that the narrowing of the absorption linewidth compared to intrinsic broadening of the level is due to an excitonic interaction of the photoionized electron with the positive charged donor in the quantum well. We investigate this effect by measuring the absorption in dependence on an applied bias voltage.

References:

1. B.F.Levine,C.G.Bethea,G.Hasnain,V.O.Shen,E.Pelve,R.R.Abott and S.J.Hsieh, Appl.Phys.Lett., **56**, 851, 1990

2. E.Rosencher,E.Martinet,F.Luc,Ph.Bois and E.Böckenhoff, Appl.Phys.Lett.,**59**, 3255, 1991

12.4

Increased Responsivity and Detectivity in Asymmetric Quantum Well Infrared Detectors

A. Fraenkel, E. Finkman, G. Bahir, and A. Brandel
Department of Electrical Engineering and Solid State Institute
Technion - Israel Institute of Technology, Haifa 32000, Israel

G. Livescu, and M.T. Asom
AT&T Bell Laboratories, Breinigsville, PA 18031, USA.

Quantum well infrared detectors received an increasing interest during the last few years. Their performance, however, is far from being optimized. One of the basic parameters which was studied very little is the dependence of the device properties on the well shape. A study of a new version of asymmetric stepped GaAs/AlGaAs multi quantum well infrared detectors is reported. These asymmetric detectors utilize the usual bound to continuum transition. However, their current responsivity is remarkably asymmetric with regard to the voltage polarity. In contrast with rectangular wells, in which responsivity saturation is reached in both bias polarities, these wells exhibit saturation only for negative bias. In positive bias the responsivity continues to increase with increasing electric field. The responsivity does not depend on temperature. Dark current and noise also depend on bias polarity, but the difference between polarities is decreasing with decreasing temperature. As a result, the optimum operation voltage, with highest signal to noise ratio, is increased for positive bias at low temperatures, but stays almost constant for negative one. The highest D^* in positive polarity is much higher than in the negative one.

In order to explain these results we present a model for the transport properties of the excited electrons in the continuum. The key parameter in this model is the dwell time spent by the carrier wave packet in the well region, which is strongly bias dependent. Employing this model, we achieve a very good fit to the experimental data.

Fig 3

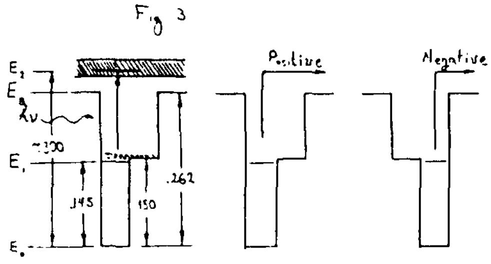

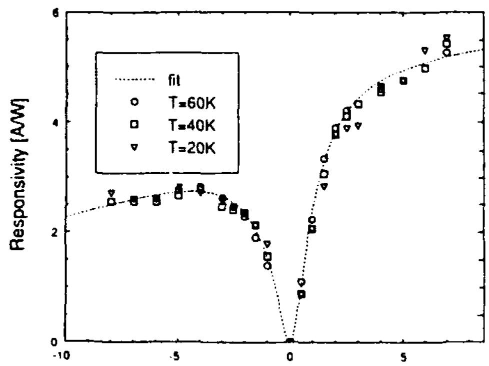

12.5

Stimulated Emission due to Magnetoelectric-Photo Effect in Narrow-Gap Semiconductors at the Quantum Limit

T. Morimoto *, M. Chiba*, G. Kido# and A. Tanaka$

* Institute of Atomic Energy, Kyoto University, Uji, Kyoto 611, Japan
# Institute of Materials Research, Tohoku University, Sendai 980, Japan
$ Electronics Materials Laboratory, Sumitomo Metal Mining Co. Ltd., Ohme, Tokyo 198, Japan

We have revealed the quantum aspects of the stimulated emission from bulk InSb at the quantum limit, being excited by the electric field E_y^* induced by passing a current density $\mathbf{J}(\|\hat{x})$ through the sample subjected to a transverse magnetic field $\mathbf{H}(\|z)$. The phenomenon has been demonstrated to be a useful tool for the determination of the band parameters such as the energy gap ε_g, the electrons effective mass m_1^* and the effective g-factor g_1, in addition to the application as a tunable infrared laser [1].

The peak frequencies, $\omega_\pm$, of the strongest emissions observed at the quantum limit can be expressed as

$$\hbar\omega_\pm = \varepsilon_g + \frac{1}{2}\hbar\omega_{c1}\left[1 \pm \frac{m_1^* g_1}{2m_0}\right] + \frac{1}{2}\hbar\omega_{c2,h} - |e|E_y^* l^* \quad , \tag{1}$$

with $E_y^* = JH/n^*|e|c$. Here ω_{c1} and $\omega_{c2,h}$ are the cyclotron frequencies of electrons and heavy holes, respectively, n^* is the effective electron concentration, and l^* is the mean free path of the lucky electrons drifting along-y direction without suffering severe damping until the annihilation by recombination.

When the inverted population is realized by the $\mathbf{J} \times \mathbf{H}$ force excitation at the quantum limit the gain $g(\omega, \mathbf{H})$ of the stimulated emission can be written as

$$g(\omega, \mathbf{H}) \quad = \quad A\frac{eH}{c\omega}\sum_\pm(\hbar\omega - \varepsilon_{0,\pm})^{-1/2} \quad , \tag{2}$$

with $\hbar\omega_\pm = \varepsilon_{0,\pm}$, so that it diverges to infinity at the frequencies $\omega = \omega_\pm$ as $\omega_c\tau \to \infty$. This singularity makes it possible to cause the stimulated emission at such an extremely low value of the critical current density J_c as 16 - 40 A/cm^2, for example being observed in InSb at 80K for H = 7T.

We shall report the latest measurements of the stimulated emission of InSb in a magnetic field extended up to 23T together with the experiments for $Hg_{1-x}Cd_xTe$, and discuss the quantum nature of the emission with the application to the band parameter determination particularly at room temperature.

[1] T. Morimoto and M. Chiba, Proc. 20th Int. Conf. Physics of Semiconductors (1990) p.1847; J. Phys. Soc. Jpn. 60, 2446 (1991).

12.6

GALVANOMAGNETIC PROPERTIES OF InSb/(001)GaAs HETEROSTRUCTURES FOR MICROMINIATURE HALL TRANSDUCERS

[illegible].A.Mironov, V.F.Igumenov, V.M.Konstantinov
Institute of Radiophysics & Electronics, Acad. of Sci. of Ukraine
12 Acad. Proskura St. 310085 Kharkov,Ukraine FAX:(7-0572)-44-11-05

The InSb films 0,3-5 μm thick were grown on semiinsulating (001) GaAs substrates using vacuum epitaxy methods. The perfection of layers were determined by the ratio of In and Sb molecular fluxes (Sb/In=1,1-2,5) and by two-stage procedure of epitaxy. During the first stage the thickness of the films (d) was less than 200 nm and substrate temperature was T_{sub} = 350-370°C. The further growth (d > 200 nm) was carried out at T_{sub} = 390-410°C with the rate of 2-3 nm per second. The X-ray rocking curves width amounted to 3'-6'. The dislocation density reached 10^7-10^8 cm^{-2}. To obtain n-type layers the latter were doped with Sn in the concentration range of $5 \cdot 10^{16}$-$2 \cdot 10^{18}$ cm^{-3}. The Hall measurements were performed in the temperature range 1,5-400 K in magnetic fields of up to 6 T. The application of methods of integrated-circuit technology (vacuum metallization of local parts of the structure, photolithography, assembly by bonding, etc.), made it possible to fabricate cross-shaped Hall probe structures with dimensions of 0,7 × 0,7 × 0,35 mm and a sensitive cross over region of 50 × 20 μm. The optimum electron concentration and mobility were $7 \cdot 10^{17}$-10^{18} cm^{-3} and $(1,5\text{-}2,0) \cdot 10^4$ $cm^2/V \cdot sec$, respectively.At the nominal operating current of 100 mA the sensitivity of the transducers was 50-160 $\mu V/mT$, the residual voltage was 5-100 μV, the divergence of Hall voltage was 0.04-0.06 %, the nonlinearity factor was 0,3-3,0 %, and the input resistance was 2,0-200 Ω. The high degree of doping of the films resulted in low values of the temperature sensitivity factor (0,005-0,05 % $\cdot K^{-1}$) and a temperature resistance coefficient (+0.09 % $\cdot deg^{-1}$). The Shubnikov-de Haas oscillations in both the Hall signal and in the tranverse magnetoresistance were measured at helium temperatures 1,5 K ≤ T ≤ 15 K by the compensation technique. The amplitude of the Hall voltage oscillations at 5-6 T was a few hundredths of a per cent of the total Hall voltage, which is an order of magnitude smaller than that of the quantum oscillations inherent to bulk InSb with comparable electrical parameters. This is due to the features of the InSb high dislocation density in the film (~10^8 cm^{-2}),which results in an effective nonthermal broadening of the landau levels without violating a linearity of Hall voltage. Using these transducers one can control the parameters of magnetic material including high-T_c superconductors in temperature range 1,5-300 K and in magnetic fields up to 25 T.

12.7

III-V MAGNETIC SENSORS

J. Heremans
General Motors Research Laboratories
30500 Mound Road, Warren, MI 48084-9055, USA

Narrow-gap semiconductors have been used for decades in the fabrication of magnetic field sensors, such as magnetoresistors and Hall sensors. Magnetic field sensors are, in turn, used in conjunction with permanent magnets to make contactless potentiometers and rotary encoders. This sensing technology offers the most reliable way to convert a mechanical movement into an electrical signal. With the proliferation of microprocessors, magnetic sensing technology is widespread in automotive applications, such as spark timing. Most current applications use Si Hall sensors integrated with amplifiers.

Recent developments in the growth of thin epitaxial layers of InAs and InSb on semi-insulating GaAs or InP substrates have resulted in the development of magnetoresistors with excellent sensitivity and operating temperatures up to 285°C. Magnetoresistors and, to a lesser degree, Hall sensors, require a very thin active semiconductor region, a high carrier density, and a high room temperature mobility. The best materials are narrow-gap III-V compounds. 2-DEG layers in InSb and InAs would be ideally suited for these devices. The accumulation layer at the surface of InAs has been used to make magnetoresistors [1], and so have n-type doped thin InSb films [2]. InSb-based magnetoresistors outperform Si-based Hall sensors, even with integrated amplification.

The talk will describe device design criteria, materials requirements, and a direct comparison of the three type of galvanomagnetic devices, magnetoresistors, Hall sensors and magnetotransistors, made from the same material, an InAs film with a strong accumulation layer of 6×10^{12} cm $^{-2}$. It will also contain comparisons of the characteristics of different magnetic field sensing technologies, such as Si and GaAs Hall sensors, and Permalloy-type magnetoresistors, with those of narrow-gap III-V-based sensors.

[1] J. Heremans, D.L. Partin, D.T. Morelli, B.K. Fuller and C.M. Thrush, Appl. Phys. Lett. 57, 291 (1990)

[2] D.L. Partin, J. Heremans, C.M. Thrush and L. Green, 1992 Solid-State Sensor and Actuator Workshop, Hilton Head Island, SC (1992)

12.8

"Hot electron and subband far infrared detectors"

E. Gornik
Walter Schottky Institut
TU München, D-8046 Garching

A review on the present state of the art of hot electron detectors for the far infrared spectral range is given. A significant improvement in the performance of n-type InSb detectors was achieved by passivating the surface and avoiding surface state recombination. The responsivity of passivated detectors mounted on brass or steel is increased by two orders of magnitude. The spectral range in the cyclotron mode is extended from 10 cm^{-1} to 400 cm^{-1} with magnetic fields up to 8T.

In specially designed GaAs heterostructures a tunable single line photoconductive response in the magnetic field with a linewidth of 0.1 cm^{-1} is demonstrated. This detector represents a high resolution spectrometer in a wide frequency range.

The potential for wave length selective quantum well detectors in the infrared and far infrared is discussed. A double wavelength selective detector with high resolution based on GaAs/GaAlAs quantum wells is demonstrated. Using surface plasmon in coupling techniques for normal incident light a very high responsivity (2.2 A/W) is achieved.

12.9

Superconducting Structures on Narrow Gap Semiconductors

Hideaki Takayanagi, Tatsushi Akazaki and Junsaku Nitta
NTT Basic Reserach Laboratories, Musashino-Shi, Tokyo 180 Japan

Semiconductor-coupled superconducting devices have recently attracted much interest as a so-called superconducting transistor [1]. Since the superconducting characteristics of these devices strongly depend on the induced pair potential Δ_N of the semiconductor side at the superconductor/semiconductor interface, it is very important to know the semiconductor carrier concentratiuon n dependence of Δ_N at the interface. A Nb/n-type InAs/Nb junction with oxide-free interfaces is very suitable for this study, because n-type InAs has no Schottky barrier. We have fabricated such Nb/InAs/Nb junctions and have obtained the n -dependence of Δ_N.

A schematic cross-sectional view of the fabricated device is shown in Fig.1. Both the p-type InAs buffer layer with a thickness of 1.0 μm and the n-type InAs channel layer with a thickness of 0.4 μm were grown by MBE. Subsequently, a Nb film with a thickness of 0.1 μm was deposited without breaking vacuum. A TEM observation showed that there was no oxide layer at the interface and that the Nb film grew as a single crystalline deposit under a substrate temperature condition [2].

According to the superconducting proximity effect theory, in the Superconductor /Semiconductor/Superconductor junction, the maximun supercurrent density is given as [3],

$$J_c \propto n\mu\, \Delta_N^2 \exp(-L/\xi_N)\,/\xi_N\,, \qquad (1)$$

where μ is the mobility of the semiconductor, L is the length between two superconducting electrodes (see Fig.1), and ξ_N is the coherence length of the semiconductor given as $(\hbar D/2\pi k_B T)^{1/2}$, where D is the diffusion constant. We measured the J_c's of devices with n ranging from 4.2×10^{17} to 2.5×10^{19} cm^{-3}. Using the measured J_c, n, μ, and L, Δ_N was derived from eq.(1). Figure 2 shows the obtained n-dependence of Δ_N when L=0.3 μm. It is shown that Δ_N has a weak dependence on n and it is almost constant when n is larger than ~ 10^{18} cm^{-3}. This is consistent with the boundary condition proposed by de Gennes [4] with some assumptions.

[1] A.W. Kleinsasser and W.J. Gallagher, §9 in *Superconducting Devices*, edited by S.T.Ruggiero and D.A. Rudman (Academic Press, 1990)
[2] T. Akazaki, J. Nitta, and H. Takayanagi, Appl. Phys. Lett., **59**, 2037 (1991)
[3] H. Takayanagi and K. Kawakami, *Tech. Digest Int. Elect. Devices Meet.*, Washington D.C. (1985) 98
[4] P. G. de Gennes, *Superconductivity of Metals and Alloys* (Benjamin, New York, 1969)

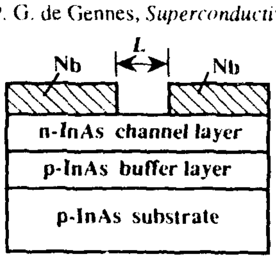

Fig 1. Schematic cross sectional view of a semiconductor-coupled superconducting device.

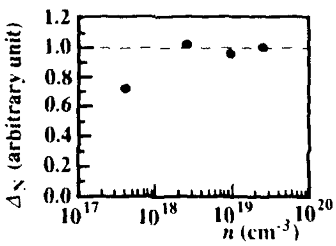

Fig.2. The n-dependence of Δ_N which is normalized by Δ_N of the highest n.

12.10

APPLICATIONS OF NARROW GAP STRAINED LAYER SUPERLATTICES

L. Ralph Dawson
Sandia National Laboratories
Albuquerque, New Mexico, USA

The conventional superlattice (SL), composed of alternate layers of lattice matched materials, provides structures with unique optical and electronic properties due to quantum size and band offset effects. To a lesser extent, SLs also provide some metallurgical advantages, such as dislocation filtering, likely due to small differences in the elastic properties of the different materials. In contrast to the conventional superlattice, the strained-layer superlattice (SLS) is fabricated from thin layers of materials whose lattice constants are significantly different, leading to nearly uniform strain within each layer. The relaxation of the lattice matching requirement leads to a much broader range of artificially-structured optical and electronic properties, due to the wider choice of constituent materials and the addition of another significant variable, the strain. In addition, the SLS plays a much more active role than the SL in controlling the metallurgical properties of the structure, particularly with respect to the ability to adjust the lattice constant of buffer layers without unacceptable densities of threading dislocations. The latter property is extremely important, since many interesting device structures have no lattice matched substrate on which they may be grown.

This talk will focus on the MBE growth of narrow gap SLSs, particularly InAsSb and InGaSb, with emphasis on their application as materials for long(8-12μm) and mid (2-5 μm)-wavelength IR detectors and emitters. Since these superlattices are not lattice matched to any commercially available substrate, suitable buffer layers are needed. To date, growth of such structures on InSb substrates, which places the SLS under net tension, usually leads to cracking of the epitaxial material, precluding the fabrication of detector arrays. We will discuss steps taken to mitigate this problem. In addition, we will discuss the growth of similar structures on GaSb and InAs substrates, which places the SLS in net compression and eliminates the cracking problem, but requires a much larger mismatch between SLS and substrate. A key factor in the successful growth of these structures is the use of the InAlSb/AlSb SLS as a digital alloy buffer. Nearly dislocation-free buffers with lattice mismatch in excess of 2% can be achieved in this manner. These techniques may have strong implications for the growth of other materials whose lattice constants are substantially different from that of any available substrate materials.

12.11
Review on n-i-p-i Structures

Josef Oswald, Institut für Physik, Montanuniversität Leoben, Austria

The concept of n-i-p-i structures, based on a system of alternatively n- and p- doped or δ-doped layers, is not limited only to the realization of a periodic band edge modulation. As shown for the case of PbTe p-i-n-i-p structures, a system of p-n-p-n-p... doped layers can also be used to design arbitrary potential shapes.

There is a long tradition of investigating n-i-p-i structures in both, narrow gap (e.g. PbTe, InSb) and wide gap (e.g. GaAs, InP, Si) semiconductors. Their major features, expected from the n-i-p-i concept, are common to all types of semiconductors.

However, the experimental conditions to observe all these effects vary over a wide range depending on the parameters of the bulk materials and the technological limits. Therefore the topics concerning 2D-confinement, tunneling, transport by use of selective contacts, excess carrier lifetime and detector application will be discussed in terms of a comparison of different bulk materials. Mainly GaAs will be used as representative for a wide gap and PbTe for a small gap system. Due to the high dielectric constant of PbTe ($\varepsilon_S \sim 500...1000$) the thickness of the potential wells resulting at moderate doping levels (N_A, $N_D = 1...3 \times 10^{17} cm^{-3}$) is too large to allow tunneling phenomena to be observed. Therefore single period structures, consisting of p-n-p layers, are sufficient to study all relevant effects in PbTe. It is shown, that selective contacts to n-type channels in PbTe structures can easily be made. Due to the small barrier height, the leakage of the selective contacts has to be taken into account for the interpretation of the conductivity experiments. This disadvantage, on the other hand, can be exploited for a new photo conductivity mechanism which enhances the photoconductive response by orders of magnitude above the contribution of the photo generated carriers themselves. The potential modulation is very sensitive to screening by excess free carriers, which in turn controlls the excess carrier lifetime. This builds up an efficient feed back loop. All the observed trends of photo Hall experiments as well as the results of time dependent and steady state photoconductivity experiments can be modelled successfully taking static and dynamic screening effects into account. The sensitivity of the potential modulation to the number of excess carriers determines also the I-V-characteristic of the selectively contacted n-channel in a p-n-p-structure. The built in voltage drop can produce some kind of pinch off and leads to a well formed plateau in the I-V-curve which changes drastically with illumination. It is shown that interdiffusion of Indium into the p-n-p-structure near the In-contact is of major importance for the successful modelling of the I-V-curves. This interdiffusion also explains the high voltages (up to 10 Volts) the selective contacts can withstand. Another phenomenon, related to the screening effect is the drastic enhancement of the ambipolar diffusion of locally generated non-equilibrium electron hole pairs. The local change of the carrier density changes locally the potential modulation and carrier diffusion is driven by the strong electric field which is built up in lateral direction. This effect, first systematically demonstrated by Döhler in GaAs p-n-p structures, also plays an important role in PbTe structures and makes, as will be shown, the n-i-p-i concept attractive for novel infrared detector applications.

12.12

MCT versus Quantum well structures for IR Detectors

S.C. Shen

1) Center for Condensed Matter and Radiation Physics
CCAST (World Laboratory) P.O.Box 8730, Beijing, China

2)National Lab for Infrared Physics
Chinese Academy of Sciences, Zhong Shan Bei Yi Road #420
Shanghai 200083, China

The Mercury Cadmium Telluride ($Hg_{1-x}Cd_xTe$) mixed crystal has been developed as a superior infrared detector material for more than two decades. From fundamental consideration, the HgCdTe provides the highest detectivity D^* for the detectors applications and can be modulated to fit all important wavelength regions of 1-3 µm, 3-5 µm, and 8-14 µm simply by adjusting the composition x. The material and detector technology has been developed quite well for the wide use of the mixed alloy. Nevertheless this material also suffers from some fundamental difficulties, such as large tunneling dark currents, and the fast Auger recombination rates, especially for making high-performance array responding to longer wavelength (8-14 µm).

Rapid progress has been made in last few years for the investigation and development of the quantum well infrared photodetectors (QWIP). Quite a lot of approaches and structures have demonstrated the great potential for the practical use of the QWIP, especially for making large arrays. The advantages of the quantum well materials against HgCdTe in uniformity, controllability and yield are clear, and the shortcomings of the materials have also been improved a lot in last few years, while they are still inferior, in point of view of detectivity D^*, to HgCdTe.

A comprehensive discussion will be made in this report, and the competition and comparison between the two material systems are expected to be lasted for a long period.

P1.1

NOVEL GAPLESS COMPOUNDS, MAGNETICS: $CuFeS_2$ and $CuFeTe_2$

L.V. Kradinova, A.M. Polubotko, V.V. Popov, V.D. Prochukhan, Yu.V. Rud, V.E. Skoriukin
Physico-Technical Institute Russia Academy of Sciences, Politekhnicheskaya 26, 194021 Sankt Petersburg, Russia

The nonmagnetic gapless compounds such as α-Sn, HgTe, HgSe, and HgS were known for a long time. We have investigated the temperature dependences of the Hall coefficient R(T), specific conductivity σ (T), and electron concentration n(T) in monocrystalls $CuFeS_2$ and $CuFeTe_2$. The measurements point out the power character of these values. For the compound $CuFeS_2$ R(T), σ (T), and n(T) are proportional to T^k, where k=-3 for R(T) and k=3 for σ (T) and n(T) in the temperature range $1.5 < T < 20K$. For $T > 20K$ these values are propotional to T^k too but with k=-3/2 for R(T) and k=3/2 for σ (T) and n(T). The electron mobility is small $\mu \sim 1\ cm^2V^{-1}s^{-1}$ and is practically independent on temperature. For the compound $CuFeTe_2$ these values are proportional to T^k too with k=-1.9 for R(T), k=1.9 for n(T) and k=1.15 for σ (T). The electron mobility is also small and changes as $\mu \sim T^{-0.75}$. The power dependences of R(T), σ (T), and n(T) are characteristic for gapless semiconductors. Therefore we have concluded, that both substances refer to the gapless compounds. The small temperature independent mobility is characteristic for the ferron (magnetopolaron) character of transfer with the ferrons of a large radius [1]. The observed mobility dependence $\mu \sim T^{-0.75}$ for $CuFeTe_2$ is close to the dependence $\mu \sim T^{-1}$ which is characteristic for the Mott, diffusional mechanism of transfer with the ferrons of a small radius [1]. All these peculiarities incline us to opinion that we deal with new type of compounds -the gapless magnetic semiconductors with the ferron type of charge transfer. The crystalline structures of $CuFeS_2$ and $CuFeTe_2$ are different. Because of unknown crystalline and magnetic structures of $CuFeTe_2$, realization of the theoretical group analysis is possible for $CuFeS_2$ only. The magnetic group of chalcopyrite is the single-colour one. Therefore all the results, which refer to the nonmagnetic case are correct for the magnetic one. The analysis of the irreducible representations established that the gapless state in the chalcopyrite structure can be realized in the P point of the Brillouin zone only. It corresponds to the special case of the space symmetry in accordance with the Abrikosov-Beneslavskii classification. The ferron states are special type of excitations, characteristic for antiferromagnetics and can be described in the frames of the spatial crystall and magnetic symmetry. In accordance with the temperature dependence $n(T) \sim T^3$ it was established that the gapless state in $CuFeS_2$ refers to the gapless state of the first type. Existence of the hole ferron follows from the facts of the gapless state and the ferron state of the conductance electrons.

1. T. Kasuya, A. Yanase, T. Takeda, Solid st. Comm. 8, 1551 (1970).

P2.1

WHY VARIOUS TYPES OF DONORS CAN EITHER ENHANCE OR REDUCE ELECTRON MOBILITY IN NARROW GAP SEMICONDUCTORS?

C. Skierbiszewski[1], Z. Wilamowski[2], T. Suski[1] and J.Kossut[2]

[1] High Pressure Research Center, Polish Academy of Sciences, Sokolowska 29/37, 01-142 Warsaw, Poland

[2] Institute of Physics, Polish Academy of Sciences, Al. Lotnikow 32/46, 02-668 Warsaw, Poland

It is well known that, under conditions of a fractional occupancy of impurity states, it is possible for the charges localized on the impurities to correlate their mutual positions. As a consequence, the electron mobility in such samples can exhibit greatly enhanced values. The effect has, in fact, been observed in narrow gap semiconductors where a configuration of the band edges with respect to impurity levels can be often found, that makes the fractional occupancy possible with the band carriers being present at the same time. Particularly suitable for this situation to arise is the case of resonant donors or acceptors.

In real samples it is common that several types of impurities are present, e.g., the resonant (which are fractionally occupied) and shallow donors. Intuitively, additional donors, when fully ionized, should lead to a drop of the mobility. Here we study the case of HgSe doped with Fe (resonant donor) and Ga ("shallow" donor). The concentrations of both dopants can be controlled in this system with sufficient accuracy for a quantitative study to be made. In particular, keeping the concentration of Fe constant and changing the concentration of Ga in the sample we can vary the critical parameter that rules the degree of spatial correlation, i.e., the ratio of the number of unoccupied to total number of donors. As the alternative method of tuning the discussed ratio we employ the hydrostatic pressure.

With this purpose we studied samples of HgSe with $n_{Fe} = 2 \cdot 10^{19} cm^{-3}$ (corresponding to maximum of mobility) with n_{Ga} in the range $0 - 1 \cdot 10^{19} cm^{-3}$ (i.e., up to complete filling of Fe - donor states).

The results of the conductivity and Hall effect measurements are compared with short-range correlation model modified appropriately in order to account for the presence of Ga ions. A quantitative agreement is observed. As a result of our analysis we obtain a set of conditions necessary for achieving very high mobility values in doped narrow gap semiconductors.

P2.2

TRANSPORT PHENOMENA IN A QUANTUM WELL CONTAINING MIXED VALENCE IMPURITIES

I.I.Lyapilin, I.G.Kuleev, and V.V.Karyagin

Institute of Metal Physics, Ural Branch, Ekaterinburg

On the basis of the Anderson model we consider transport phenomena in a quantum well containing mixed valence impurities. An example of such structure is [$Hg_{1-x}Cd_xSe$ / $Hg_{1-y}Fe_ySe$ / $Hg_{1-x}Cd_xSe$] ,with the appropriate choise of the composition parameter y. We analyze the energy spectrum of two-dimensional electrons, calculate the density of states with allowance for the hibridiza- tion of the d-level with band states and also study behaviour of conductivity and thermoelectric power as a function of both the iron content of a quanttum well and temperature.

The energy spectrum of 2D conduction electrons splits up into two or more branches, according to the number of dimensionally quantized energy levels lying below the d-level of iron if neglect of damping d-level. In another case the renomalized energy spectrum has anomalous dispersion at $E \sim E_d$.

In the vicinity of the resonance d-level the density of electron states suffers a radical change. The two-dimensionality of the electron gas results in the stepwise shape of the pumping and pump-out regions in the density of states and leads to the N_d threshold in the onset of the additional rectangular peaks and minima. At high iron concentration a gap arises in the density of states.

The increase of the gap as the iron conentration is raised lead to a decrease in conducivity with decreasing temperature and thus to an increase in the coefficient of thermoelectric power.

P2.3

THE "ANOMALY" OF ELECTRON SCATTERING BY A CORRELATED SYSTEM OF CHARGED DONORS

Tsidilkovski I.M., Kuleev I.I., Lyapilin I.I.

Institute of Metal Physics, Ekaterinburg, Russia

The HgSe:Fe crystals exhibit an unusual temperature dependence of the electron mobility μ: in a wide interval of iron concentrations N_{Fe} the mobility caused by Fe^{3+} impurity ion scattering increases when the temperature is loweved, $T \to 0$, in contrast to the Brooks-Herring theory. In order to explain this $\mu(T)$ "anomaly" the space correlatioon of Fe^{3+} ions due to short-range ordering induced by Coulomb repulsion should be taken into account.

We have considered the $\mu(T)$ "anomaly" in framework of the short-range-correlation model. The calculation is made in the direct inter-ion correlation and quantum screening approximations. The results of calculations of $\mu(T)$ for the importent iron concentrations interval ($1.8\text{x}10^{19} \leqslant N_{Fe} \leqslant 5.3\ \text{x}10^{20}$ cm^{-3}) without use of fitting parameters agree well with the experimental data in the temperature region (4.2-80)K.

We have also considered another approach to the $\mu(T)$ problem based on the assumption that Wigner crystalization of the Fe^{3+} ion set occurs at low temperatures. The method of long-wave fluctuations of the charged donor concentration has been used. We succeded in obtaining a qualitative agreement of measured curves with calculations, in which two fitting parameters were employed, only for a small T-interval (1.5-7)K. We can surely state that the idea of long-range Wigner ordering doesn't correspond to the experimental data at least at $T \geqslant 1K$.

Thus, our analysis shows that the short-range correlation model in which the modified Thomas-Fermi potential for inter-ion interacton and the Mayer coorrela-tion function are used, is a quite satisfactory approximation.

P2.4

ANISOTROPY OF THE MAGNETIC INTERACTIONS IN HgFeSe

Z. Wilamowski, H. Przybylinska
Institute of Physics PAS, 02-668 Warsaw, Al Lotnikow 32

W. Joss and M. Guillot
MPI-HML/SNCI-CNRS, BP 166X, 38042 Grenoble

We present the experimental studies of magnetic properties of HgFeSe. The magnetisation was measured at magnetic fields H up to 20 T, for $Hg_{1-x}Fe_xSe$ with iron content x in the range of 0.003 - 0.04. The temperature dependence of the magnetisation shows a behaviour corresponding to Van Vleck magnetism. The anisotropy of magnetisation is studied directly by measuring the torque for different orientations of the external magnetic field in respect to the crystallographic axes. The measured torque originates from two subsystems interacting with each other: the system of magnetic ions and the system of free electrons. In this paper we analyse the former.

At low magnetic fields the magnetic susceptibility, and hence the magnetization, is well described with use of isotropic tensors. At higher magnetic fields, as soon as the magnetization ceases to be linear in H, the magnetization is found to be strongly anisotropic. The angular dependence reflects mainly the anisotropy of the fourth order tensor, typical for the cubic symmetry.

A systematic analysis of all the symmetry allowed sources of anisotropy is presented.

P3.1

Fourier Transform Photoluminescence Excitation Spectroscopy on Medium-Band-Gap $Hg_{1-x}Cd_xTe$

F.Fuchs, K.Kheng, K.Schwarz, and P.Koidl

Fraunhofer Institut für Angewandte Festkörperphysik, Tullastrasse 72, D-7800 Freiburg, Fed. Rep. of Germany

Abstract

We report on Fourier-transform photoluminescence excitation (FTPLE) experiments in the spectral range of 1 to 4 μm wavelength. Bulk $Hg_{1-x}Cd_xTe$ (MCT) samples, as well as LPE layers and MBE grown MCT superlattices were investigated. The FTPLE results demonstrate the possibility to use this technique in the detection range of an InSb detector, thus extending the long wavelength limit of excitation spectroscopy into the mid infrared (5.5 μm). We show that new information on the origin of optical transitions observed by photoluminescence can be obtained.

In the case of bulk MCT, the FTPLE spectra reveal additional spectral details, not resolved in the photoluminescence spectra. For a $Hg_{0.66}Cd_{0.34}Te$ sample the FTPLE spectra are discussed in terms of band-to-band, band-to-acceptor, and band-to-donor transitions. In addition, the low energy-tail of the luminescence spectra can be identified as a band-to-band transition with participation of holes which are localized in disorder induced tail states of the valence band.

PACS numbers: 07.60.Ly, 78.20.-e, 78.55.Et

P.3.2

BLOCK BOUNDARIES CONDUCTIVITY AND SIZE EFFECT IN MOSAIC (HgCd)Te CRYSTALS

V.A.Pogrebnyak, D.D.Khalameida, V.M.Yakovenko

Institute of Radiophysics and Electronics, Ukrainian Academy of Sciences, Kharkov 310085 Ukraine

In this paper we present results of an experimental and theoretical study of block boundaries effect on electric conduction of mosaic (HgCd)Te (MCT) crystals. The mosaic structure of MCT single crystals results from a particular aspects of the procedure by which these materials are synthesized. X-raying and metallographic investigatons show that MCT samples have a small-angle disorientation of blocks with the average block size 100-400 μm.

The experiments reveal 2D electron channels at block boundaries in MCT single crystals. Thus MCT samples have p- or n-type bulk conductivity and two-dimensional electron conductivity along small-angle boundaries. In the work the surface electron density, electron masses and mobility in 2D channels have been determined by analisis of the set of Shubnikov-de Haas oscillations at Helium temperature. It is shown that the conductivity along 2D channels is comparable with p-type bulk conductivity of the sample at 77K. On definite conditions the bulk conductivity can be essentially decreased, then the sample will conduct along the random network of 2D electron channels. The percolation conductivity of such network are discussed in connection with anomal Hall constant behaviour of some MCT samples.

It is shown that with decreasing thickness of the sample up to the value, comparable with the average block size, one can reveal size effect and anisotropy of the magnetoresistance with respect to the orientation of the magnetic field.

P3.3

A possibility of observation of the correlated disorder effects in A_2B_6 semiconductor through the exciton spectroscopy.

M.I.Vasilevskiy, S.N.Ershov, V.V. Nikonorov

Faculty of Applied Physics, N.Novgorod University,
37 Sverdlova str., Nizhni Novgorod,603000,Russia

It was shown by a number of experimental methods that semiconductor solid solutions of A_2B_6 group, both bulk and epitaxial samples, are not perfectly random. One of the most unambigous observations of this fact is that by Zamir et.al.[1], who studyed $Cd_xHg_{1-x}Te$ alloy by means of the nuclear magnetic resonance technique. However, this technique is able to register just local deviations from randomness in occupation of the cation sites by Cd or Hg atoms. It would be interesting to have more detailed information about this non -random short-range order, namely, the spatial correlation function (with the correlation length L) , and to relate it to the method and conditions of sample preparation.

One of the methods which seems to be able to give this information is the exciton spectroscopy.Broadening of the exciton line in semiconductor alloys was observed by many researchers, and associated with composition fluctuations. It can be shown [2] that if $R_L \gg a_o$ (R_L is the exciton localization length, and a_o is the exciton Bohr's radius), the width of the line W is determined by the mean-square-root fluctuation for electron potential. Since electron states in A_2B_6- based semiconductor solid solutions follow the virtual crystal approximation,

$$W^2 \sim x(1-x)$$

and it do not depend on the correlation length. At $R_L < a_o$, however, the smoothing of small-scale fluctuations becomes quite important [2]. Accordingly, the line width should be sensitive to the correlation length:

$$W^2 \sim x(1-x)(1+ \text{const.}\frac{L}{a_o}).$$

Thus, L can be evaluated from exciton spectroscopy data.

We have studyed experimentally exciton absorption at 4.2 K in $Cd_xHg_{1-x}Te$ of different composition using samples of two kinds : thinned bulk samples and epilayers grown by the PEMOCVD tecnique. Results of preliminary processing of our experimental data show that some clustering takes place in both kinds of samples, and the correlation length is about several interatomic distances.

1. D.Zamir et. al. J.Vac. Sci. Technol. A6, 2612 (1988)
2. A.L. Efros, M.E. Raikh. In:Optical properties of mixed crystals, eds., R.J. Elliott and I.R. Ipatova, Elsevier Publishers, p.133(1988)

P3.4

TRANSIENT AND STEADY STATE LIFETIME MEASUREMENTS ON EPITAXIALLY GROWN $Cd_xHg_{1-x}Te$

S.Barton, P.Capper, A. McAllister, C.L.Jones and N. Metcalfe

Philips Infrared Defence Components, Southampton, Hants., U.K.

ABSTRACT

There is still considerable controversy in the field of recombination mechanisms in $Cd_xHg_{1-x}Te$, (CMT), particularly with regard to those operating in p-type material. It is vital to understand this behaviour, in the particular type of material being used to produce devices, if improvements are to be made. This paper reports on lifetime measurements made on both Liquid Phase Epitaxial (LPE) and Metal-Organic Vapour Phase Epitaxial (MOVPE) layers. Factors studied include the influence of surfaces, using various passivants, substrate/layer interfaces, via comparisons of data from samples still 'on-substrate' with that obtained in thin 'monolith' form and dependence of lifetimes on carrier concentration and temperature. The carrier concentrations were obtained from Hall measurements made at temperatures down to liquid Helium. The effects of various post-growth annealing schedules have also been investigated. Comparisons have been made between MOVPE material doped with acceptor impurities and that controlled by metal vacancies. As the expected trends were not always observed when transient photoconductive decay was used to determine lifetimes, measurements have been made under steady state conditions for representative samples. The former technique uses a GaAs laser as a source while the latter employs a blackbody source. In common with reported results, we find that the steady state technique produces lower lifetimes, in general. The problem of determining the electron mobility in p-type material, which is required for the steady state lifetime determination, has been addressed and both theoretical fitting to Hall data and measurements on diodes made in the particular samples have been developed [1]. It is concluded that Shockley-Read recombination governs the behaviour of most of our material at 77K while Auger 1 recombination may be dominant at 192K.

[1] N.T.Gordon et.al. (this conference).

P3.5

RAMAN INVESTIGATION NARROW-GAP SOLID SOLUTIONS OF HgCdMnTe

Yu.I.Mazur, V.P.Denisov*), S.I.Kriven, V.V.Strelchuk and G.G.Tarasov

Institute of Semiconductors of Academy of Sciences, Ukraine, Kiev

**)Institute of Spectroscopy of Russian Academy of Sciences, Troitsk*

Solid solutions of HgCdMnTe possess a number of attractive properties, due to the Mn activated strengthening of interatomic bounds, that gives new possibilities for variation of zone parameters without noticeable failure in photo-electric properties in comparison with HgCdTe. However, the increase of number of components, as a rule, leads to increase of defect-generation, in particulary, to clusters or microphases of different components appearence. We present here new data on disordered lattice dynamics of HgCdMnTe obtained under Raman investigation. Mixed semiconducting $Hg_{1-x-y}Cd_xMn_yTe$ ($x = 0.1$, $y = 0 \div 0.14$), grown by modified Bridgman technique, were of n-type with $n = (3\div15)\cdot10^{15}$ cm^{-3} at nitrogen temperature. Home-made polychromator was used with high parameters for weak signal detection. Raman spectra were excited by argon laser ($\lambda = 514.5\mu$) and investigated in geometry "on reflection". At the pumping level below 10 mWt we obtain a reproducible spectra of enriched mode content. Strong Raman lines are found for LO-phonons under the excitation at the planes (100) and (111). Numerous Raman features below the range of LO-TO splittings of HgCdTe and above it give new information on the role of structural disordering in multicomponent solid solution. A complicated spectral distribution takes place at $\nu = 95 \div 110$ cm^{-1}. We find here all signs of resonant interaction between the impurity-induced localized modes and the modes of perfect crystal. The two-phonon scattering caused by LA and TA modes of HgTe, CdTe is also out of the experimental errors. Strong modification of Raman spectra takes place under the laser power exceeding 10 mWt. The preliminary analysis shows that directed Te diffusion occurs to crystal surface, and the Te-lines dominate in Raman spectra. All other features are strongly suppressed. The data obtained give also new insight for the Mn role in lattice dynamics of HgCdMnTe.

P3.6

VIBRATIONAL MODES ACTIVATED BY STRUCTURAL DISORDERING IN FIR TRANSMISSION OF HgCdMnTe

Mazur Yu.I., Kriven S.I., Tarasov G.G. and Shevchenko N.V.

Institute of Semiconductors of Academy of Sciences, Ukraine, Kiev

A number of different vibrational states are usually observed in phonon spectra of $Hg_{1-x}Cd_xTe$ crystal which are cousistent with its two-mode behaviour under x variation. However, this set of vibrations can be substantially enriched in the case of HgCdMnTe, due to both the multimode behaviour and the increase of structural disordering of crystal lattice. We show here the experimental data for the transmission spectra of $Hg_{0.65}Cd_{0.33}Mn_{0.02}Te$ (n-type, $n = 1.5\cdot10^{15}$ cm^{-3}, thickness d = 0.2 mm) at different temperatures which are of great generality for wide range of Mn^{2+} content. Comparing spectral features observed with the data for binary and ternary components we conclude that the broad absorption band at $\nu = 30\div45$ cm^{-1} can be refered to the transverse acoustic modes of HgTe- and CdTe- type. These modes are activated by structural disordering of each of component, as well as by impurity ions of Mn^{2+}. The latters can be responsible for the band at $\nu = 53$ cm^{-1} with strong temperature dependence, which was acribed by Shen et al to resonant vibration of Mn^{2+} in CdTe. The strong absorption developes at $\nu = 95$ cm^{-1}, much lower than $\nu = 118$ cm^{-1}, which is low-energy limit of LO-TO ranges for HgCdTe. We attribute this frequency to LA mode of HgTe activated by structural disordering of HgCdTe lattice, taking into account its polarization and energy position. The complicated nature of $\nu = 190$ cm^{-1} mode is discussed. Different impurities can be responsible for this absorption as well as the 2LA(L) mode of HgTe. For the range of two-phonon transitions the striking feature is the band at $\nu = 220$ cm^{-1} which keeps its complicated structure up to T=300 K. We present some proves in favour of its side-band nature for the vibration localized at $\nu = 190$ cm^{-1}. All other features from the $\nu \approx 220 - 310$ cm^{-1} range are analyzed with symmetry arguments on account. In the range of three-phonon transitions the main feature is the peak at $\nu = 380$ cm^{-1}, which is undoubtedly the overtone of local vibration at $\nu = 190$ cm^{-1}. It should be noted an out-of-the-way modification of absorption line-shape with temperature increasing. Thus, we find new direct evidence for the change of dynamical properties of narrow-gap semiconductors at structural disordering.

P3.7

DOMINANT RECOMBINATION MECHANISM CHANGE
IN UNIAXIALLY PRESSED $Hg_{1-x}Cd_xTe$

S.G.Gasan-zade, G.A.Shepelsky, M.V.Strikha and F.T.Vas'ko

Institute of Semiconductors, Academy of Sciences of Ukraine, Kiev, 252650, Ukraine

The intrinsic recombination channels (radiative and Auger) in narrow gap semiconductors of $Hg_{1-x}Cd_xTe$ are of principal importance, because they determine the upper theoretical limit for the carriers lifetimes τ. In this report we show, that the dominant recombination pass may change due to energy spectrum transformation under uniaxial elastic pressure, and τ may essentially increase.

The recombination rates changes were obtained here as a results of radiative (τ_R) and Auger (τ_A) lifetimes computation within Kane model with an allowance for uniaxial pressure along [001] axis (energy spectrum is given in the figure). Due to the decrease of the effective masses in the upper of the two splitted bands (V_+) the direct radiative transitions occures more intensively, so that τ_R decreases with pressure. The Auger process rate on the contrary decreases, so that τ_A essentially increases.

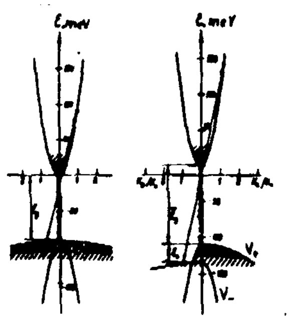

P = 0   P = 2 kBar

Experimental dependences of the lifetimes as functions of deformation $\tau(P)$ were obtained from measurements of stationary photoconductivity in n-$Hg_{1-x}Cd_xTe$ (x=0,20-0,30). They correspond well theoretical curves $\tau(P)$, so that for maximal deformation P=2kBar τ changes in 2-2,5 times. It is important, that the type of τ change with pressure unambiguously determine the intrinsic recombination mechanism.

P3.8

Electron Subband Structure in Inversion Layer of p-type $Hg_{0.79}Cd_{0.21}Te$

J.H. Chu, R. Sizmann*, K. Liu, Z.Y. Mi, S.C. Shen, and F. Koch*

National Lab for Infrared Physics
Shanghai Institute of Technical Physics
Chinese Academy of Sciences, Shanghai 200083, China

*Physik-Department E-16, T. U. Munchen
D-8046 Garching, F. R. Germany

It was found that a resonant defect level exists in p-type $Hg_{0.79}Cd_{0.21}Te$ bulk materials with high native doping concentration[1]. The subband model that was used to derive the subband structure directly from experimental results[2] can be more general after it is modified by taking account of the influence of the resonant defect states on subband structures. By using the modified model the subband structures of n-type inversion layer in the MIS structure of p-type $Hg_{1-x}Cd_xTe$ (x=0.21) bulk materials with different doping concentrations ranging from $N_A=3\times10^{16}$ to 7×10^{17} cm^{-3} have been derived quantitatively from the experimental results of capacitance spectroscopy, SdH oscillations and cyclotron resonance. Therefore, the dependence of the subband structure on doping concentration and energy gap adjusted by applied pressure has been obtained for the first time.

The p-type $Hg_{1-x}Cd_xTe$ samples with high doping concentration are very much helpful for the investigation of subband electron Landau levels because the effect of k-linear term of subband electron spin-orbit interaction is significant for the samples. Based on the subband structure obtained from the above model, the shifting and crossing effect as well as the wave-function mixture effect of the Landau levels and the effective g^* factor of the subband electrons for p-type $Hg_{0.79}Cd_{0.21}Te$ have been quantitatively investigated from both theory and experiments such as SdH oscillations, cyclotron and spin resonance of subband electrons.

[1] J.H. Chu, Z.Y.Mi, R. Sizmann, F. Koch, J. Ziegler, and H. Maier, The US workshop on physics and chemistry of HgCdTe and other II-VI compounds, Dallas, TX, Oct.8-10, 1991.
[2] J.H. Chu, Z.Y. Mi, R. Sizmann, and F. Koch, Phys. Rev. B44(1991), 1717.

P3.9

The Study of Far-infrared Phonon Spectra in $Hg_{1-x}Cd_xTe$

J.H. Chu and S.C. Shen

National Lab for Infrared Physics
Shanghai Institute of Technical Physics, Chinese Academy of Sciences, Shanghai 200083, CHINA

The far infrared absorption and reflection spectra measurements were performed on the $Hg_{1-x}Cd_xTe$ samples with x=0.18 to 0.45 in the wavenumber region of 15-500 cm^{-1} at temperatures from 4.2K to 300K.

In addition to the absorption structures of two-phonon combination on both sides of the reststrahlen band of the material, a low frequency absorption band has been observed between 20-50 cm^{-1} in all the measured samples. By comparing it with the phonon spectra of $Hg_{1-x}Cd_xTe$, which have been estimated by means of the ab initio density functional calculations of planar force constants, we have attributed the low frequency absorption band to the TA band modes induced by the disorder and "doping" effects resulting from the crystalline mixing in the material. The dependence of the two-phonon combination absorption on temperature and composition was determined in the alloy compositions ranging from 0.18 to 0.45 for temperatures from 4.2 to 300 K.

In the measured reflection spectra of the samples, we observed not only the fine structures of the CdTe-like optical phonon reflection band, but also the complex structure of the HgTe-like band for the low composition samples. The dependence of the spectral structures on the composition and the temperature of the samples, and the plasmon-LO phonon coupling effect have been investigated. The fine structures of the reflection spectra have been explained based on the multi-mode quasi-harmonic oscillator model. By means of the classical oscillator matching method, the curve-fitting calculations were performed for the experimental reflection spectra. The complex dielectric function spectra and the complex refractive index versus frequencies have been obtained from a satisfactory fitting.

P3.10

Bias Effects on the Electrical Characterization of Deep Levels in HgCdTe

Susan J Zachman, Eliezer Finkman and Gad Bahir

Department of Electrical Engineering
Technion - Israel Institute of Technology
Haifa 32000, Israel

A study of deep traps in HgCdTe n-type $x = .3$ and $x = .225$ MIS capacitor samples is presented using Deep Level Transient Spectroscopy (DLTS). It is shown that DLTS is a useful electrical characterization tool, but care must be taken when analyzing results obtained for a narrow band gap semiconductor such as HgCdTe.

Our measured DLTS scans show a marked bias effect. The emission rate is strongly affected by bias, and consequently, the deduced activation energy is a strong function of the measurement bias used. The Poole-Frankel effect cannot sufficiently account for this bias dependence. We explain the effect by assuming that emission alone is the dominant process near the interface, whereas capture and emission processes compete near the bulk end of the depletion region. The relative proportion of the widths of the two regions is strongly bias dependent. Analysis that includes this effect gives corrected values for the emission rate, and hence a bias independent energy level for the trap. This energy is extracted from DLTS measurements on the assumption that the trap energy (E_T) follows the majority carrier band edge. Under this standard definition we find $E_T = E_c - .035$ eV for the $x = .3$ sample and $E_T = E_c - .023$ eV for the $x = .225$ sample.

The above assumption was examined and deemed questionable since the band gap in HgCdTe changes significantly with temperature during the DLTS measurement. There is no reason to believe that the trap energy will follow the majority carrier band edge. In general, E_T will be a function of temperature. To derive this function we measure the capture cross section over the temperature range. We then combine this information with the corrected expression for the emission rate, and use thermodynamic considerations to calculate the temperature dependence of the trap energy.

P3.11

Precision of the Hall Quantization in Naturally Occurring Two-Dimensional System–HgCdMnTe Bicrystals.

G. Grabecki[1], A. Wittlin[1,2], T. Dietl[1], P.A.A. Teunissen[2], S.A.J. Wiegers[2] and J.A.A.J. Perenboom[2]

1) Institute of Physics, Polish Academy of Sciences, Al. Lotnikow 32/46, PL-02-668 Warsaw, Poland

2)High Field Magnet Laboratory and Research Institute for Materials University of Nijmegen, Toernooiveld NL 6525 ED Nijmegen The Netherlands

ABSTRACT

Magnetoresistance measurements on naturally occurring two-dimensional electron system–inversion layers adjacent to grain boundaries in narrow gap semimagnetic semiconductor $Hg_{0.75}Cd_{0.23}Mn_{0.02}Te$ (E_g=185 meV) have been performed. In order to establish a most favorable conditions for the occurrence of the quantum Hall effect, magnetic fields up to 20 T simultaneously with millikelvine temperatures have been applied. Regardless of the natural (and therefore uncontrolled) origin of the studied samples, precise Hall quantization (*plateau* flatness up to $5 \cdot 10^{-5}$ has been measured) as well as nearly vanishing diagonal resistance minima were observed (see Figure). This result may be regarded as a subsequent evidence of the quantum Hall effect universality. Additionally, detailed analysis of the magnetoresistance data revealed severe macroscopic electron density gradients in our system. We have found that in high magnetic fields the inhomogeneities lead to formation of the network of Hall resistors with different quantum indices. Temperature dependence of the both Hall and diagonal magnetoresistances has been studied in the range between 100 mK and 40 K. The mobility gaps associated with Landau splittings were found to be about 10 times larger than those arising from spin splittings. Such result is hard to be understood within a framework of the conventional theory of narrow gap systems which predicts that these gaps should be nearly equal. However, the observed behaviour may be explained in terms of the exchange interaction between conducting electrons and magnetic $Mn^{2}+$ ions in our semimagnetic system.

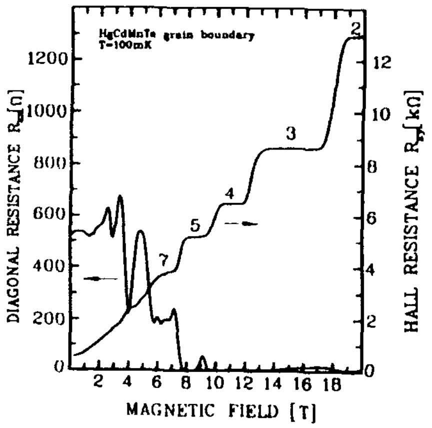

P3.12

The Optical Absorption Coefficient of HgTe-CdTe Superlattices - Theory and Experiment

E. Bangert, P. Boege, V. Latussek and G. Landwehr

Physikalisches Institut der Universität Würzburg, Am Hubland, 8700 Würzbu g

During the last decade a rather large number of papers concerning the calculation of semiconductor superlattice states have been published

This is mainly due to the difficulty of being confronted with the following problems: First, the incorporation of realistic band structures for both materials and which are basically founded on translational symmetry. Secondly, this symmetry is broken at the interface of barrier and well. Finally, the special and interesting features of superlattices just originate from this symmetry violation. In other works, inside each layer the dynamic of the electrons is determined by the E(k)-relations, based on a one or multi band approach, but dynamic of electrons crossing the interface cannot be formulated in a straightforward fashion of band structure concepts.

Among the various approaches of trying to solve these problems are two extrema, namely the tight binding and the envelope function method. In both cases experimental results must be used to fit the unknown parameters of the theories in order to obtain a realistic band structure. The tight binding calculations fit the coupling integrals of atomic wave functions of adjacent atoms. Therefore, these coupling integrals are known inside the material, but not for the crossing of the interface. The envelope function method utilizes band parameters like γ_1, γ_2, γ_3, m^* and Ep which are again known for each material, but even defined close to the interface region.

P4.1

Field-Effect Controlled Resonant Interband Tunneling in Electron Surface Layers on InAs and $In_{53}Ga_{47}As$

B. Föste[1], U.Kunze[2], G. Zwinge[3], A.Schlachetzki[3]
([1]Institut für Elektrophysik and Hochmagnetfeldanlage der Technischen Universität Braunschweig, [2]Institut für Technische Physik, Universität Erlangen-Nürnberg, [3]Institut für Halbleitertechnik, TU Braunschweig, Germany)

We report on an experimental study of a novel three-terminal negative differential conductance (NDC) device. Interband tunneling from a 2D electron inversion layer through the depletion barrier into resonant states of the bulk valence band is controlled via an applied gate voltage of an MIS structure.

Sample preparation started either from bulk n-type InAs with 1 µm Zn diffused p^+-layer or from MOVPE grown p^+-InGaAs (1 µm) layers on n-InGaAs (2 µm) on n^+-InP substrates. After 1.5 µm mesa etching an oxide layer (20...100 nm) was anodically grown. Subsequently Yb/Al gate and p^+-contacts were formed by evaporation and standard lithography.
An overlap of the mesa by the gate electrode provides an ohmic contact of the n-type substrate to the electron inversion layer at the InGaAs-oxide interface if the gate voltage V_G is kept above the threshold of -1.4V (+1.2V) for InAs (InGaAs). At T=77 K and T=4.2 K upon increasing V_G, the peak current can be varied by a factor of 5,000 (500) with a maximum peak-to-valley current ratio in excess of 2 (16). The peak voltage is shifted from 30 mV to 300 mV.

From the decrease of the peak current under magnetic fields up to B=15T, applied parallel or perpendicular to the interface, we infer that the effective tunneling electric field is independent of V_G. In perpendicular orientation, the InGaAs samples show oscillations in d^2I/dV^2-vs-B curves which reflect the Landau quantisation of the surface electrons .

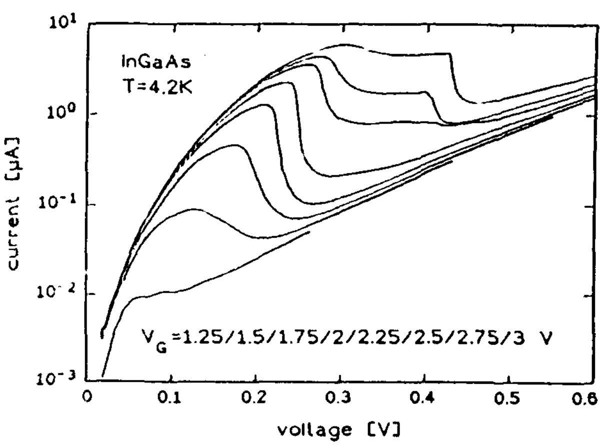

Semi logarithmic plot of the current-voltage characteristic of an InGaAs tunnel junction with gate voltage as a parameter.

P4.2

Far infrared spectroscopy of strained AlSb/InAs/AlSb quantum wells

M.J. Yang, P.J. Lin-Chung, R.J. Wagner, J.R. Waterman, W.J. Moore, B.V. Shanabrook, and M. Fatemi
Naval Research Laboratories, Wahsington D.C., USA

We have systematically studied the far infrared absorption due to InAs TO phonons in strained InAs single quantum wells, for the first time. We have found that the TO phonon energy (ω_{TO}) is virtually unchanged when the well thickness is varied from 40Å to 250Å. Th ..dependence of ω_{TO} on the confinement effect implys that the TO phonon branch is dispersionless up to 15% of the Brillouin zone. In contrast, ω_{TO} shifts to a lower energy when the strain in InAs is increased. The degree of the strain in InAs is varied by using different buffer layers. When thick GaSb or AlSb layers are grown as the buffer layers, the InAs is under biaxial tension and its vertical lattice constant, measured by x-ray diffraction, is reduced to 6.0171Å or 6.0000Å, respectively. We obtain an empirical expression for the strain dependence of TO phonon energy, $\Delta\omega_{TO} = (1.36\varepsilon_{\perp})\omega_{TO}$, where $\Delta\omega_{TO}$ and $\varepsilon_{\perp}$ are the relative change of ω_{TO} and the vertical strain, respectively.

The electron effective mass in InAs is expected to be reduced as a result of biaxial tension. To examine this effect, we have performed cyclotron resonance measurements at 1.2K, with magnetic fields of up to 12T. The CR linewidth increases as the well width is decreased. This can be explained by two factors. One is that the electron wave function penetrates deeper into the barrier as the well width becomes narrower, and the interface roughness would reduce the electron lifetime (homogeneous broadening). The other is that the nonuniformity of the well thickness would result in inhomogeous broadening in subband energy. In addition, the electron effective masses are found to be insensitive to the degree of the strain and vary from $0.034m_o$ for the 187Å sample to $0.047m_o$ for the 63Å sample. The measured effective masses are all much larger than the unstrained band edge mass, $0.023m_o$. We carried out a detailed calculation of subband energies and subband in plane effective masses using the four band $\mathbf{k}\cdot\mathbf{p}$ model, including the strain effect and the effect due to the penetration of the electron wave function into the AlSb barriers. We find that the enhancement of the observed effective mass results partially from the nonparabolic band of InAs, and partially from the penetration of the wave function into the barrier. Excellent agreement with experiment is achieved for samples with narrow well widths, while the calculation still predicts smaller masses than those observed for samples with larger well widths. Possible explanations such as the space charge effect will be discussed.

P4.3
The Effect of Landau Quantization on Cyclotron Resonance in a non-parabolic Quantum Well

J. Scriba, A. Wixforth and J. P. Kotthaus
Sektion Physik, LMU München
C. Bolognesi, C. Nguyen, G. Tuttle, J. H. English and H. Kroemer
Department of Electrical and Computer Engineering, UC, Santa Barbara

Quantum wells consisting of epitaxial layers of AlSb and InAs are characterized by unusually high confinement energies (≈1.3 eV), high carrier densities ($10^{12}cm^{-2}$) and relatively high electron mobilities (400000 cm^2/Vs)[1]. The electronic properties make the system a promising candidate for transistor applications. Moreover, the small effective mass of the active layer InAs yields high quantization energies which make electro-optical applications attractive such as tunable detectors based on resonant quantum effects.

To exploit such mechanisms it is necessary to take into account the effects of band non-parabolicity which has a much stronger influence in InAs-quantum wells than in the widely used GaAs-systems. We investigate cyclotron resonance absorption (CR) at low temperatures (T=2K) and high magnetic fields (B<15T). By detecting discrete CR transitions between different Landau states, we observe directly the effect of subband non-parabolicity on the Landau ladders.

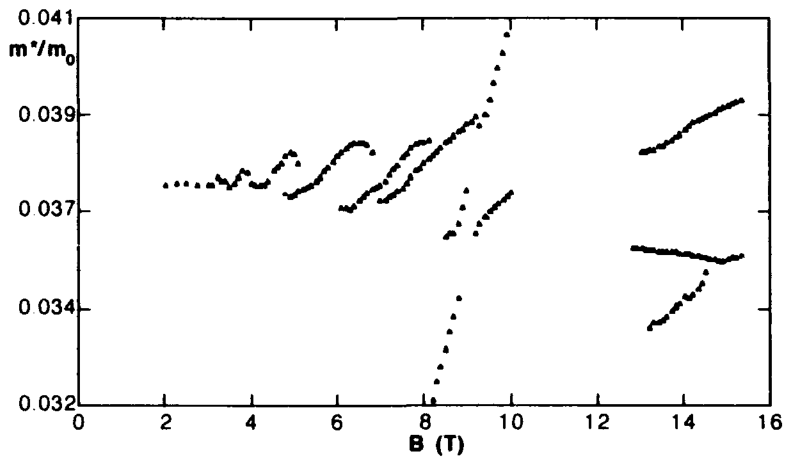

Oscillations of the effective mass in InAs/AlSb quantum wells as extracted from cyclotron resonance measurements.

The resonance positions and splittings of the CR are explained in a straightforward single particle model. Since subband energies can easily be calculated by self-consistent methods for the "infinitely deep" quantum well, our model employs no fit parameter once the carrier density and the well width are known. The results of our analysis can also be applied to other quantum well and heterojunction systems. It remains surprising why discrete CR lines of different simultaneous Landau transitions haven't yet been observed in other non-parabolic 2D electron systems. The differences to our observation will be discussed.

---

[1] Gary Tuttle, Herbert Kroemer and John H. English, J. Appl. Phys. 65, 1989

P4.4

Photoconductivity in AlSb/InAs Quantum Wells

C. Gauer, J. Scriba, A. Wixforth and J. P. Kotthaus
Sektion Physik, Universität München, 8 München 22, Germany
Ch. Nguyen, G. Tuttle, J. H. English and H. Kroemer
Quest Center, UC Santa Barbara, CA 93106, USA

The enormous progress in epitaxial growth techniques during the last years has made it possible to grow even exotic, lattice mismatched heterostructures. In particular, the AlSb/InAs system is a promising candidate for future electro-optic applications. It combines large confinement energies ($\approx$1.3 eV) with high carrier concentrations ($\leq 3 \cdot 10^{12}$cm^{-2}). To date, despite the large lattice misfit between the GaAs substrate and the active heterostructure very high electron mobilities can be obtained ($\mu_{max} \approx 60$m^2/Vs).
We investigate the electrical and optical properties of such AlSb/InAS quantum wells. The system forms a type II staggered heterojunction in which we study quantum wells of widths between 12 and 20 nm. In contrast to other material combinations the photoconductivity can be persistently enhanced and reduced depending on the incident wavelength. We determine the carrier densities and the electron mobilities as well as their temperature dependence from cyclotron resonance and Shubnikov-de-Haas experiments. In a typical sample the carrier density decreases from $n \approx 1.6 \cdot 10^{12}$cm^{-2} for E_{ph}=1.3eV to $n \approx 0.9 \cdot 10^{12}$cm^{-2} for E_{ph}=2.2eV at T=4K. The reduction of the electron mobility due to reduced screening for the same light energies makes this negative persistent photo effect even more pronounced. It is only quenched by heating the sample to T>130K.
We ascribe our experimental findings to the electron-hole recombination via deep defects at the AlSb/InAs interface leading to a loss of electrons in the well. It was suggested that these interface states are Tamm states since the high mobility of the electrons in the well indicates that the potential of the defects must decrease much more strongly than the Coulomb potential.[1] The holes are believed to be generated in the GaSb cap layer of the structure and to follow the field gradient to the AlSb/InAs interface. One set of our samples shows an oscillatory structure superimposed on the photoconductivity spectrum. We attribute this phenomenon to multiphonon emission of holes in the AlSb layer. Our experiments thus provide new insight into the band lineup and the nature of electronic defects of this novel system.

---

1) H. Kroemer, Ch. Nguyen, Bobby Brar, "Are there Tamm State Donors at the InAs-AlSb Quantum Well Interface?", to be published.

P5.1

Insulator-Metal Transition in HgTe in Crossed Magnetic and Electric Fields

P. Pfeffer and W. Zawadzki

Institute of Physics, Polish Academy of Sciences, 02668 Warsaw, Poland

Zero-gap semiconductor HgTe is considered theoretically in the presence of crossed magnetic and electric fields.

The external magnetic field opens an energy gap between the Landau levels in the conduction and the heavy-hole valence bands. An electric field in the crossed-field configuration closes this gap, inducing an insulator-metal transition at low temperatures.

The structure of Landau levels in HgTe in crossed fields has been calculated using Pidgeon and Brown model for B ‖ (111) crystal direction. The energies of the system have been found using the Evtuhov procedure. It has been shown that in principle the electric field shifts the conduction Landau levels downwards and the hole levels upwards. However, the Luttinger ("quantum") effects for the lowest quantum numbers in both bands complicate this simple picture. In order to decide whether (and between which levels) the gap really closes, we have also calculated the k_z-dependence of the Landau subbands in both spin sets. It turns out that the insulator-metal transition occurs between the "a" set (spin up) levels, in spite of the fact that the lowest conduction level 0^+ moves upwards in the electric field, contrary to semiclassical expectations. For B = 2 T the insulator-metal transition occurs at [illegible] $\approx$ 1 kV/cm.

Finally, we have considered effects related to the center of electron and hole oscillations in crossed fields and showed that the insulator-metal transition is preceded by tunneling effects.

P5.2

INFLUENCE OF HEAVY HOLE SCATTERING ON THE MAGNETOTRANSPORT BEHAVIORS OF P-TYPE ZERO-GAP $Hg_{1-x}Mn_xTe$

Guozhen Zheng Jinxi Shen Shaoling Guo Dingyuan Tang

National Laboratory for Infrared Physics
Shanghai Institute of Technical Physics
Chinese Academy of Sciences

The transport behaviors of zero-band gap p-type $Hg_{1-x}Mn_xTe$ samples (X=0.03 and 0.065) are investigated for temperatures from 0.3K to 4.2K and magnetic field up to 7T . The striking anomalies of the magnetoresistance have been observed in both samples.

A giant increase in the magnetoresistance and broadness of the last two SdH oscillation have been found for $Hg_{1-x}Mn_xTe$ with X=0.03 experimentally. The dependence of the energy of Landau levels in the Γ_8 band for K_z=0 on the magnetic field has been calculated using the modified Pidgeon-Brown model for the $Hg_{0.97}Mn_{0.03}Te$ alloy at different temperatures. It indicated that the conduction energy levels, $a_c(0)$, $a_c(1)$ are below the highest valance level $b_v(-1)$. The overlap between the highest valance band $b_v(-1)$ and the conduction energy levels $a_c(0)$, $a_c(1)$ leads to a new scattering mechanism of free electrons i.e. the threshold scattering of conduction electrons, which prevails over intraband scattering if there exists a finite overlap between the valance and conduction energy levels[1].

A step negative magnetoresistance associated with the minimum Hall mobility for B=1.5T at T=0.3 occurred in another $Hg_{1-x}Mn_xTe$ sample (X=0.065) while the Hall coefficient exhibited a sign reversal near B=0.4T. Because $a_v(-1)$ and $b_v(-1)$ heavy hole Landau subbands are shifted towards the conduction band strongly with increasing field B, there are two heavy hole bands in the vicinity of the Fermi level. When the Fermi level is merged into the top of $a_v(-1)$ band, the scattering of the holes of $b_v(-1)$ band would be the largest.

(1). I.I.Lyapilin Phys. Lett., 93A, 5, 245(1983)

P5.3

Magnetotransport Investigations at InSb and $Hg_{1-x}Cd_xTe$ Bicrystals in Tilted Magnetic Fields

G. Nachtwei, N.J. Bassom*, W. Kraak, R.J. Nicholas* and M. Watts*

Fachbereich Physik der Humboldt- Universität zu Berlin
Institut für Festkörperphysik
Invalidenstraße 110, Berlin D-O-1040, FR Germany
* University of Oxford, Clarendon Laboratory
Parks Road, Oxford OX1 3PU, England, UK

Abstract

The Hall effect and the Shubnikov- de Haas effect of a quasi-two-dimensional inversion layer adjacent to grain boundaries in InSb and $Hg_{0.23}Cd_{0.77}Te$ bicrystals are investigated in magnetic fields up to 14.5 T, temperatures down to 0.4 K and at different angles between the grain boundary plane and the magnetic field.
For magnetic fields perpendicular to the grain boundary interface a complicated pattern of Shubnikov- de Haas oscillations and well developed quantum Hall plateaux with the quantum numbers j= 7 and j= 9 are observed at a HgCdTe sample.
A cosine dependence of the Hall coefficient and the oscillation period of the ground subband in tilted fields was found for both InSb and HgCdTe bicrystals, whereas the first excited subband showed remarkable deviations from the two dimensional behaviour. From these deviations, an estimate of the spatial extension of the wave function is given. The diamagnetic Shubnikov- de Haas effect yields depopulation fields which can be explained within the Reisinger- Koch model.
First results of cyclotron resonance measurements show well separated transmission dips for different subband masses at HgCdTe bicrystals.

Correspondence to: Dr. G. Nachtwei (address as above)
fax: Berlin (Ost) 372 / 2803 477
Tel: 2803 347

P5.4

Phonon-Assisted Interband Magneto-Optical Transitions in HgCdMnTe

W. Zawadzki*, E. Dudziak+, L. Z. Jedral+,
E. Placzek-Popko+, and J. Bozym+
*Institute of Physics, Polish Academy of Sciences
Warsaw, Poland 02-668
+ Institute of Physics, Technical University of Wroclaw
Wroclaw, Poland 50-370

Magneto-optical properties of narrow-gap $Hg_{1-x-y}Cd_xMn_yTe$ photo-diodes have been investigated. The samples were grown by isothermal vapor phase epitaxy, they had a Cd content of $x < 0.22$, a Mn content of $y < 0.012$, and were characterized by the energy gaps $70 < E_g < 150$ meV. Optical measurements were performed in the Faraday configuration with the use of circularly polarized light.

The photovoltaic effect showed oscillatory behavior, related to the interband $\Gamma_8 \rightarrow \Gamma_6$ magneto-optical transitions. The data were analyzed using the Pidgeon-Brown model, completed by the exchange terms. In addition to the usual interband transitions, well described by the theory, we have observed for the first time interband magneto-optical transitions assisted by the emission of optic phonons. The measured phonon energies were $15.8 < \hbar\omega_L < 17$ meV, depending on the chemical composition of the sample.

A detailed theoretical analysis has shown that the inetrband phonon-assisted transitions possess resonant character only if they originate from the "camel-back" shaped Γ_8 Landau subbands $\epsilon_n(k_z)$. Thus, our observation confirms the existence of "camel-back " Γ_8 subbands, which have been predicted theoretically for a long time, but never observed.

P5.5

Band Offsets in Eu-containing Lead Chalcogenides and Lead Chalcogenide Superlattices from Spectroscopical Data

K. H. Herrmann, K.-P. Möllmann, J. W. Tomm[1]
H. Böttner, A. Lambrecht, M. Tacke[2]
I. V. Kolesnikov, A. E. Yunovich[3]
A. I. Fedorenko, O. A. Mironov, A. Y. Sipatov[4]

[1] Humboldt-Universität Berlin, Institut für Festkörperphysik, O-1040 Berlin, FRG
[2] Fraunhofer-Institut für Physikalische Meßtechnik, W-7800 Freiburg, FRG
[3] Lomonossov Moscow State University, 117 234 Moscow, Russia
[4] Polytechnical Institute Charkov, Ukraina

The results of an experimental study of the optical (transmittance, luminescence) and photoelectrical properties (photocurrent exciting spectroscopy, photocurrent decay) of europium containing alloys ((Pb,Eu)Se, (Pb,Eu)S) and superlattices (PbS-EuS, PbSe-PbS) are presented.

From the study of the alloy properties in the narrow-gap region a model of the bandstructure of the mixed crystal system for rather small Eu contents was deduced. The extrapolation of these data to the binary wide-gap components (EuSe, EuS) allows estimating the band offsets.

From the fit of luminescence spectra from PbS-EuS and PbSe-PbS superlattices independent band offset data are obtained.

Both sets of data confirm the thesis, that the valence band edges of the lead chalcogenides (PbSe,PbS) formed by the p-orbitals of the chalcogenes have a comparable distance to the vacuum level as the valence band edges of the europium chalcogenides formed by the 4f-orbitals of the europium atoms.

P5.6

SHUBNIKOV-de HAAS OSCILLATIONS IN $Cd_3(As_xP_{1-x})_2$

A. Nateprov * [a], I. Laue [a], M. von Ortenberg [a], and E. Arushanov [b]

[a] Institut für Halbleiterphysik und Optik, Hochmagnetfeldanlage, Technische Universität Braunschweig,
D-3300 Braunschweig, F.R. Germany
[b] Institute of Applied Physics, Kishinev, Moldavia

In the ternary semiconductor $Cd_3(As_xP_{1-x})_2$ for x=0.70 the forbidden gap vanishes. It was shown earlier by [1] that for this situation the evaluation of the Shubnikov-de Haas (SdH) yields a spherical Fermi surface for the electrons involved with a cyclotron mass $m_c = (0.05 \pm 0.01)m_0$ for a carrier concentration of $n = 1.8{*}10^{24}$ m^{-3}. We report now on SdH experiments in a variety of $Cd_3(As_xP_{1-x})_2$ with different values of x near the zero-gap condition. "As grown" samples were obtained by the sublimation technique. The measurements were carried out in in the 2 - 10 K temperature range in quasi-stationary magnetic fields up to 17 T using Bitter solenoids. Interesting results were obtained for samples with $x = 0.68 \pm 0.03$ exhibiting an electron concentration from the Hall effect of $n = 2.6{*}10^{23}$ m^{-3} and a mobility $\mu_H = 5.6$ $m^2/(Vs)$ at 4.2 K. SdH-like oscillations were observed in both the transverse magnetoresistance (curves 1, 2) and the Hall voltage (curve 3). A splitting of the n = 0 and n = 1 quantum states (see curve 1) is clearly resolved for a 40° angle between the C_4-axis and the external magnetic field B. An unexpected result is the disagreement between the electron concentrations as calculated from Hall and SdH effects respectively ($n_H/n_{SdH} = 3.9$). Comparison of our data with those reported in [1] suggests that the Fermi surface of $Cd_3(As_xP_{1-x})_2$ at the electron concentration of $n = 2.6{*}10^{23}$ m^{-3} is more complex than of the spherical, single-valley type. This may result from the influence of lattice vacancies on the energy band structure of $A_3^{II}B_2^{V}$ compounds as predicted by [2].

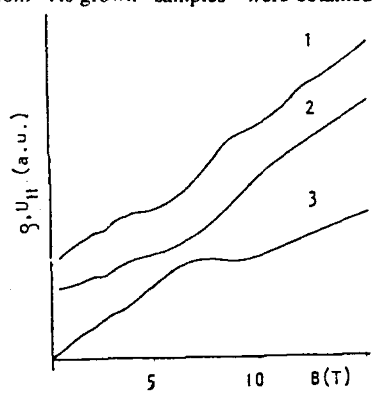

[1] E.K. Arushanov et al., Sov. Phys. Semicond. **16**, 1216 (1982)
[2] B. Plenkiewicz, P.R. Wallace, P. Plenkiewicz, Solid State Comm. **50**, 681 (1984)

* On leave of absence from Institute of Applied Physics, Kishinev, Moldavia

P6.1

Excess currents in narrow gap $Cd_xHg_{1-x}Te$ p-n junctions

N.L.Bazhenov, S.I.Gasanov, V.I.Ivanov-Omskii

A.F.Ioffe Physico-Technical Institute, St.-Petersburg, Russia

The performance of IR photodiodes fabricated in narrow gap semiconductors is limited by the value of dark reverse currents. In some cases the value of reverse current exceeds one calculated taking into account the well known mechanisms - thermally generated current, band to band and trap to band tunneling current .

The starting material was undoped LPE epylayers with hole concentration about 10^{16} cm^{-3}. The photodiodes have been formed by implanting boron. It was shown that the current-voltage characteristics of the samples with excess currents had peculiarities. The excess currents proved to be connected with the fluctuations of charged impurities density which changed the local transparency of the barriers. A quantitative analysis of current-voltage characteristics based on the Raich-Ruzin theory [1] was made. The analysis indicated that the samples with excess currents were strongly compensated. The influence of the compensation degree on the excess currents as well as on the dark current nonuniformity in the multi element system are discussed.

1. Raich M.E., Ruzin I.M. Physica i Technika poluprovodnikov (Sov. Phys. Semicond.),1985, v.19, p.1217 (in Russian).

P6.2

ELECTRON MOBILITY IN P-TYPE EPITAXIALLY GROWN $Cd_xHg_{1-x}Te$

N.T.GORDON

DRA (ED), RSRE, Malvern, Worcs, U.K.

S.Barton, P.Capper, C.L.Jones and N.Metcalfe

Philips Infrared Defence Components, Southampton, Hants, U.K.

ABSTRACT

There is a need to predict photodiode parameters from measurable material properties in $Cd_xHg_{1-x}Te$, (CMT). These properties are doping levels in both the p-type and n-type sides, minority carrier lifetimes and mobilities, intrinsic carrier concentration and composition,x. This paper is primarily concerned with the electron mobility in p-type material. Electron mobility values in n-type material are well established from Hall effect measurements, however, in p-type material these values are likely to be lower due to both ionised impurity and electron-hole scattering mechanisms. In this work, the electron mobility has been deduced from the variation of the reverse saturation current (I_{sat}) with magnetic field [1]. Measurements as a function of temperature (77K - room temperature) have been performed on cylindrical (LOOPHOLE) diodes made in epitaxially-grown CMT layers. The measured mobilities are considerably below those obtained in low doped n-type material which can largely be accounted for using ionised impurity scattering [2]. Comparisons are made between these measured electron mobilities and values derived from theoretical fitting to Hall data. This shows that the mobility ratio, b is not, in general, constant with temperature. The measured values of the electron mobility have been used in determining steady state lifetimes measures in the same samples[3]. Finally, these lifetimes have been compared to values predicted from diffusion length measurements, from Electron Beam Induced Current (EBIC) studies, in the same diode arrays.

[1] F.E. Schacham and E.Finkman, J.Vac.Sci.Technol.,A7(2),(1989),378
[2] D.L. Rode, Phys.Rev.B,3(10)(1971),3287.
[3] S.Barton et al. (this conference)

P6.3

(Hg,Cd)Te layers grown by MBE on GaAs using different buffer layers

N. Hoffmann, K. Jacobs, L. Parthier, T. Teubner[1)]

K. H. Herrmann, W. Hoerstel, K.-P. Möllmann, J. W. Tomm[2)]

[1)] Humboldt-Universität Berlin, Institut für Kristallographie und Materialforschung, O-1040 Berlin, FRG

[2)] Humboldt-Universität Berlin, Institut für Festkörperphysik, O-1040 Berlin, FRG

GaAs is a common substrate material for Molecular Beam Epitaxy of II-VI compounds. The lattice mismatch between (Hg,Cd)Te and GaAs is more than 14 %. In order to obtain (100) epitaxial overgrowth only, a thin ZnTe layer is grown first. In order to reduce the effect of the large misfit, different buffer layers were applied.

In this paper the following buffer layers are investigated: CdTe layers of various thickness, (Cd,Zn)Te of different composition and thickness, and superlattices of the types CdTe/ZnTe as well as CdTe/(Cd,Zn)Te. The narrow-gap top layer was investigated by the following methods:

- X-ray diffraction,
- infrared photoluminescence excited with c.w. and pulsed YAG laser,
- galvanomagnetic measurements,
- photoconductivity spectroscopy and p.c. decay.

The properties of (Hg,Cd)Te layers grown on different buffers are compared with each other.

The recombination of non-equilibrium carriers is strongly influenced by the different kinds of buffer layers. This will be related with the influence of the buffer layer on crystallographic perfection and impurity accumulation at the interfaces.

P6.4

Identification of Extended Defects in n-$Hg_{1-x}Cd_xTe$ by Galvanomagnetic Measurements

N.N. Berchenko[1], J.S. Budzhak[2], K.R. Kurbanov[1] and G. Sasvari[1,2]

[1] Lvov Polytechnical Institute, Lvov, Ukraine
[2] Research Institute for Technical Physics of the Hungarian Academy of Sciences, Budapest, Hungary

In this work we show that the measurement of the Hall constant, R(H), versus the magnetic field in n-$Hg_{1-x}Cd_xTe$ at 77K permits to identify and characterize extended defects. Bulk, stochiometrically annealed crystals of $Hg_{1-x}Cd_xTe$ ($x = 0.2$, $n < 2x10^{14} cm^{-3}$, $\mu > 2x10^5 cm^2/Vsec$ at 77 K) were studied. R(H) was measured in the range of 0.1-1.6 kG for steady and up 100kG in pulsed magnetic fields. Based on the behaviour of the R(H) curves obtained on a great number of samples they can be classified into three groups. The first group, to which the most perfect crystals belong, is characterized with the classical field dependence of R(H) consisting of two plateaux in weak and strong (53 kG) magnetic fields in agreement with the theoretical value of Hall-factor in n-$Hg_{1-x}Cd_xTe$. For samples belonging to the second group, a minimum appears on the R(H) curve between the plateaux due to the influence of isolated inhomegeneities having higher conductivity than the conductivity of the surrounding medium. These are presumably Te-rich precipitates transformed during the anneal into HgTe inclusions. The distinctive feature of the third group is a monotonous decrease of R(H), reaching saturation in fields > 50 kG. This is attributed to a second set of electrons, which appear when the dislocation density in the sub grain boundaries exceeds a critical value at a certain misorientation along the boundary, corresponding to the appearance of percolation threshold.

Finally the influence of such defects on electron localisation in $Hg_{1-x}Cd_xTe$ at low temperatures is discussed.

P6.5

CRYSTALLIZATION OF HgSe BULK CRYSTALS UNDER HIGH GAS PRESSURE AND THEIR ELECTRICAL CHARACTERISATION

J.C.Tedenac, M.C.Récord, R.M.Ayral-Marin

Laboratoire de Physicochimie des matériaux,
Université de Montpellier II, Sciences et Techniques du Languedoc, 34095 Montpellier cedex 5, France

L.Konczewicz*, J.Jun

"Unipress", High Pressure Research Center of Polish Academy of Sciences, 01-142 Warsaw, Poland

J.L.Robert

Groupe d'Etudes des Semiconducteurs,
Université de Montpellier II, Sciences et Techniques du Languedoc, 34095 Montpellier cedex 5, France

ABSTRACT :

The gradient freeze method, under high pressure conditions, was applied to elaborate the bulk HgSe material. A tree zones furnace, specially constructed, with possibility of programmable gradient was installed inside a gas pressure chamber of 30 mm internal diameter and the experiments were carried out under gas pressure of argon or nitrogen up to 1.5 GPa. The crystals grown under different pressure conditions for the two of gas medium were characterised by electrical transport measurements. The Hall effect and conductivity were studied as a function of pressure (up to 1.3 GPa) and temperature (in the range 4.2 - 300 K)

* present address :
Groupe d'Etudes des Semiconducteurs,
Université de Montpellier II, Sciences et Techniques du Languedoc, 34095 Montpellier cedex 5, France

P7.1

ENERGY SPECTRUM IN QUANTUM DOTS OF IV-VI NARROW-GAP SEMICONDUCTORS

V.K.Dugaev, V.I.Litvinov, O.A.Mironov, P.P.Petrov

Institute of Radiophysics & Electronics, Academy of Sci.of Ukraine, 12 Acad. Proskura St.,Kharkov 310085, Ukraine, FAX:(7-0572)44-11 05

M.Oszwaldowski

Technical University of Poznan, Piotrowo 3, 60-965 Poznan, Poland

We calculated the size-quantised levels of a system consisting of two narrow-gap semiconductor materials with different energy gaps. For instance it could be a small PbSnTe ball inside a PbTe sample. Such a quantum dot is assumed to be spherically symmetric. Since the bare energy spectrum anisotropy varies sufficiently for IV-VI semiconductors, we had to consider two extreme cases of weak and strong anisotropy.In the first case the problem is entirely spherical symmetric and it allows us to look for solutions in terms of spherical spinors. The initial Hamiltonian is taken in a Dirac form which includes interband transitions with possible spin changes. When considering the problem we ran into two possibilities related with relative signs of energy gap parameters. While the real gap is always positive the gap parameters can have both signs. In the normal case of equal signs for semiconductors inside and outside the ball we obtained by numerical calculations the dependences of energy levels upon the ball radius. In the opposite band-inverted case of different signs we obtain the system of levels for boundary states.The wave functions of these boundary states are localised in the vicinity of a ball surface. They correspond to the Weyl states in plane band-inverted contacts,investigated by B.Volkov and O.Pankratov[1].

We also investigated the case of strong anisotropy. For the Dirac model under consideration it is the anisotropy of interband interaction parameters for one valley. The different valleys are independent in the model. With this assumption we calculated the size-quantised energy spectrum in the adiabatic approximation.

1. B.A.Volkov and O.A.Pankratov. JETP Lett. 42,178(1985).

PO.1

$Cd_xHg_{1-x}Te$ Doping by Ion Beam Treatment

V.I.Ivanov-Omskii, K.E.Mironov, K.D.Mynbaev

A.F.Ioffe Physico-Technical Institute

194021 St.Petersburg, Russia

Low-energy ion treatment ("ion-beam-milling", IBM) is known to be the effective way to convert conductivity type and create p-n junctions in p-$Hg_{1-x}Cd_xTe$ (MCT) [1]. However, real mechanism of conductivity type conversion caused by IBM has not been accurately established yet.

To specify the mechanism and to evaluate IBM method abilities, the effect of IBM on both p- and n-type epitaxial layers and bulk crystals of MCT with x=0.20÷0.24 has been studied.

We have suggested that the process of conversion was caused by interstitial mercury generation, its diffusion by dissociative mechanism and subsiqent recombination with vacancies. IBM treatment of p-type MCT with $N_A-N_D \leqslant 2\cdot10^{17}$ cm^{-3} was found to result in n-type material with low electron concentration ($\sim10^{14}$ cm^{-3}), high mobility ($>10^5$ $cm^2/V\cdot s$) and carrier lifetime (>2 μs) for x=0.22 composition at 77 K. Application of IBM treatment to n-type material makes it possible to increase electron mobility and to obtain practically uncompensated material. The electron concentration in subjected to IBM samples was proportional to the concentration of uncompensated acceptors in initial material. The reason is that generation of acceptor defects during pre-IBM annealing is accompanied by appearance of donor ones. This effect seems to clear up the direct way to control the properties of material subjected to IBM by varying pre-IBM annealing conditions.

IBM treatment abilities in application to device multielement structures (photodiodes and photoconductors) have been demonstrated. It have been shown that using IBM it was possible to obtain p-n junctions with dark reverse currents less than in ion implanted ones. The main dark currents mechanisms and photoelectric parameters have been investigated on IBM high-performance photodiodes in the temperature range 20÷300 K.

[1] C.T.Elliott et al. El.Letters. 1987, v.23, N 19, p.978-979.

P8.2

ASSESSMENT OF DOPED $Cd_xHg_{1-x}Te$ STRUCTURES USING BEVELLED SECTIONS

I.G.Gale, C.D.Maxey and J.B.Clegg

Philips Research Laboratories, Redhill, Surrey, U.K.

S.Mugford, S.Barton, P.Capper and C.L.Jones

Philips Infrared Defence Components, Southampton, Hants., U.K.

ABSTRACT

Doped homo- and hetero-structures of $Cd_xHg_{1-x}Te$, (CMT), are required for some types of new generation devices. These structures have been grown by Metal-Organic Vapour Phase Epitaxy (MOVPE) at 350°C onto both CdTe and GaAs (buffered with CdTe) substrates. The structures were produced using both acceptor and donor doping, with arsenic and iodine respectively, and the junctions formed following annealing in Hg to eliminate metal vacancies. This paper summarises progress in characterising these junctions both in terms of x and electrical behaviour. Techniques are described for making bevel sections by either angle-polishing, chemical etching or ion beam rastering in a Secondary Ion Mass Spectrometry (SIMS) instrument. Detailed surface profiles were taken to ensure that accurate positional information on junctions could be obtained. Assessment on these bevels has included Auger Electron Spectrometry (AES) profiling to determine x variations and Electron Beam Induced Current (EBIC) measurement to reveal the position (to within $\pm$ 0.5 μm) and width of the electrical junction. This information can then be linked to the dopant profiles determined by SIMS and the position of the electrical junction estimated from Hall and strip depth profiling. Agreement has been found between the various techniques with regard to the position of the electrical junction. A comparison is made between the position of the electrical junction and the position of the x change within a hetero structure. Narrow interface widths have been revealed, by AES, between the GaAs substrate and CdTe buffer (0.1 μm) and between both the CdTe buffer and the CMT layer and the x change within the CMT heterolayers, (0.5 μm).

P8.3

EFFECT OF TRAP ATHERMAL RECHARGE ON DLTS MEASUREMENTS IN NARROW GAP SEMICONDUCTORS

Soltanovich O.A., Yakimov E.B., Yarykin N.A.
Institute of Microelectronics Technology,
Russian Academy of Science
Chernogolovka Moscow distr., Russia 142432

Investigation of deep level centers in narrow gap semiconductors is very important because these centers control recombination properties of materials and parameters of related devices. Deep level transient spectroscopy (DLTS) based on the analysis of carrier thermal emission from non-equilibrium filled traps is widely used for deep level defect characterization. As the probability of the processes which can be responsible for trap athermal recharge (e.g. tunneling) in narrow gap semiconductors is sufficiently high, an effect of these processes on DLTS spectra is expected to be especially remarkable.

The DLTS signal simulation is made taking into account athermal recharge of deep levels competing with their thermal emptying during DLTS measurements. The shape of the DLTS curves is found to be dependent on whether athermal emptying or athermal filling of traps occurs. In the frame of the model assuming the athermal recharge rate to be constant with distance from junction plane the possibility to obtain correct deep level center parameters and to estimate athermal recharge rate is demonstrated.

An analysis of DLTS peak amplitude vs "rate window" dependence observed on p-$Hg_{1-x}Cd_xTe$ crystals with x=0.2 and x=0.4 is performed. It is shown that such behavior is likely due to athermal filling of deep levels by majority carriers during DLTS measurements. Two possible ways of athermal filling of deep levels (conductance band - deep level tunneling and hole capture due to leakage current) with various dependences of athermal filling rate versus distance from the junction plane were considered. Comparison of experimental dependences of DLTS peak amplitude vs "rate window" with calculated ones has allowed to determine the most probable mechanism of trap athermal filling for p-$Hg_{1-x}Cd_xTe$ crystals with x=0.4 .

P8.4

Cavity structure effects on $Cd_xHg_{1-x}Te$ photopumped heterostructure lasers.

J.Bonnet-Gamard, J.Bleuse, H.Mariette†, L.Ulmer, N.Magnea, and J.-L.Pautrat

DRF-MC/ SP2M/ Laboratoire de Physique des Semiconducteurs
Centre d'Etudes Nucléaires de Grenoble
85X F-38041 Grenoble CEDEX

†Laboratoire de Spectrométrie Physique (CNRS - URA 08)
Université Joseph Fourier, Grenoble I

Separate confinement heterostructures (SCH) designed for laser emission in the range from 2 to 2.5 µm were grown by molecular beam epitaxy. Under pulsed photoexcitation, they display stimulated emission up to room temperature[*]. In the present work, we particularly studied the effect of the nature of the active layer, and lateral confinement of photons through gain guiding, provided by the suppression of the luminescence by ion implantation.

Lasing characteristics of a SCH laser with a 'bulk-like' active layer are compared with those of an identical laser whose active layer is made of 6 quantum wells, 100 Å wide. The consequences of the non-identity of the wells' thickness are investigated.

Boron ion implantation, at accelerating voltages of 150 to 200 keV, and doses of 10^{13} to 10^{14} cm^{-2} strongly reduces the luminescence intensity from the buried active layer of SCH laser structures, which is approximatively 0.5 µm deep. For photolithographic requirements, a 3 µm-thick resist layer is enough to protect the underlying sample. We therefore use implantation through a resist mask to define 5 to 50 µm-wide bands of intact material. These bands are perpendicular to the cleaved facets used as cavity mirrors. Lasing characteristics of such structures are presented.

[*] J.Bleuse, N.Magnea, L.Ulmer, J.-L.Pautrat, and H.Mariette, proceedings of the Fifth International Conference on II-VI Compounds, Tamano, Okayama, Japan, 1991, to be published in J. Cryst. Growth.

P8.5

The Performance of p^+-n $Hg_{1-x}Cd_xTe$ Photodiodes

A. Rogalski, A. Joswikowska, K. Joswikowski and J. Rutkowski
Institute of Technical Physics, WAT, 01-489 Warsaw 49, Poland

In the last decade HgCdTe photovoltaic detector technology efforts focused almost exclusively on n^+-p junctions. The main problem in fabrication of these photodiodes is probably connected with surface control of the p-side of junctions.[1] However, in 1985 Rogalski and Larkowski[2] indicated that due to low mobility of holes in n-type region of p^+-n junctions, diffusion limited R_oA product of such junctions is larger than for n^+-p ones. This prediction has been recently confirmed by several papers.[1,3-6]

In the paper the performance of p^+-n photodiodes in comparison with n^+-p ones is analyzed. The consideration are carried out for the 77-300 K temperature region and 3-15 μm cutoff wavelengths. The effects of doping profiles on the photodiode parameters (R_oA product, quantum efficiency) is solved by forward-conduction steady-state analysis.[7] The influence of different junction current compositions (diffusion current for radiative and Auger 1 recombination mechanism, tunneling and depletion layer currents) on the R_oA product is considered. It is clearly shown that the R_oA product for p^+-n junctions is higher especially for long wavelength photodiodes. In medium wavelength region the R_oA product for both type of junctions is similar, because it is determined by depletion layer current. Results of calculations are compared with experimental data reported by several authors. An attempt is made to explain the discrepancy between theoretical calculations and experimental data.

References

1. C. C. Wang, J. Vac. Sci. Technol. B9, 1740 (1991).
2. A. Rogalski and W. Larkowski, Electron Technology 18(3/4), 55 (1985).
3. J. M. Arias, S. H. Shin, J. G. Pasko, R. E. DeWames and E. R. Gertner, J. Appl. Phys. 65, 1747 (1989).
4. L. O. Bubulac, D. D. Edwall, D. McConnell, R. E. DeWames, E. Blazejewski and E. R. Gertner, Semicon. Sci. Technol. 5, S45 (1990).
5. J. M. Arias, M. Zandian, J. G. Pasko, S. H. Shin, L. O. Bubulac, R. E. DeWames and W. E. Tennant, J. Appl. Phys. 69, 2143 (1991).
6. G. N. Plutz, P. W. Norton, E. E. Krueger and M. B. Reine, J. Vac. Sci. Technol. B9, 1724 (1991).
7. M. Kurata, Numerical Analysis of the Semiconductor Devices, Lexington Books, Lexington 1982.

Removal of Oxygen and Carbon Contamination from (100) CdZnTe Substrates

Y.S.Wu, C.R. Becker, A. Waag, R.N. Bicknell-Tassius, and G. Landwehr
Physikalisches Institut der Universität Würzburg
D-8700 Würzburg, FRG

CdZnTe is an important substrate for infrared detectors containing either HgCdTe or HgZnTe because it offers tunability of the lattice constant and band gap. The lattice constant varies from 6.102 Å for ZnTe to 6.481 Å for CdTe and can be lattice matched to HgCdTe or HgZnTe alloys.

Surface treatment is very important for both device processing and MBE growth. A number of workers have recently studied the surface of CdTe substrates with various analytical tools, such as X ray photoelectron spectroscopy (XPS) and Auger electron spectroscopy (AES). In this investigation we have employed XPS and the reflection of high energy electron diffraction (RHEED) to study various in situ cleaning techniques.

Heating CdZnTe (Zn 4%) substrates at 300 °C can eliminate oxygen contamination, but can not completely remove carbon from the surface. Heating at higher temperatures decreases the carbon contamination only slightly, while increasing the Zn to Cd ratio on the surface considerably, which affects the CdZnTe (Zn 4%) surface stoichiometry. We have found that carbon contamination could be nearly eliminated from the surface by sputtering with Argon ions at an incident angle ranging between 20 and 60° at temperatures between 200 and 250 °C. The RHEED pattern after sputtering under these conditions displays (2 × 1) reconstruction.

P8.7

INFRARED ABSORPTION AND STRUCTURAL PROPERTIES OF HgCdTe QUANTUM WELLS

by

Richard Sizmann, Torbjørn Skauli, Thierry Colin, Kjersti Gjønnes and Stian Løvold
Norwegian Defence Research Establishment
P O Box 25, N-2007 Kjeller, Norway

We study the growth, infrared absorption and structural properties of HgCdTe quantum wells with ≈78% Hg (x = 0.22) between CdTe barriers. The samples are grown on (111)B CdTe or CdZnTe substrates in a Riber MBE machine. We can grow "twin free" (less than 2% twins) HgCdTe with X-Ray (333) rocking curve widths less than 50 arc sec (FWHM), measured with a four-crystal monochromator X-ray diffractometer. We measure the structures with high resolution X-ray diffraction before and after sample preparation, in order to determine a possible change in the structural quality with sample preparation.

The infrared absorption of the quantum wells is measured in a waveguide geometry with the light incident on a 45° polished facet. In this geometry it is possible to distinguish between absorption of light polarized parallel and perpendicular to the quantum well layers.

P8.8

MAGNETOTUNNELING IN Pb-p-HgCdTe SHOTTKY BARRIERS.

V.V.Zav ialov, V.F. Radantsev.
Institute of Physics & Applied Mathematics
of Ural University, Ekatherinburg, Russia.

It is known that in Kane semiconductors the tunneling in electric E and magnetic H fields depends on their mutual orientation and magnitude ratio [1]. At H⊥E under the condition that $H > H_{cr} = cE/s$ (s is Kane velocity) the tunneling current is supposed to vanish. But tunneling in "magnetic limit" $H > H_{cr}$ for Kane semiconductors was not investigated experimentally because of large electric fields in tunnel diodes $E \sim 10^6 - 10^7$ V/cm^2. InSb diode where $E \sim 10^5$ V/cm^2 was not investigated in this limit also. We investigated tunneling in parallel and crossed fields in Shottky barriers Pb-p-$Hg_{1-x}Cd_xTe$ ($x \sim 0.2$, 0.3) which are effective for tunneling at small $E \sim 10^4$ V/cm ($H_{cr} \sim 10$ kOe) because of narrow energy gap ~0,1 eV. In contrast to p-n junctions it is easy to realize in Shottky barriers the condition of homogeneous electric field which is important for comparison with theory. Tunneling current at H= 50kOe in both orientations decreases aboute ten times. In parallel fields the magnitude of effect is in accordance with theory and gives correct value of electric field (according to E determined from I-V characteristics at H=0). At H⊥E orientation any peculiarities near H_{cr} were not observed in contrast to the theory [1]. In the whole range of H=0- (2--5)H_{cr} the magnetic field dependences at H⊥E are similar to those at H∥E. Experimental results for the case H⊥E may be explained quantatively if we take into account nonresonant scattering of light holes during tunneling under barrier [2]. The length of scattering determined from the ratio of tunnel currents for two orientations is proportional to H and is about magnetic length as to be expected for quantum diffusion in magnetic field.

1. A.G.Aronov, G.E.Picus JETF 51, 281 (1966).
2. B.I.Shklovskii, A.L.Efros JETF, 84, 811 (1983).

P8.9

STATIONARY CHARACTER OF 2D STATES IN INVERSION AND ACCUMULATION LAYERS ON ZERO GAP HgCdTe

T.I. Deryabina, V.F. Radantsev.
Institute of Physics & Applied Mathematics
of Ural University, Ekatherinburg, Russia.

Recently performed numerical calculations [1,2] showed that interband tunneling slightly influences broadening and energy of subband levels in inversion layers on narrow gap semiconductor even for very small energy gap E_g. We present experimental evidence of such surprising behavior. 2DEG in inversion and accumulation layers on gapless ($E_g<0$) $Hg_{1-x}Cd_xTe$ was investigated by using capacitance spectroscopy in magnetic fields. Althouth in investigated systems with $E_g<0$ the barrier, separating subband states from the continuum of bulk band states is absent and 2D states are supposed to be resonant states, capacitance magnetooscillations are distinctly resolved. Broadening of Landau levels does not differ from that in $Hg_{1-x}Cd_xTe$ with $E_g>0$. The experimental subband parameters are in very good agreement with theoretical calculations,which ignore the interband tunneling.Stationary character of 2D states in Kanes semiconductor may be understand in the framework of the conception, developed for the description of vacuum condensate of electrons near the nuclei with supercritical charge [3]. Even for $E_g=0$ the effective quasirelativistic potential provides nonpenetrating barrier for 2D states with energy $E(p) > E_F-ps$ (E_F is Fermi energy, s is Kanes velocity, p is 2D momentum) and such states are true stationary states. For energy $E_F-ps > E > E_F-ps\sqrt{4\beta+1}$ the barrier transmission is exponentially small.As result above 97% of subband states are well-defined. If we take into account spin polarization terms in effective potential the all states turn out to be true stationary.

1. A.Ziegler, U.Rossler, Europhys. Lett. 8, 543, (1989).
2. P. Sobcowicz, Semicond. Sci. Technol. 5, 183, (1990).
3. A.B.Migdal et al, JETF Lett. 24, 164 (1976).

P9.1

SPIN POLARIZED TUNNELING CURRENT IN METAL-INSULATOR-GAPLESS SEMICONDUCTOR STRUCTURES IN MAGNETIC FIELD.

A.V.Germanenko, V.V.Kruzhaev, G.M.Minkov, E.L.Rumyantsev & O.E.Rut
Institute of Physics & Applied Mathematics of the Ural University, Lenin st. 51,Ekaterinburg 620083, Russia

Tunneling spectroscopy in quantized magnetic field is the unique method for investigation not only energy spectrum but the peculiarities of behavior of states near the surface.

We report experimental investigations of tunneling conductivity oscillations of M-I-gapless semiconductor p-$Hg_{1-x}Cd_xTe$ (x<0.16) structures at different orientations of magnetic field relative to the normal to the surface ($\vec{n}$). It was revealed that splitting of oscillation maxima at H$\parallel$n is due to spin splitting of Landau levels and maxima amplitudes at tunneling into both spin states "a" and "b" are close. When magnetic field turns from H$\parallel$n the amplitudes of low bias (i.e. connected with tunneling into "a" states) maxima decrease monotonously and at H$\perp$n oscillations due to tunneling only into "b" states are observed. Thus at H$\perp$n spin-polarized tunneling current takes place.

Tunneling current at H$\perp$n is defined by dependencies of $(\hat{V}_x\Psi)^2_{x=0}$ ($\hat{V}_x$ -velocity operator) and energy of states versus distance of oscillator center from the surface (x_0). Our theoretical analysis shows that in gapless semiconductors with spectrum described by Luttinger Hamiltonian these dependencies are different for "a" and "b" states and significantly distinguish from those in semiconductor with nondegenerate band. As a result the "b" states are "attracted" to the surface and it leads to larger contribution of these states to the tunneling current at H$\perp$n. Thus tunneling spectroscopy, for the first time, made it possible to reveal the peculiarities of behavior of different spin states near the surface in gapless semiconductors.

P9.2

Contactless Local Determination of the Recombination Parameters of Narrowgap Semiconductors Using the Laser Interferometry

A.B. Fedortsov, Y.V. Churkin, A.S. Ivanov, K.F. Komarovskikh, D.G. Letenko and L.E. Vorobjev*
Northwest Polytechn. Inst. 5 Millionnaja, 191065, St. Petersburg, Russia
*State Techn. University, 29 Polytechnicheskaya, 195251, St. Petersburg, Russia

The presented method of investigation of the excitation energy of the recombination centers, their concentration, electron and hole cross sections of these centers is based on the analysis of the electron and hole lifetime experimental dependencies [1]. Both these dependencies are measured in one experiment using the laser interferometry of plane-parallel semiconductor sample. The probing beam from IR CO_2-laser passes through the sample. Its intensity measured by photodetector is a function of the reflection index n and the absorption coefficient α of the semiconductor and thus of the electron and hole concentrations. The sample is also illuminated by the shortwave laser, which generates the electron-hole pairs and changes n and α of the sample and so modulates the intensity of the probing beam. The analysis of two modulation values measured for each temperature using two different probing beam incidence angles allows to determine the τ_n and τ_p separately [2]. Using the wavelength attunable source, for example our CO-laser [3], for the excess carriers generation one can determine separately the surface recombination velocity and bulk lifetime [4]. By the effective focusing of the laser beams it is possible to investigate recombination parameters locally. We have investigated lifetime dependencies in such semiconductors as InSb, $Cd_{0.3}H_{g0.7}Te$ in the internal from 77K to 300K. The lowest τvalues we can measure are 3.10^{-10} sec and the locality is 100μm.

[1] L.E. Vorobjev, D.G. Letenko, A.B. Fedortsov, Sov. Teh. Phys. Lett. 17 (2), to be published.

[2] A.B. Fedortsov, Y.V. Churkin, Sov. Teh. Phys. Lett. 14 (2), 142 (1988).

[3] D.G. Letenko, V.N. Sawateev, A.B. Fedortsov, Y.V. Churkin, Instr. and Exper. Tech., to be published.

[4] V.B. Voronkov et al, Sov. Phys. Tekch. Phys. 36 (2), to be published.

P9.3

A new technique for the interpretation of photo-Hall measurements in semiconductors

J.I.L. Hughes[1] and H.A. MacKenzie[2]

[1]Now with Shell Research Ltd., Thornton Research Centre, Chester

[2]Department of Physics, Heriot-Watt University, Edinburgh EH14 4AS

A new method of intepretation of photo-Hall measurements in semiconductors will be described. It will be shown that previously used geometrical scaling factors used to account for small areas of illumination on a sample are only valid over a small range of photo-generated carrier concentrations. A model has been developed which takes an arbitrary geometry Hall sample with an incident laser beam, and, assuming a resultant Gaussian distribution of photo-generated carriers, the voltage at each point in the sample may be determined. This method allows unambiguous and accurate determination of the photo-generated carrier concentration from the measured photo-Hall voltage. The model was tested with predictions of the dark Hall voltage for an experimental sample of n-type indium antimonide, and these predictions agreed with the measured values to within 13% at the four different measurement temperature from 20 to 77K.

Application of this model to interpret experimental photo-Hall measurements will also be discussed. This technique has proved valuable in the study of the recombination of photo-excited carriers, and the process of saturation of absorption in n-type InSb.

The recombination time of photo-generated carriers in n-type InSb was found to change with carrier concentration, showing an increase from 350 ns to 850 ns as the concentration of photo-generated carriers increased from 6×10^{11} to $4 \times 10^{13} cm^{3}$. These results match well with a theoretical model of the recombination of carriers using a single-level trap recombination mechanism.

Combining the inhomogeneous Hall modelling and the recombination time results, provides a basis for the investigation of nonlinear absorption in InSb. Measurements of saturation of optical absorption have been made at four different temperatures from 20 to 77K and these results are compared with the direct band-blocking or Burstein-Moss model of absorption saturation. This new photo-Hall technique has provided direct information relating the saturation of optical absorption to the photo-generated carrier concentration.

P9.4

Interband and intraband contributions to refractive index in narrow-gap semiconductors

K. H. Herrmann, U. Müller

Humboldt-Universität Berlin, Institut für Festkörperphysik, O-1040 Berlin, FRG

Several narrow-gap mixed-crystal semiconductors offer the possibility to vary the energy gap without changing the nature of the electronic states responsible for the (near to edge) interband transitions. On the other hand, the resonances giving the major contributions to dielectric constant (interband, optical phonons) are quite neighboured, thus their separation from each other and from the free-carrier contribution is critical. These facts together with the new possibility to investigate the wide-gap to narrow-gap transition in high-quality bulk crystals or MBE layers of (Hg,Cd)Te, (Pb,Sr)Se (our own experiments), (Pb,Eu)Se and other ones are the reasons for this critical reexamination of the topic.

Following steps of analysis are included:

- Use of E_g as the diffence between two levels (bands) rather than of its absolute value in systems with level-crossing.
- Direct fitting of the experimental values $n(\lambda)$ to a formula containing both a long-wave (phonons, free carriers) and a short-wave (interband) oscillator.
- Microscopic interpretation of the interband oscillator in terms of calculated absorption edge combined with a Kramers-Kronig analyis of the absorption at higher energies.
- Classification of the systems depending on whether the near-to-edge transitions deliver the main contribution to the interband oscillator or transitions between other pairs of bands.
- Comparison of samples with different energy gap within the $\mathbf{k}\cdot\mathbf{p}$ band structure.
- Account for the influence of strong doping on the optical dielectric constant in samples exhibiting Burstein-Moss shift of the absorption edge in a second step.

The refractive indexes data of about 10 different mixed-crystal systems from literature are included in the analysis. Recommendations are given for parametrization of dispersion formulae as well as application of general $\epsilon_{opt}(E_g)$ interrelations to different materials.

P10.1

PHOTOCONDUCTIVITY SPECTRUM AND KINETICS OF
$Pb_{1-x}Sn_xTe/PbTe/BaF_2$ MULTI-QUANTUM-WELL STRUCTURES

I.I.Zasavitsky, B.N.Matsonashvili, V.T.Trofimov
P.N.Lebedev Physical Institute, Moscow

To determine the heterojunction energy diagram the photoconductivity (PC) spectra and kinetics of $Pb_{0.89}Sn_{0.11}Te$/ $PbTe/BaF_2$ multi-quantum-well (MQW) structures and superlattices have been studied.

PC decay signal consists of three components which differ each other by relaxation times and excitation long wavelength limits. The first component is due to usual interband transitions and has decay time of $\leq 10^{-7}$s.

Decay time of second component is decreasing in thermoactive way from 10^{-2} to 10^{-6}s with increase of temperature from 20 to 100 K. Activation energy is about 20 meV. The long wavelength limit is 66 meV that is almost by two times lower than the narrowest gap in the MQW structure.

Decay time of third component is decreasing also in thermoactive way from 10^{-2} to 10^{-6}s with increase of temperature from 30 to 170 K. Activation energy is about 80 meV. This component is exciting only with photon energy higher than 350 meV that is by 1.5 times higher than the widest gap in the MQW structure. The polarity of third component is positive for p-type MQW structures and negative for n-type MQW structures.

A model of type-II staggered superlattice was used to explain the experimental results. The long wavelength limit of second PC signal component is attributed to the indirect optical transitions from $Pb_{0.89}Sn_{0.11}Te$ quantum wells to PbTe barrier layers. Relaxation of captured electrons takes place through the potential barrier due to conduction band offset. The third PC signal component is explained by electron capture to the resonant deep level in conduction band, and the layered staggered structure allows to manifest this level. The level is located by 130 meV above the bottom of PbTe conduction band.

P10.2

The Resonant Defect Superconductivity in the Narrow Gap A_4B_6 Semiconductors

I.A. Chernick, S.N. Lykov

St. Petersburg University, St. Petersburg (Leningrad), C.I.S.

Abstract

The experimental data connected with the discovery and research in the narrow gap A_4B_6 semiconducting compounds of a new nontrivial kind of superconducting state - the resonant defect superconductivity (RDS) are considered and analyzed.

The principal peculiarities of the RDS indicating that its physical mechanism is essentially (by an order) more effective (from the point of view of the value of the superconducting transition critical temperature) as compared with the ordinary BKS-mechanism are discussed and formulated.

An attempt of the comparing empirical data on the RDS with the predictions given in a number of theoretical investigations devoted to the working out of the nonconventional (not BKS) models of superconductivity is made.

A high probability of a similarity (identify) between the physical mechanism of *the RDS* and the high temperature superconductivity discovered by Bednorz and Muller in the HTSC-ceramics is marked.

P10.3

Sasaki Effec: in the Narrow Gap Semiconductor $Bi_{1-x}Sb_x$ Alloys

E.V. Bogdanov

Physics Department, Moscow State University, Moscow, Russia

For samples of n- and p-type multivalley narrow gap semiconductor bismuth-antimony alloys oriented in the binary bisector plane at 4.2 K, electromotive force perpendicular to the flowing current is observed. The deviation angle of electric field vector from current vector exceeds 10° in some cases. This effect is observed only in samples for which the current direction doesn't lie on any of the symmetry axes of the crystal and at high electric fields for which the current voltage characteristic is nonlinear. So it can be connected with Sasaki effect i.e. the anistropy in electric conduction of hot electrons due to the ellipsoidal energy surfaces. All peculiarities of the dependence of the deviation angle on the current orientation and longitudinal field strength can be qualitatively described on the basis of the theory of Sasaki effect and known band structure of bismuth-antimony alloys.

P10.4

FERROELECTRIC PHASE TRANSITIONS IN QUATERNARY LEAD-TIN CHALCOGENIDES

A.I.Lebedev and I.A.Sluchinskaya
Physics Dept., Moscow State University, Moscow, 119899, Russia

Quaternary solid solutions of IV-VI semiconductors, in which energy band gap and lattice parameter can be changed independently, are widely used for IR laser and photoconductive device fabrication. In this work the ferroelectric phenomena, affecting the properties of these devices, are shown to be characteristic for all quaternary solid solutions with Pb→Sn substitution.

Solid solutions were studied by means of electrical and X-ray methods. The investigation of $Pb_{1-x}Sn_xTe_{1-y}Se_y$ showed that the ferroelectric phase transition can be observed starting from x=0.08. At constant y the temperature of phase transition T_c increased with x, at constant x T_c varied nonmonotonously with y, reaching a maximum at $y \approx 0.25$. The resistivity hysteresis and relaxations observed near T_c in crystals with $x<0.35$ make it possible to consider this phase transition as the order-disorder one. Disappearance of these features at $x>0.35$ indicates the change of type of phase transition to displacive one.

Similar strong increase of T_c with isoelectronic substitution, hysteresis and relaxations of resistivity near T_c were found in $Pb_{1-x}Sn_xTe_{1-y}S_y$ solid solutions. All features of electrical properties, which usually precede the onset of ferroelectric phase transition, were also found in $Pb_{1-x}Sn_xSe_{1-y}S_y$, although the phase transition itself was not observed.

All peculiarities of phase transitions observed in $Pb_{1-x}Sn_xY$ solid solutions (including rise of T_c when substituting in anion sublattice and crossover from order-disorder to displacive phase transition) were explained by the existence of off-center Sn_{Pb} atoms with strong tunneling.

P10.5

Lead Telluride-Based Photodetectors: a New Approach

B.A. Akimov, D.R. Khokhlov

Physics Department, Moscow State University, Moscow, Russia

Narrow-gap semiconductors based on the group III - doped lead tellurides received a lot of attention last year as a new promising candidate for the photodetection in the middle- and far-infrared. The Fermi level pinning effect results in the high spatial homogeneity of the material electric properties. In some cases the Fermi level is pinned within the bandgap, so one has a very unusual situation, when a heavily doped narrow-gap semiconductor with high number of the growth defects acts electrically as an ideal one with practically zero background free carrier concentration at the low temperatures. Another effect that defines the behaviour of these materials is the persistent photoconductivity that is observed at the low temperatures. Use of this "internal integration" effect in the photodetecting systems improves greatly their parameters. We discuss the main features of these materials and the ways of construction of the respective photodetecting systems.

P10.6

Magnetic Field-Induced Localization in $Pb_{1-x}Sn_xTe(In)$

D.R. Khokhlov, I.I. Ivanchik

Physics Department, Moscow State University, Russia

A. de Visser

Van der Waals-Zeeman Laboratory, University of Amsterdam, The Netherlands

A.V. Nikorich

Institute of Applied Physics, Kishinev, Moldova

We report on the high-field ($H < 40\,T$) magnetoresistance measurements of $Pb_{0.75}Sn_{0.25}Te(In)$ at the temperature $T = (1.4 - 4.2)K$. The concentration of the free nonequilibrium electrons n was changed by means of the infrared illumination. The sample magnetoresistance increases in time for the relatively low n. The Hall effect measurements show that the resistance rising is due to the electron localization. The localization characteristic time τ depends on H and T as $\tau = \tau_0(1 - T/T_0) \exp(H/H_0)$. The parameter $H_0 \approx 5T$ practically does not depend neither on the temperature, nor on the degree of photoexcitation (n). The characteristic temperature T_0 does not depend on the magnetic field applied, and reduces for higher n. We discuss the processes that could lead to the effect appearance.

P10.7

STRUCTURAL DEPENDENCE OF THE OPTICAL ABSORPTION IN $TlBiSe_2$ THIN FILMS NEAR THE FUNDAMENTAL ABSORPTION EDGE

C.L. Mitsas, E.K. Polychroniadis and D.I. Siapkas

University of Thessaloniki, Dept. of Physics, Solid State Section
313-3, Thessaloniki 54006, Greece

$TlBiSe_2$ belongs to the family of semiconductive compounds of the general type $TlAB_2$ (A:As, Sb, Bi and B:Te, Se, S). It is usually referred to as a "pseudo" lead salt compound since it is isoelectronic with the corresponding lead salt, PbSe. $TlBiSe_2$ crystallizes in the rhombohedral structure, the primitive unit cell having parameters a=7.728 Å and $\alpha=31.92^o$ and has been identified as a narrow gap semiconductor. Among the various applications for which it has been proposed we mention its potential use as an acousto-optic detector, infrared detector, thermoelectric, switching and memory element.

In this work we present the characterization of epitaxial thin films of $TlBiSe_2$ by IR reflectivity measurements and electron microscopy which were grown on NaCl substrates with varying deposition parameters, such as substrate temperature, deposition rate and film thickness. In particular we will focus on the optical transitions occuring in the as-grown films in the region near the fundamental absorption edge in an attempt to correlate the observed, by TEM and SEM, geometrical and physical imperfections existing in the films to the different contributions to the absorption coefficient. Thus it will be shown that defects such as incoherent grain boundaries and deviations from stoichiometry are responsible for sub-gap absorption and that their contribution , as well as the affect of surface and interface roughness, should be taken into account in order to extract a meaningful value of the energy gap from the variation of the absorption coefficient in the above specified spectral range.

P10.8

The Electrical Characteristics of $Pb_{1-x}Eu_xSe$ Homojunctions

Jianren Xu, Bernard Halford, Maurus Tacke

Fraunhofer Institute of Physical Measurement Techniques
Heidenhofstraße 8, D-7800 Freiburg, Germany

Semicomductor laser diodes based upon the ternary IV-VI compound material $Pb_{1-x}Eu_xSe$ are important tunable infrared lasers. Presently, microstructures are developed for optimizing these lasers, e.g. for achieving monomode behavior. However, the efficiency of these laser diodes is still quite low. Trying to improve the laser performance, we have analysed the electrical chacteristics of our main material $Pb_{1-x}Eu_xSe$. As a first step towards this goal, homojunctions were made by MBE. The R_0A product of $Pb_{1-x}Eu_xSe$ diodes with composition x from 0 to about 0.1 have been theoretically and experimentally investigated over a wide temperature region 30-300 K.

Theoretical analysis of the R_0A product as function of temperature T and composition x shows that the R_0A product at high temperatures is diffusion limited for small x, and depletion limited model for large x, but also depletion for x=0. At low temperatures, it is dominated by tunneling. The dependence on the carrier concentration is less important compared to the other factors x and T.

The experimental results are in accordance with these calculations. For the samples with x about 0.03, the R_0A product is diffusion limited at high temperatures. It is depletion limited for x about 0.045 and 0.085. It is also depletion limited for x=0. This evidence confirms that the Roseman/Katzir model based upon the non-parabolic effect of energy band is reasonable for small energy gap materials. And Emtage model is still quite good for large gaps. From these models, the minority carier life time can be derived, which is of the order of nanosecond. The low temperature data can't be explained by assuming the band to band tunneling model. At present, we favour the trap-assistant tunneling model as dominant mechanism at low temperatures, based on our experimental results on diodes made by MBE with different doping levels, and also by diffusion and ion implantation. It is probably responsible for the significant nonradiative recombination in our laser diodes.

P10.9

Two-Dimensional Electronic States on the Interface of the Stressed Piezoelectric Semiconductor

V G Kantser and N B Malkova

Institute of Applied Physics, 277028, Kishinev, Moldova

The internal strains in multilayered semiconductor structures generate polarization fields through the piezoelectric effect. The influence of the induced polarizations on the electron spectrum of the strained heterojunction is studied. Interface electron states are shown to exist in such structures. These states occur due to the supersymmetry of a two-band Hamiltonian with the polarization effect included and exist only in definite energy and momentum intervals, which are determined by the supersummetry condition of the Hamiltonian. The energy spectrum is essentially linear as a function of in-plane momentum.

P10.10

MBE Of Lead Chalcogenides At Increased Residual-Gas-Pressures

M.Griesinger, H.Böttner, S. Kuhn, A. Seifert and M. Tacke
Fraunhofer-Institut for Physical Measurement Techniques (IPM),
Heidenhofstr.8, D-7800 Freiburg, Germany
Tel. : (49)-(0)761-8857-0, Fax: (0)761-8857-224

Semiconductor diode lasers made of IV-VI-semiconductor-compounds, the lead chalcogenides, emit in the mid infrared region between $3\mu m$ and $30\mu m$. These lasers are commonly used for high resolution spectroscopy.
Molecular-beam-epitaxy equipment is used for the production and development of advanced IV-VI diode lasers, usually at residual gas pressures around 10^{-12} mbar to 10^{-9} mbar. Diode lasers made under reduced high-vacuum-conditions show no decrease in device quality compared to those made under UHV-conditions. Nevertheless a systematic measurement of the influence of the residual gas pressure has not yet been performed.
The residual gas pressure at high vacuum was achieved by controlled influx of the gases N_2, O_2 and H_2O during the MBE growth process. The samples were characterised by Hall-measurements. The important parameters investigated are the Hall-coefficient and the resulting carrier-concentration and the carrier-mobility. The Hall-data were taken in the temperature range from 320 K to 28 K.
Aside from PbSe-samples, we produced $Pb_{1-x}Sr_xSe$-samples under the same conditions. We found that the influence on the above mentioned parameters is greater in $Pb_{1-x}Sr_xSe$ samples than in PbSe-samples. For example, the $Pb_{1-x}Sr_xSe$-samples are p-type with carrier-concentrations of about $10^{18}cm^{-3}$ at high O_2 residual gas pressure. We noticed that higher N_2 residual gas pressure induces n-typ conductivity in some $Pb_{1-x}Sr_xSe$-samples and in others a change of the polarity of the Hall-voltage at low temperatures. The samples which were produced under higher O_2 and H_2O residual gas pressures also showed different carrier concentrations. The systematic examinations show that the residual gas pressures of N_2, O_2 and H_2O which usually occur in high-vacuum have no negative influence on the electrical properties of the lead chalcogenides.

P10.11

DISLOCATION SUPERLATTICES BASED ON LEAD AND TIN CHALCOGENIDES AS MODELS FOR HIGH T_c SUPERCONDUCTORS

O.A.Mironov, A.I.Fedorenko, V.V.Zorchenko, A.Yu.Sipatov,
O.N.Nashenekina, A.A.Konchits, I.M.Zaritskii
Institute of Radiophysics & Electronics, Academy of Sci.of Ukraine,
12 Acad. Proskura St.,Kharkov 310085, Ukraine, FAX:(7-0572)44-11-05

The results of investigations of galvanomagnetic, superconductive and microwave properties of epitaxial superlattices (SL) based on lead and tin chalcogenides (PbTe, PbS, PbSe, SnTe) are presented [1-4]. The epitaxial n-type SL both with homogeneous pseudomorphic and nonhomogeneous layer deformations were under consideration. The SL periods were varied from 2 nm up to 150 nm. It is shown that SL with regular misfit dislocation networks (MDN) can be considered as HTSC models. The highest critical temperature of superconductive transition $T_c \sim 6,5$ K was observed in SL (001)PbTe-PbS with MDN period of 5,2 nm. It is found that T_c is non-monotonic function both of number of electrons per node of MDN and of SL period. The sheet resistance proves to be non-monotonic function of SL period as well. It is revealed that electron pairing begins on the MDN nodes at $T > T_c$ and is stabilized by the interactions between carriers on the adjacent MDN at lower temperatures.

The spectrum of quasi-particle excitations obtained from point-contact measurements of SL (001)PbTe-PbS with MDN is extended up to an energy of 90 meV being six times as high as optical phonon energy in PbTe and PbS bulk materials [5]. The microwave absorption in SL shows peculiarities similar to ones found in HTSC previously [6-7]. The supposition about the same mechanism of superconductivity in SL and HTSC is done.

1.D.Agassi and T.K.Chu. Phys.stat.sol.(b) 160,601(1990) .
2.O.A.Mironov et al.JETP Lett.48,106(1988);49,335(1989);50,334(1989)
3.O.A.Mironov et al.Acta Phys. Pol.A. 80,329(1991); 77,251(1990).
4.O.A.Mironov et al.Superlat.& Microstruct. 8 ,361(1990).
5.N.L.Bobrov et al. Sov.J.of Low Temp.Phys.16,862(1990).
6.I.M.Zaritskii et al.Supercond.:Phys.,Chem.,Technology.4,1400(1991)
7. O.A.Mironov et al.Physica C. 180,196(1991); 185-189,2737(1991).

P10.12

INTERFACE ENERGY SPECTRUM OF REAL PbTe/SnPbTe HETEROJUNCTION

V. I. Litvinov[*)] *and M. Oszwaldowski*[**)]

[*)] *Institute of Material Science Problems, Ukr. Acad. Sci.*
Krasnoarmeyskaya 60-63, 274029 Chernovtsy, Ukraine

[**)] *Instytut Fizyki, Politechnika Poznanska*
Piotrowo 3, 60-965 Poznan, Poland

In heterojunctions formed by semiconductors having inverted order of the bands and overlapping gaps, there were found bands of electron and hole interface states which are gapless and have a linear dispersion. A model of such a heterostructure is a PbTe/SnPbTe heterojunction formed in the (111) plane. So far, all considerations were limited to a single [111] valley [1,2]. The interface energy spectrum obtained for this case is

$$E_{\pm}(111) = \pm v^{\perp} p^{\perp} \sqrt{(1-\lambda^2)} \qquad (1)$$

where $v^{\perp}$ and $v^{\parallel}$ are interband velocity matrix elements, $p^{\perp}$ is the in-plane momentum, λ is a parameter which depends on the gaps offset, and "+" and "−" refer to electrons and holes respectively

In the present contribution we consider the effect of the remain three <111> valleys and interface strain on the interface spectrum. We find that in addition to the non-degenerate branch (eq.(1)), there appears threefold degenerated branch

$$E_{\pm}(111) = \pm \frac{5v^{\perp} + 4v^{\parallel}}{9} \; p \sqrt{(1-\lambda^2)} \qquad (2)$$

For the heterojunction formed in the (100) plane there exists fourfold degenerated branch

$$E_{\pm}(100) = \pm \frac{2v^{\perp} + v^{\parallel}}{3} \; p \sqrt{(1-\lambda^2)} \qquad (3)$$

The phase volume, where the bound-states exist is largest for the branch described by eq.(2). The strain effect deduced from the deformation potentials is remarkable. It considerably affects the gaps and their alignment, and by that it affects the phase volume of the interface states.

1. *B. Volkov & O. Pankratov, Pisma v Zh. Eksp. Teor. Fiz. 42 (1985) 145*
2. *D. Agassi & V. Korenman, Phys. Rev B37 (1988) 10095*

P10.13

EFFECT OF ANNEALING ON THE ELECTRICAL AND STRUCTURAL PROPERTIES OF Sb_xSe_{1-x} THIN FILMS

H.A.Kenawy, H.A.Zayed, A.M.Abo-Elsoud* and A.M.Ibrahim
University College for Girls, Ain Shams University,
Cairo, Egypt
* National Research Center, Cairo, Egypt.

Thin films of $Sb_x\,Se_{1-x}$ with $0<x<1$ and thickness ranging from 500-1000 °A, were prepared by thermal deposition under vacuum on glass substrates. The electrical resistance (ρ) and thermoelectric power (s) were determined at different temperature in the range 300-473 K for different thin film compositions.

Electron microscopic and x-ray diffraction techniques were used to determine the crystallinity and lattice parameters for these structures. The results showed that Sb_xSe_{1-x} alloys have hexagonal structure with lattice parameters which vary linearly with the cmposition with a ranging from 4.362°A to 4.306°A and C in the order of 6.504°A to 11.234°A for x=0.1 to x=0.9.

The resistivity at room temperature was found to be in the order of 10^{11} Ω.cm for the Se rich compositions and 10^3 a.cm for the Sb rich compositions. The activation energy as calculated from $\ln(\rho)$ Vs $1/T$ polts was given as 0.125 ev for x=0.9 and 1 ev for x=0(Se) thin films. The resistance was found to decrease by increasing both film thickness and annealing temperature. The temperature coefficient of resistance decreased from 11×10^{-2} to 2.3×10^{-2} as x increased from x=0 to 0.9.

The value of the thermoelectric power (s) was found to be 100 μv/K for $Sb_x\,Se_{1-x}$ thin films of x=0.1 then it gradually decreased with increasing x ramaining positive up to x=0.4 showing the majority carriers to be holes i.e. p-type conduction. For $0.4<x<0.6$ the thermoelectric power appears to be negative and equals 540 μv/K for x=0.5 i.e. n-type conduction. It turns again to be positive for $0.6<x<0.9$.

P11.1

ELEMENT OF A NEW INFRARED DEVICE —OPTICAL TRANSISTOR

Qian Dingrong
National Laboratory For Infrared Physics, Academia Sinica
420 Zhong Shan Bei Yi Road, Shanghai 200083, China

The energy dispersion relation of free-carriers in narrow-gap semiconductors of which the energy bands can be well described by Kane model turns out to be linear in the case of highly degeneration resulted from either doping or light injection. This influences the behavior of free-carriers profoundly, one of the consequences is the absence of the energy coupling between collective oscillation and electron-hole pair excitations, so that the damping to plasma, as a result, is rather weak and the plasma edge in the reflectivity spectrum of narrow-gap semiconductors is very steep. The edge reflectivity is so sensitive to the variation of carrier concentration that a small amount of excess carriers created by weak infrared radiation in the sample can result in an appreciable increase in reflectivity there. If, in the meantime, a light beam of which the photon frequency is equal to the frequency on the edge is shining on the sample, then the changed edge reflectivity will certainly cause a strong increase in the strength of the reflected shining beam. The sample, in this case, works like a optical transistor: a weak infrared beam controls another infrared beam which is stronger in power and lower in frequency by virtue of reflecting it on plasma edge. It is a versatile device and can be, in its function, a infrared modulator and light switch being prosperous in infrared measurement and detection. The device physics has been discussed in detail and the possible design of various optical transistors with different functions have been proposed. The merit parameters of optical transistor have been discussed, the results are impressive. For example, if a photoconductive infrared detector is coupled to optical transistor, then the detectivity for it can be enlarged by $(t_{pl}t_{pc})^{1/2}/l$ times, where t_{pl}, t_{pc} are the thickness of optical transistor and photoconductive infrared detector, respectively, l is plasma absorption distance.

P11.2

Damage Induced Changes in the Electronic Properties of InSb(100): Implications for Surface Preparation

M.O. Schweitzer[1], W.T. Yuen[2], T.S. Jones[3], C.F. McConville[4], N.V. Richardson[1] and R.A. Strading[2]

1 IRC in Surface Science, University of Liverpool, Liverpool L693BX, UK.
2 Department of Physics & IRC in Semiconductor Materials, Imperial College London SW7 2BZ, UK.
3 Department of Chemistry & IRC in Semiconductor Materials, Imperial College, London, SW7 2AY, UK.
4 Department of Physics, University of Warwick, Coventry, CV4 7AL, UK.

Abstract

Ion bombardment is generally used to prepare chemically clean surfaces of InSb substrates prior to the growth of epilayers by molecular beam epitaxy. Although this method is successful in producing clean surfaces, there are considerable problems associated with the induced changes to the electronic properties of the near-surface region of the material. We have applied a combination of surface sensitive techniques and electron transport measurements to characterise the effects of argon ion bombardment and annealing on a series of p-type InSb(100) ($p \sim 2 \times 10^{14} cm^{-3}$) samples. High resolution electron energy loss spectroscopy (HREELS) has been used *in-situ* to monitor the changes in the surface and interfacial plasmon excitations, and the formation of an n-type accumulation layer, as a function of post-bombardment annealing over a temperature range of 300-700K. Using electron energy dependent measurements and model calculations based on dielectric theory the depth of damage has been determined. It is found that the n-type layer is ~500Å thick and located ~200Å below a surface depletion layer. *Ex-situ* magneto-transport measurements involving the two-dimensional accumulation layer, using the Shubnikov-de-Haas effect, have also been used to independently determine the relative occupancy of the sub-bands and provide a value for the spatial extent of the conducting region. Consistency between the Shubnikov-de-Haas and HREELS measurements is found if the electron concentration in this region is $\sim 9 \times 10^{17} cm^{-3}$ and the carriers are confined below the surface in a layer of thickness ~500Å.

P11.3

Anisotropy and Polarization of Hot Electron Intraband Luminescence

O.M. Bulashenko, A.G. Kollyukh, V.K. Malytenko and V.A. Morozhenko

Institute of Semiconductors, Ukrainian Academy of Sciences, 252650, Kiev-28, Ukraine

Far infrared luminescence ($\lambda \sim 100$mkm) ofn-InSb ($n \sim 10^{13}cm^{-3}$) and n-$Cd_xHg_{1-x}Te$ ($n \sim 10^{14}cm^{-3}$) samples due to the intraband transition of hot electrons in the high electric field ($10<E<150$V/cm) has been investigated both theoretically and experimentally at low temperature ($15<T<150$K). *It was shown that the light emission intensity increases with* increasing the lattice temperature and/or the electric field strength. Besides, the measurements of luminescence in transverse and longitudinal directions with regard to the electric field allowed us to detect the anisotropy of radiation.

To explain the experimental results the calculations of the electron distribution function and the probabilities of photon emission in the passive energy range (the photon energy is less than the optical phonon energy) were carried out by the Monte Carlo method. Electron-photon interaction with simultaneous acoustic, optic and ionized impurity scattering was considered i the second-order perturbation theory. An acoustic phonon scattering gives the main contribution to the light emission intensity among the different scattering mechanisms.

An angular dependence of the matrix element of the electron-photon interaction results in the luminescence anisotropy when the electric field is rather strong, so that the electron distribution function is anisotropic and close to streaming at high fields.

The polarization of the light emission transverse to electric field is the other consequence of angular dependence of the matrix element. The polarization degree of luminescence was also calculated using the Monte Carlo method. The results of the numerical simulation are in good agreement with experimental data.

The investigation of the hot electron luminescence anisotropy as well as the polarization degree of the light emission, transversal to electric field may be used as experimental method for studies of non-equilibrium electron gas behaviour and scattering processes in the narrow gap semiconductors.

P12.1

Low-Temperature Switching in PbTe(Ga) at High Electric Fields

B.A. Akimov, A.V. Albul, E.V. Bogdanov

Physics Department, Moscow State University, Moscow, Russia

Abstract

Current-voltage characteristics (CVC) were measured in PbTe(Ga) (concentration of Ga is 0.2 - 0.4 at %) at high electric fields $E \leq 3000$ V/cm and temperatures $T = 4.2 - 77$K. CVC of PbTe(Ga) drastically differ from CVC of pure PbTe: the pronounced linear region is observed only at $T \geq 70$K and for very weak electric fields $E \leq 1$ V/cm; at higher fields CVC become superlinear and fulfil Poole-Frenkel law; at last switching to high-conductivity state takes place at $E \geq 500 \div 1000$ V/cm. In helium the relaxation time of this conductivity induced by high electric field exceeds 10^4s. At higher temperature relaxation time drops drastically and becomes 10^{-2}–10^{-3}s at 77 K. Under the effect of high electric fields the increase of the conductivity can exceed seven orders of magnitude and CVC change and obtain long linear and sublinear regions characteristic for pure PbTe. The processes that could lead to the switching are discussed.

P12.2

INFRARED PHOTOCONDUCTIVITY AND LUMINESCENCE OF MULTIPLE QUANTUM WELLS $GaAs/Ga_{1-x}Al_xAs$

V. A. Gorbylev*, I. D. Zalevski*, V. B. Kulikov*, A. I. Petrov*, M. V. Chukichev**, A. E. Yunovich**.
*) "Sigma-Plus", Moscow, Russia;
**) Moscow State (Lomonosov) University, 119899, Moscow, Russia.

Optical absorption and photoconductivity due to electron transitions from the levels localized in quantum wells (QW) to continuum states are discussed in connection with luminescence spectra.

For the first time multiple QW's and SL's of heterostructures $GaAs/Ga_{1-x}Al_xAs$ ($x \approx 0.3$) were grown by MOCVD (700°C, 65 Torr) with thickeners of QW GaAs $L_z = 3...5$ nm, of barriers GaAlAs $L_B = 30...50$ nm and number of periods up to $N = 70$.

Energy of the ground eigenstates in QW's was calculated in the approximation of envelope function. For the sample with MQW ($x = 0.3$; $L_z = 4.0$ nm; donors in QW $N_D(Si) = 5 \cdot 10^{17}$ cm^{-3}; $L_B = 31.0$ nm; $N = 70$) in conduction band $\Delta E_{1c} = 89.5$ meV; in valence band $\Delta E_{1vh} = 20.2$ meV; the barrier in conduction band was assumed $\Delta E_c = 228$ meV. In cathodoluminescence spectra at $T = 5$ K a high-energy line with a peak $\hbar\omega_m = 1.613 \pm 0.002$ eV and halfwidth $\Delta(\hbar\omega)_{1/2} = 13...15$ meV was seen. The peak corresponds to radiative transitions between E_{1c} and E_{1vh} levels if exciton or donor ionization energy is taken into account. Halfwidth is caused by QW thickness fluctuations of one atomic layer, $L_z \pm a_0/2$. Two other low-energy lines were lower in intensity and will be discussed later.

The optical absorption and photoconductivity in the infrared region ($\lambda = 7...14$ µm) is due to electron transitions from E_{1c} levels to the continuum states higher than the barrier height ΔE_c. Evaluation of density of states and transition probabilities gives value of the absorption coefficient $\alpha \approx 10^3$ cm^{-1}. The long-wavelength edge of absorption is smoothed by fluctuations.

For electrical characterization the QW's structure was processed into 50x50 µm^2 mesas. Dark I-V curves had one or two steps ($T = 77$ K) in different samples. The measured activation energy of conductivity varied with bias from 84 meV (1 V) to 54 meV (5 V). The device dark current was $4 \cdot 10^{-8}$ A, photoresponse was 0.8 A/W (2 V).

Similar structures but grown by MBE with $N \leq 50$ were described previously by B. F. Levine et al. /Appl. Phys. Lett., v. 56, pp. 851, 1990/.

Index

PROGRAMME OUTLINE - by first authors

Time	Monday	Tuesday	Wednesday	Thursday
	Introduction	**5. Magnetism/ Magnetooptics**	**8. CMT (structure)**	**11. III-V (devices)**
8.45	Welcome	Dietl-inv	Arias-inv	Lakrimi-inv
9.00	McGill Opening			
9.15		Geist	Montenat	Phillips
9.30	**1. Novel Growth**	Story	Dutton	Bougnant
	Abstreiter-inv	Eggenkamp	Bubalac	Ashley
10.00	Norman-inv	Manasses-inv	Tardot-inv	Malutenko-inv
10.30	**Coffee**			
	2. DMS (mainly Fe)	**6. II-VI growth**	**9. Linear and NL optics**	**12. Special Symposium** Chair:D G Seiler
11.00	v.Ortenberg-inv	Maxey-inv	Vodopyanov-inv	Levine-inv
11.30	Skierbizewski	Lusson	Klann	Sheng Li
11.45	Wilamowski	Funaki	Hofmann	Sizman
12.00	Szuszkiewicz	Mitra	Kremser	Fraenkel
12.15	Dobrowolski	Astles	Littler	Morimoto
12.30	Lahderanta	He	Kushev	Mironov
12.45	**Lunch**	**Lunch**	**Lunch**	**Lunch**
	3. II-VI (elect/opt.)	**POSTERS**	**10.Material (mainly IV-VI)**	**12. contd.**
13.45	Meyer-inv	P1.1 to P12.2	Tacke-inv	Heremans-inv
14.15	Cheong		Lambrecht	Gornik-inv
14.30	Kraus		Zogg	
14.45	Takita		Herrmann	Takyanagi-inv
15.00	Esquivias		Schweitzer	
15.15	Andrukhiv			Dawson-inv
15.30	**TEA**	**TEA**	**Conference Excursion**	------------
				15.45- TEA
	4. III-V (InAs/GaAs)	**7. Dots/Novel Confinement**		
16.00	Mendes-inv	Ploog-inv		------------
				16.15 Oswald-inv
16.30	Miles	Tournie		
16.45	Waterman	Zawadzki		**16.45 Shen-inv**
17.00	Golding	Freytag		
17.15	Omaggio	Kubisa-inv		**Close**
17.30	Golding			
17.45	Inoui			Landwehr